

TECHNISCHE UNIVERSITÄT MÜNCHEN

Wissenschaftszentrum Weihenstephan für Ernährung, Landnutzung und Umwelt

Lehrstuhl für Entwicklungsgenetik

Identification of Sox2 as a key regulator of cell-matrix adhesion in Schwann cells

Elen Raquel Sarabasti Torres Mejía

Vollständiger Abdruck der von der Fakultät Wissenschaftszentrum Weihenstephan für Ernährung, Landnutzung und Umwelt der Technischen Universität München zur Erlangung des akademischen Grades eines

Doktors der Naturwissenschaften

genehmigten Dissertation.

Vorsitzender: Prof. Dr. Harald Luksch

Prüfer der Dissertation: 1. Prof. Dr. Wolfgang Wurst

2. Prof. Dr. Magdalena Götz

Die Dissertation wurde am 10.07.2017 bei der Technischen Universität München eingereicht und durch die Fakultät Wissenschaftszentrum Weihenstephan für Ernährung, Landnutzung und Umwelt am 18.12.2017 angenommen.

Table of contents

1. Summary	7
1.1. Abstract	7
1.2. Zusammenfassung	9
2. Introduction	12
2.1. Peripheral nervous system	13
2.1.1. Structure of the PNS	13
2.1.2. Glial cells of the PNS	14
2.2. Schwann cells	15
2.2.1. Schwann cell differentiation	15
2.2.2. Schwann cell migration during development	16
2.2.3. Schwann cells in adult nerves	17
2.3. Regeneration of the PNS	17
2.3.1. Nerve injuries	17
2.3.2. Cellular changes during nerve repair	18
2.3.3. Schwann cell responses after nerve damage	20
2.3.4. Sox2	21
2.3.4.1. Role of Sox2 in the nervous system	21
2.3.5. Molecular changes in Schwann cells during nerve repair	22
2.4. Extracellular matrix in the peripheral nerves	24
2.4.1. ECM during regeneration of the PNS	24
2.4.2. Fibronectin	25
2.4.2.1. FN structure	26
2.4.2.2. FN receptors: the integrins	27
2.4.2.3. FN activation	28
2.4.2.4. FN during PNS regeneration	31
2.5. Aim of the thesis	31
3. Results	33
3.1. Sox2 overexpression modify Schwann cell behavior	33
3.1.1. Development of an in vitro model to study the role of Sox2 in Schwann cells	33
3.1.2. Sox2 overexpression promotes the repair Schwann cell phenotype in vitro	34

3.1.3. Schwann cells proliferation remains at the same levels after Sox2 overexpression	36
3.1.4. Sox2 induces Schwann cell organization and directional migration	37
3.2. Identification of genes and pathways downstream of Sox2, important for Schwann cell behavior	39
3.2.1. ECM- and cell adhesion-related genes are significantly up-regulated in Sox2-positive Schwann cells	39
3.2.2. Sox2 induces FN up-regulation and fibrillogenesis in Sox2-positive Schwann cells	45
3.2.3. FN fibrillogenesis is present in Sox2-positive primary rat Schwann cells	48
3.2.4. Cell-Matrix adhesions are modified upon Sox2 overexpression ...	49
3.2.5. Sox2 directly controls FN expression in Schwann cells	52
3.3. FN is important for Schwann cell organization and directional migration	56
3.3.1. Generation of the Fn1 knock-out rat Schwann cell line using CRISPR/Cas9 genome-editing system	57
3.3.2. FN fibrillogenesis induces Schwann cell aggregation and organization	59
3.3.3. Directional migration of Schwann cells is dependent of FN expression	61
3.3.4. Schwann cell-cell adhesion is independent of FN expression	62
3.4. FN-dependent Schwann cell organization is necessary for axon guidance	63
3.4.1. Axons from dorsal root ganglion neurons follow Schwann cell orientation	64
3.4.2. Human iPSC-derived motoneurons are oriented by self-organized Schwann cells	68
3.4.2.1. Characterization of human iPSC-derived motoneurons	68
3.4.2.2. Axon of human motoneurons regrow following Schwann cells direction	69
3.4.3. FN is necessary for the growth of human motoneurons	72
3.4.4. SC-dependent axonal growth is not affected by the FN produced by embryonic fibroblasts	73
3.5. In vivo expression of Sox2 and FN during regeneration of the peripheral nervous system	77

3.5.1.	Sciatic nerve injury in adult rats	77
3.5.1.1.	Sciatic nerve surgery model	77
3.5.1.2.	Sox2 and FN fibrillogenesis are up-regulated after sciatic nerve transection	79
3.5.1.3.	FN containing the spliced domain EIIIA is co-expressed in Sox2-positive Schwann cells after nerve injury.....	81
3.5.2.	Study of Sox2 expression in the posterior lateral line of zebrafish larvae	83
3.5.2.1.	Development of the pLL of zebrafish.....	84
3.5.2.2.	Regeneration of the pLL of zebrafish after axotomy.....	85
4.	Discussion	87
4.1.	Sox2 controls Schwann cell behavior and modulates the expression of cell adhesion and ECM-related genes	87
4.2.	Sox2 as a novel direct regulator of FN in Schwann cells	90
4.3.	Sox2 regulates cell-matrix adhesion dynamics in Schwann cells	91
4.3.1.	Integrin expression in SC ^{Sox2+}	91
4.3.2.	Focal and fibrillar adhesion structures are present in Sox2-positive Schwann cells.....	93
4.3.3.	FN expression could modulate N-Cadherin-dependent Schwann cell-cell adhesion.	94
4.4.	FN controls Schwann cell alignment and directional migration.....	95
4.5.	Cell to cell contact between axons and Schwann cells is necessary for proper axon guidance	96
4.5.1.	Self-organized Schwann cells control axon guidance.....	96
4.5.2.	Self-organized Schwann cells guide the axons of mouse sensory neurons and human motor neurons.....	97
4.5.3.	FN fibrillogenesis from fibroblasts is not necessary for axonal guidance	99
4.6.	Schwann cell migration: comparison of 2D and 3D in vitro models ...	100
4.7.	Role of Sox2 in Schwann cells during regeneration in vertebrates	101
4.7.1.	Sox2-dependent FN fibrillogenesis could regulate the formation of the Band of Büngner in mammals.....	101
4.7.2.	Sox2 could induce FN expression in repair Schwann cells also in vivo	102
4.7.3.	The FN containing EIIIA spliced domain could be important for Schwann cell matrix assembly in vivo.....	102

4.7.4. Sox2 is not involved in the zebrafish posterior lateral line regeneration.....	103
4.8. Concluding remarks and future perspectives.....	104
5. Materials and Methods.....	106
5.1. Materials.....	106
5.1.1. Animal strain.....	106
5.1.2. Cell lines.....	107
5.1.3. Bacteria strain.....	107
5.1.4. Reagents.....	108
5.1.5. Consumables.....	109
5.1.6. Commercial Kits.....	110
5.1.7. Cell culture media and solutions.....	111
5.1.8. Immunohistochemistry solutions.....	113
5.1.9. Immunocytochemistry solutions.....	115
5.1.10. Molecular solutions.....	116
5.1.11. Protein isolation solutions.....	117
5.1.12. Plasmid list.....	119
5.1.13. Antibody list.....	119
5.1.14. Primer list for semiquantitative RT-PCR.....	121
5.1.15. Primer list for evaluation of Sox2 binding in the rat Fn1 promoter by semi-quantitative PCR.....	124
5.1.16. Primer list for real time RT-PCR.....	124
5.1.17. Primer list for site-directed mutagenesis.....	125
5.1.18. sgRNA sequences for generation of fibronectin-knockout Schwann cell line by CRISPR/Cas9.....	125
5.1.19. Instruments.....	126
5.1.20. Software and databases.....	126
5.2. Methods.....	128
5.2.1. Cell culture.....	128
5.2.2. Retroviral transduction.....	128
5.2.3. Surgical Procedure of rat sciatic nerves.....	129
5.2.4. Live-cell imaging.....	129
5.2.5. Immunocytochemistry.....	130
5.2.6. Immunohistochemistry.....	130

5.2.7.	In situ hybridization	131
5.2.8.	DAB staining	132
5.2.9.	Immunoblotting	133
5.2.10.	RNA isolation and reverse transcription.....	133
5.2.11.	Semiquantitative-PCR and real time PCR	134
5.2.12.	Transformation.....	135
5.2.13.	Cloning procedure	135
5.2.14.	Plasmids purification.....	135
5.2.15.	Microarray analysis.....	136
5.2.16.	In silico promoter analysis	138
5.2.17.	Chromatin immunoprecipitation	139
5.2.18.	Lucia luciferase reporter assay.....	139
5.2.19.	Generation of Fn1 knockout Schwann cell line	140
5.2.20.	FN depletion in normal serum.....	140
5.2.21.	Dorsal root ganglion neurons extraction and co-culture.....	141
5.2.22.	Preparation of the extracellular matrix layer.	142
5.2.23.	Human pluripotent stem cell derived-motor neurons	142
5.2.24.	Human pluripotent stem cell derived-motor neurons co-culture..	143
5.2.25.	Primary Rat Schwann cell culture	143
5.2.26.	Zebrafish experiments	143
5.2.27.	Statistical analysis	144
6.	References	145
7.	Appendix.....	154
7.1.	Abbreviations.....	154
7.2.	Acknowledgements.....	159

1. Summary

1.1. Abstract

Nerve regeneration is an essential process that allows animals after nerve damage to restore brain function, muscle control and sensation, among others. However, not all animals have the same capacity of nerve regeneration. In mammals, it is limited to the peripheral nervous system (PNS) and the efficiency of regeneration depends on the severity of the damage. Schwann cells (PNS glial cells) are one of the major players that guide the regrowing axons to their original targets. During this process, Schwann cells have a high plasticity. After nerve damage, these cells acquire a specific phenotype defined as repair Schwann cells. The transcription factor Sox2 is an important modulator of this repair phenotype. Sox2 induces a change in Schwann cell behavior from cell repulsion to cell-cell adhesion. This change is crucial for their collective migration and the formation of a chain of Schwann cells that acts as a path for axons during their regrowth *in vivo*. This path is also dependent on Schwann cell-basal lamina composed of different extracellular matrix (ECM) protein. ECM proteins influence the cells of the regenerative nerve acting as scaffold and as signaling molecules to promote nerve repair. The exact mechanism by which Sox2 controls Schwann cell behavior during regeneration is not completely understood. Until now it was not known if Sox2 was able to modulate the ECM of Schwann cells to modify their own behavior to promote nerve repair.

The present study aimed at deciphering the role of the transcription factor Sox2 in Schwann cell behavior and its influence on ECM remodeling. To address this, I used an *in vitro* model system where I overexpressed Sox2 in the rat Schwann cell line RSC96 and studied its effect on the expression of ECM proteins. I found that specifically Fibronectin (FN) was directly regulated by Sox2. Live imaging of the Schwann cell line in our *in vitro* model system showed that Sox2 controls Schwann cell aggregation and directional collective

migration. A broad expression profile approach, using microarray analysis of mRNA, revealed that Sox2 modulates the expression of ECM- and cell adhesion-related genes in Schwann cells. Subsequent bioinformatic studies allowed the identification of FN as a main candidate responsible for the directed migration of Schwann cells. FN expression and activation in Sox2-positive Schwann cells was confirmed by western blot analysis and immunostaining. *In silico* promoter analysis identified Sox2 as a new direct regulator of FN expression in Schwann cells and this was confirmed by Chromatin Immunoprecipitation techniques and reporter assays. Sox2-positive Schwann cells showed an increase on focal adhesion and fibrillary adhesion which was quantified by high-content image analysis. I found that FN fibrillogenesis in Schwann cells was necessary for their directed migration. This was confirmed using a FN knockout Schwann cell line generated with CRISPR/Cas9 genome editing technology which showed a random migration pattern and a loss of organization. I also found that FN-dependent Schwann cell organization controlled axon guidance. Co-culture strategies of Schwann cells with mouse sensory neurons and human iPSC-derived neurons, showed that the ability of Schwann cells for guiding the regrowing axons is lost after the disassembly of the Schwann cells due to the absence of FN fibrillogenesis. Additionally, I found that FN produced by embryonic fibroblasts does not influence axonal growth. Some of these results were finally tested *in vivo* in two different animal models. In rat sciatic nerves after injury, the FN splice domain EIIIA was found to be up-regulated and co-expressed with Sox2 in repair Schwann cells. On the contrary, in zebrafish, a non-mammal vertebrate, Schwann cells guided the axons independently of Sox2 expression. In conclusion, I showed that in the established *in vitro* system Sox2 directly controls FN fibrillogenesis in Schwann cells to provide a highly oriented ECM, which supports their directional collective migration to guide the regrowing axon. These results provide new insights into the mechanism for the modification of the ECM by glial cells during neuronal regeneration in mammals.

1.2. Zusammenfassung

Die Regeneration von Nerven ist ein essenzieller Prozess, der es Tieren nach einer Nervenläsion ermöglicht, unter anderem Hirnfunktionen, Muskelkontrolle und Sinnesempfindung wiederherzustellen. Jedoch besitzen nicht alle Tiere die gleiche Fähigkeit zur Regeneration von Nerven. In Säugern ist diese Fähigkeit auf das periphere Nervensystem (PNS) beschränkt und hängt stark vom Grad der Nervenschädigung ab. Eine Hauptrolle nehmen dabei Schwann-Zellen ein, indem sie nachwachsende Axone zu ihren ursprünglichen Zielstrukturen führen. Während dieses Prozesses zeigen diese Zellen ein hohes Maß an Plastizität. Nach einer Nervenschädigung verändern sich Schwann-Zellen zu einem speziellen Phänotyp, der als Reparatur Schwann-Zelle definiert ist. Ein wichtiger Modulator dieses Phänotyps ist der Transkriptionsfaktor Sox2. Sox2 induziert in Schwann-Zellen die Änderung von einem repulsiven zu einem adhäsiven Verhalten. Dieser Wechsel ist entscheidend für die kollektive Zellmigration und die Aneinanderreihung der Reparatur Schwann-Zellen zu einer Kette, die nachwachsenden Axonen *in vivo* als Pfad dient. Dieser Pfad ist auch von der Basal-Lamina von Schwann-Zellen abhängig, die aus verschiedenen Proteinen der extrazellulären Matrix (EZM) besteht. Proteine der EZM modulieren zum einen als Scaffold als auch als Signalmoleküle die Zellen des regenerierenden Nervs und fördern damit seine Reparatur. Der genaue Mechanismus, über den Sox2 das Verhalten von Schwann-Zellen während der Nerv-Regeneration steuert, ist noch nicht vollständig verstanden. Außerdem war bisher nicht bekannt, ob Sox2 auch über die EZM von Schwann-Zellen das Verhalten dieser Zellen während der Regeneration von Nerven modulieren kann.

Das Ziel der vorliegenden Arbeit war es, die Rolle des Transkriptionsfaktors Sox2 im Verhalten von Schwann-Zellen und während der Remodulierung der EZM zu untersuchen. Um dieser Fragestellung nachzugehen, etablierte ich ein *in vitro* Modell indem ich Sox2 in einer Schwann-Zell-Zelllinie der Ratte, RSC96, überexprimierte und die Effekte von Sox2 auf die Expression von EZM Proteinen analysierte. Dabei fand ich heraus,

dass Fibronectin (FN) der direkten Regulierung von Sox2 unterliegt. Die Analyse der -Zellen dieses Modells durch Live-Cell Imaging zeigte, dass Sox2 das Zusammendrängen und die gerichtete kollektive Migration von Schwann-Zellen steuert. Durch eine Genexpressionsanalyse mittels microarray chips fand ich heraus, dass Sox2 in Schwann-Zellen die Expression von Genen steuert, die mit der EZM und mit der Zelladhäsion assoziiert sind. Die bioinformatische Auswertung dieser Daten führte zur Identifikation von FN als Hauptkandidat für die Steuerung der kollektiven Migration von Schwann-Zellen. Die Expression und Aktivierung von FN in Sox2-positiven Schwann-Zellen wurde durch Western Blot Analysen und immunhistochemische Färbungen bestätigt. *In silico* Promotor Analysen identifizierten Sox2 als neuen, direkten Regulator der FN Expression in Schwann-Zellen. Dieses Ergebnis wurde durch Chromatin-Immunopräzipitation und Reporter-Assays bestätigt. Sox2-positive Schwann-Zellen zeigten eine vermehrte fokale und fibrilläre Adhäsion, die mittels High-Content-Imaging Analysen quantifiziert wurde. Weiterhin fand ich heraus, dass die Fibrillogenese von FN erforderlich für die gerichtete Migration von Schwann-Zellen war. Dieses Ergebnis bestätigte ich durch die Analyse von Schwann-Zellen, in denen ich das FN Gen mittels CRISPR/Cas9 Technologie ausschaltete. Darüber hinaus fand ich heraus, dass die FN-abhängige Organisation von Schwann-Zellen die axonale Wegfindung steuert. Außerdem analysierte ich Co-Kulturen von Schwann-Zellen mit sensorischen Neuronen der Maus und mit humanen, aus iPSC-generierten, Neuronen. Dabei konnte ich zeigen, dass eine fehlende Fibrillogenese von FN zu einer Disassemblierung von Schwann-Zellen führt, wodurch diese Zellen Ihre Fähigkeit verlieren, nachwachsende Axone zu führen. Außerdem fand ich heraus, dass FN, welches von Fibroblasten produziert wurde, nicht den axonalen Wachstum beeinflusst. Einige dieser Ergebnisse wurden schließlich *in vivo* in zwei verschiedenen Tiermodellen überprüft. In verletzten Ischias Nerven von Ratten war die gespleißte FN Domäne E11A hochreguliert und wurde mit Sox2 in „Repair Schwann-Zellen“ co-exprimiert. Im Gegensatz dazu, war die Nervenregeneration im zebrafisch, einem nicht-säugenden Wirbeltier, nicht abhängig von der Sox2 Expression der Schwann Zellen. Zusammengefasst konnte ich zeigen, dass Sox2 direkt die Fibrillogenese von FN in Schwann-Zellen von Säugern steuert um eine hoch-orientierte EZM zur Verfügung zu

stellen. Diese EZM unterstützt die gerichtete kollektive Migration von Schwann-Zellen um nachwachsende Axonen zu führen. Diese Ergebnisse stellen einen neuen Mechanismus für die Modifizierung der EZM durch Gliazellen während der neuronalen Regeneration in Säugern dar.

2. Introduction

Regeneration allows animals after injuries to replace lost tissue, organs or even an entire part of the body. To develop the new body part, cell proliferation, migration and architectural modification in the extracellular matrix compartment should take place. Regenerative mechanisms are diverse, new tissue can originate from stem cell niches in the injured area, after cell dedifferentiation or through a trans-differentiation process (Tanaka & Reddien, 2011). In addition, the microenvironment of the new proliferative cells should be re-established where the extracellular matrix proteins, located in the cell microenvironment, are important players as scaffold and signaling driving molecules (Lu et al., 2011). The process of regeneration was discovered in Hydra by the Swiss naturalist Abraham Tremblay in 1740. Tremblay observed that after cutting half of the animal, it could completely regenerate (Tanaka & Reddien, 2011). However, not all animals have the same ability to produce new body parts, and actually, this capacity is reduced in mammals and limited to only new tissues or parts of an organ (Bely, 2010). Nowadays, regeneration is a field of intensive study due its implications in regenerative medicine to improve patient recovery after accidents or in degenerative diseases. The nervous system and specifically the PNS in mammals, have the capacity to regenerate after injuries, nevertheless this capacity can be compromised depending on the severity of the damage (Kristján R Jessen et al., 2015). Each cellular component of the PNS have a relevant role during the process of regeneration. An increase of our understanding on how these cells interact with the extracellular microenvironment is crucial for the development of new therapies that improve the recovery of functional capacities of patients after nerve trauma. Furthermore, the knowledge we acquire from PNS regeneration studies can be applied to the mammalian central nervous system where regeneration is absent. In this work, I studied the role of the transcription factor Sox2 in Schwann cells behavior throughout the modulation of extracellular matrix proteins, specially FN, to favor PNS regeneration.

2.1. Peripheral nervous system

2.1.1. Structure of the PNS

The vertebrate nervous system is anatomically divided into central nervous system (CNS) and peripheral nervous system (PNS). The CNS comprises the brain and the spinal cord, and the PNS is formed by sensory and motor neurons. Sensory neurons receive internal and external information from the sensory receptors and transmit the information through the nerves and sensory ganglia to the CNS. The motor system carries the responses from the CNS to the muscles. There are two main systems formed by motor neurons, the visceral or autonomic system that controls the smooth muscles, cardiac muscles and glands, and the somatic motor system that controls the skeletal muscles (Purves et al., 2004).

In the PNS, the cell body of the neurons is located in ganglia together with supporting cells, axons are collected in bundles that form the nerve trunk. The PNS is made of three layers: i) the epineurium, ii) the perineurium and iii) the endoneurium (Figure 1). The epineurium is the outermost layer and is formed by dense connective tissue and the vasculature. Inside the epineurium are nerve fascicles composed by the perineurium, the layer that surrounds each fascicle and contains collagen fibers and perineurial cells. Inside lays the endoneurium, where macrophages, fibroblasts, mast cells, peripheral glial cells and axons are located (Gonzalez-Perez et al., 2013).

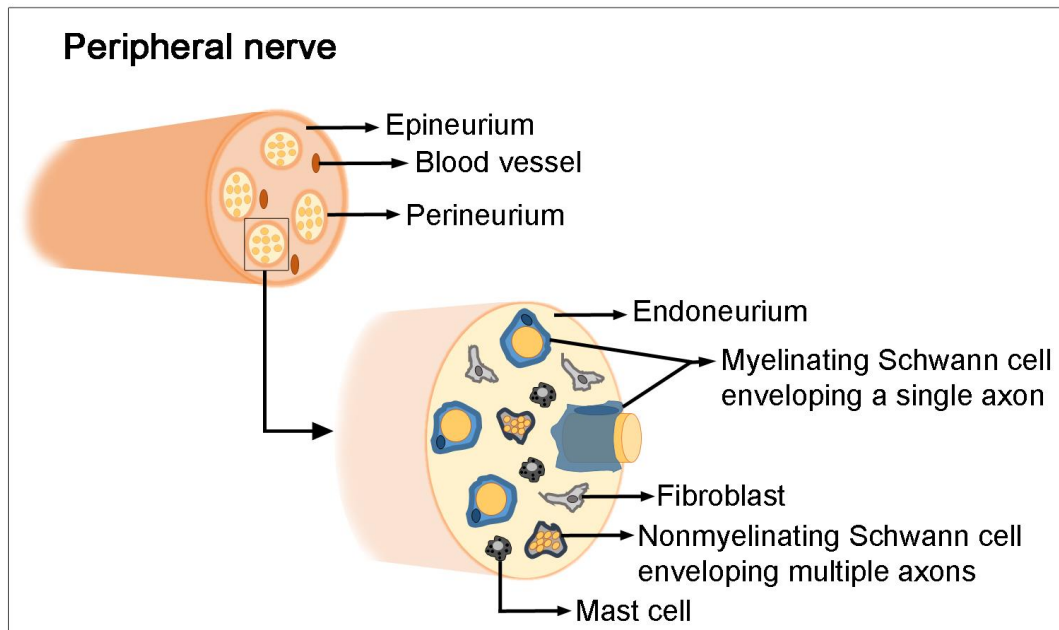


Figure 1. Schematic representation of the peripheral nerve structure. Transversal view of a nerve showing the layers and cell types.

2.1.2. Glial cells of the PNS

Glial cells are the second major cellular players in the nervous system. They outnumber neurons and maintain a close association with them (Kristjan R Jessen, 2004). Glia cells have important roles during development of the nervous system and in adulthood. They maintain nerve homeostasis, support neurons, provide trophic factors, myelinate the axons and help during the regeneration of the PNS (Kristjan R Jessen, 2004). There are different types of glial cells depending on their location and association with the neurons. Satellite glial cells envelope the cell body of sensory and autonomic neurons in the ganglia. Enteric glial cells are present in the enteric nervous system. Olfactory ensheathing cells, also associated with the CNS, wrap the primary olfactory axons. Teloglia cells are found in terminal axons at the skeletal neuromuscular junctions. Schwann cells are packaging the axons in the nerve trunk (K. R. Jessen & R. Mirsky, 2005).

2.2. Schwann cells

Schwann cells are the main glial cells of the PNS. These cells were described for the first time by Theodor Schwann in the 19th century (Bhatheja & Field, 2006). Originally, they were thought to be a passive component of the nervous system, but now it is clear that both neurons and glia depend on each other to accomplish a proper development and for survival during adulthood (Bhatheja & Field, 2006). There are two types of Schwann cells, myelinated and non-myelinated (Remak) Schwann cells. Myelinated Schwann cells envelope one large axon and non-myelinated Schwann cells wrap a bundle of small diameter axons in the nerve trunk (K. R. Jessen & R. Mirsky, 2005). Schwann cells have been subject to extensive studies due their relevance to maintain nerve homeostasis, their different roles in PNS regeneration and their implications in tumor formation (Miller et al., 2006; Shivane et al., 2013).

2.2.1. Schwann cell differentiation

Schwann cell lineage develops from neural crest, to Schwann cell precursor, immature Schwann cells and finally to non-myelinating or myelinating Schwann cells. Neural crest cells delaminate from the neuroepithelium during the formation of the neural tube and migrate to the periphery in two main directions, laterally to give rise to melanocytes and ventrally where they differentiate to sensory neurons, glia, sympathetic and parasympathetic nerve cells, and chromaffin cells (K. R. Jessen & R. Mirsky, 2005). Once neural crest cells differentiate to Schwann cell precursors at E14-15 in rats and E12-13 in mice, they proliferate and migrate along the developing axons behind the growth cones (K. R. Jessen & R. Mirsky, 2005). During this stage, they start to form their basal lamina. Schwann cell precursors control nerve fasciculation, promoting an accurate innervation of the final target of the neuron. They also secrete trophic factors to support survival of sensory and motor neurons. Schwann cell precursors develop to immature Schwann cells at E15-17 in rats and E13-15 in mice. Radial nerve sorting occurs during this stage at around E18, process by which axons and glial cells arrange prior to myelination (Kristján R Jessen et al., 2015). Schwann cell final fate (myelinating or

nonmyelinating) is determined by the axon diameter which they are in contact. (K. R. Jessen & R. Mirsky, 2005).

Differentiation of Schwann cells to mature myelinating cells is controlled by the downregulation of pathways that inhibit myelin formation. For example, downregulation of c-Jun-amino (N)-terminal kinase (JNK) pathway, involved in proliferation, and downregulation of the transcription factor Krox24 lead to the expression of Krox20, Brn-2, Sox10 and Oct6, pro-myelin genes (K. R. Jessen & R. Mirsky, 2005). Sox2 and Pax3, suppressors of myelination and differentiation, are also downregulated in mature myelinating Schwann cells. However, the exact mechanism that controls the switch from immature to differentiated cells is still not well understood (K. R. Jessen & R. Mirsky, 2005).

2.2.2. Schwann cell migration during development

Glial cells must migrate from their place of origin to the final position where they will differentiate. Migration of Schwann cell precursors during development has been extensively studied. Glial cell migration in developing peripheral nerves occurs in a collective manner, forming a migratory chain that moves behind the growth cone of the neurons (Stephan Heermann & Schwab, 2013). The leading cells are normally responsible of following the cues in the axon track and coordinate the entire migration of the chain. Leading cells possess a dynamic filopodia formation and long protrusions. Following cells are less active, they anchor in the leading cell rear ends and do not form filopodia (Klämbt, 2009). The molecular mechanisms that control the formation of the chain have been studied in zebrafish and Drosophila. In these models, the decision of leading cells behavior depends on genetic priming and competition for FGF signaling coming from the growing axons. Filopodia formation is controlled by Notch signaling which influences cytoskeleton dynamics. The GTPase RhoA controls stress fiber polymerization and Rac1 modulates lamellipodia formation in the migratory glial cells (Klämbt, 2009; Sepp, 2003).

Collective migration of Schwann cell precursors is indirectly influenced by NRG1-ErbB signaling pathway (Bhatheja & Field, 2006). NRG1 type III ligand is expressed by the developing axons and its receptor, the heterodimer ErbB2 and

ErbB3, is expressed by Schwann cells. This signaling pathway is important for the survival of Schwann cells and have an indirect impact on their migration. Blockage of the receptor in glial cells induces apoptosis which disturbs cell-cell contacts within the chain and impairs collective migration (Stephan Heermann & Schwab, 2013).

2.2.3. Schwann cells in adult nerves

During adulthood, one of the main roles of Schwann cells is to myelinate axons. Myelination is important for the electrical isolation of the axon in order to increase the conduction of the action potential (Purves et al., 2004). Non-myelinated Schwann cells, although less studied, produce trophic factors to support axons and they are necessary for pain sensation (S. Chen et al., 2003). The second major role of Schwann cells is to promote axon regeneration after nerve damage. In this regard, mature Schwann cells are very plastic cells, they have the capacity to de-differentiate, proliferate and activate proregenerative genes to help axon regrowth. Once regeneration is completed they differentiate and restore their original function (K. Jessen & Mirsky, 2016).

2.3. **Regeneration of the PNS**

2.3.1. Nerve injuries

The capacity of regeneration of the PNS depends on the severity of the nerve injury. There are two types of trauma:

- a) Axonotmesis (crush injury), this type of damage mainly affects the axons, Schwann cell basal lamina and connective tissue are not disturbed. Regeneration is highly efficient after a crush injury since axons can regrow and follow the original path through the remaining endoneurial tubes and Schwann cell basal lamina to reconnect to the original target (Kristján R Jessen et al., 2015).
- b) Neurotmesis (nerve transection or axotomy), this injury causes an interruption of the basal lamina and connective tissue. In mammals, functional recovery is generally poor due the discontinuity of the endoneurial tubes. After neurotmesis, the capacity of regrowing axons to find the original path is

impaired leading to axon atrophy or incorrect target innervation (Allodi et al., 2012; Kristján R Jessen et al., 2015). Re-attachment of the two ends of the nerve is a clinical treatment after neurotmesis. When a large segment of the nerve is lost, a common procedure is to graft healthy nerve tissue from other areas into the damage nerve. Muscle grafts have also been used, as cells in this type of tissue are organized and can guide the growing axons (X. Gu et al., 2014). Another approach is the use of biomaterial (still under development) and it aims at reconnecting the proximal and the distal nerve stumps by means of a tubular bridge made that guides the axons during the regeneration process (X. Gu et al., 2014), however, functional recovery is not efficient.

2.3.2. Cellular changes during nerve repair

Independently of the type of injury, there are general changes at the level of the injured area and in the distal stump. Peripheral nerve injuries trigger a cascade of responses in the cellular microenvironment of the nerve that promotes axonal growth and guidance to the original targets (Figure 2). Nerve damage induces Wallerian degeneration during the first days after the injury, which consists of the degeneration of the axons in the distal stump and the myelin breakdown by Schwann cells, process by which the glial cells autophagocyte the small myelin remains (myelinophagy) (Faweett & Keynes, 1990). Additionally, there is an invasion of activated macrophages, also promoted by Schwann cells, that phagocyte cellular debris in the distal stump (Figure 2). The rapid removal of the debris creates a favorable environment for the re-growing axons (Faweett & Keynes, 1990).

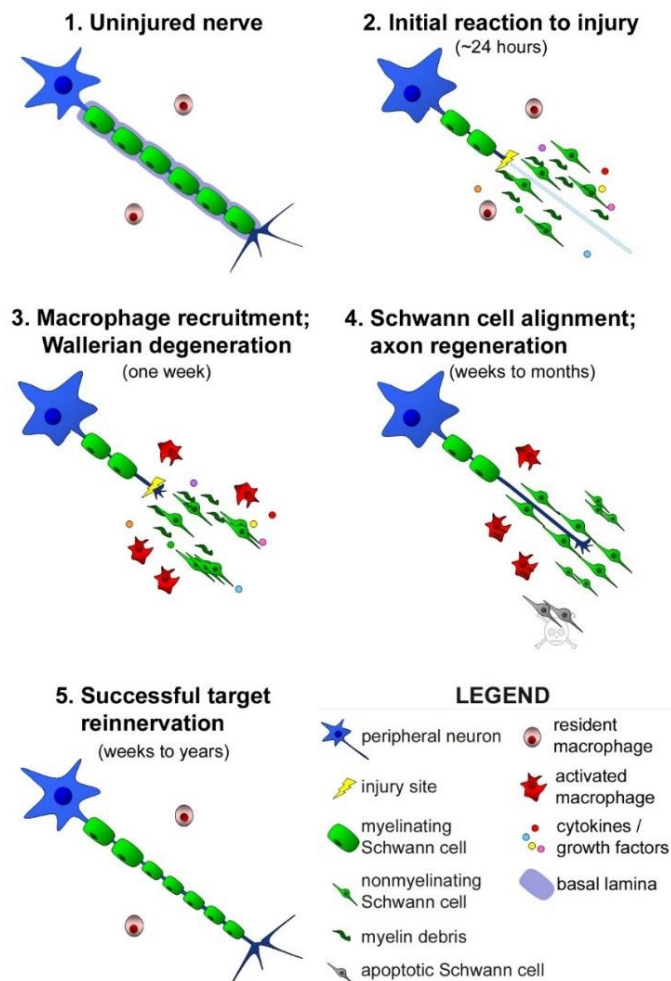


Figure 2. Main steps of peripheral nerve regeneration after axotomy.

After injury, Schwann cells downregulate myelin genes and start to proliferate (2). Macrophages and Schwann cells clear the debris to favour axonal growth (3). Schwann cells form the band of Büngner and guide the axons during the process of reinnervation (4). Finally, the axons reach their targets and Schwann cells differentiate to myelinate the axons (5). Regeneration can take weeks in rodents to years in humans (Gaudet et al., 2011).

Axon damage causes chromatolysis, (dispersal of the Nissl substance due disintegration of granular condensation of rough endoplasmic reticulum), retraction of synaptic terminals, increment of neuron metabolism and protein synthesis (Fawcett & Keynes, 1990). At the level of the injury, in the axon, there is a local rearrangement of the cytoskeleton, local production of proteins to have a rapid response to the damage and the formation of growth cones (Fawcett & Keynes, 1990). In case of neurotmesis, a tissue bridge is formed between the proximal and the distal stump to reconnect the nerve and facilitate the axonal growth to the distal stump. In the gap, macrophages stimulate the formation of blood vessels that act as a migratory scaffold for Schwann cells to migrate along the bridge (Cattin et al., 2015). Neurons by themselves have a low capacity of navigation to re-innervate the original targets. For this reason, neurons need glial cells for guidance during regeneration (Fawcett & Keynes,

1990). The growth cones follow the cues of the microenvironment, specially Schwann cells. Axons grow efficiently when they are in direct contact with the glial cells (Bunge et al., 1989). Schwann cells during regeneration, migrate collectively in front of the growth cone and form cellular channels made of Schwann cells and their basal lamina, called Band of Büngner (Fawcett & Keynes, 1990). These cellular channels are indispensable for guiding the axons across the bridge and in the distal stump in order to reconnect the original targets (Kristján R Jessen et al., 2015). Once the growth cones reach the target, they stop growing and form synapses. During the process of regeneration many axonal sprouts are generated but only the ones that make the final connection will remain. However, if the axon does not reach the target, it can form a neuroma in the proximal stump and the recovery of functionality is impaired (Allodi et al., 2012).

2.3.3. Schwann cell responses after nerve damage

Schwann cells are a key component of nerve repair. They modify their behavior and acquire a specific proregenerative phenotype (repair Schwann cells) indispensable for PNS regeneration. These changes include loss of differentiation characteristic and activation of a repair program (K. Jessen & Mirsky, 2016). Previously, it was thought that Schwann cells de-differentiate and return to an immature state, but recent evidences demonstrated that the cellular changes and expression profile of Schwann cells during nerve repair are specific to induce regeneration and not observed in immature Schwann cells (Arthur-Farraj et al., 2012). Schwann cells downregulate the expression of myelin genes, up-regulate neurotrophic factors to promote neuron survival and axon growth, express cytokines that recruit macrophages and increase proliferation (Arthur-Farraj et al., 2012; Kristján R Jessen et al., 2015).

One important characteristic of the repair Schwann cells is the change from cell repulsion to cell-cell adhesion. This modification in cell behavior facilitates their collective migration and the formation of the Band of Büngner (R. Klein, 2010). PNS regeneration depends on the capacity of Schwann cells and their basal lamina to guide the axons for a proper reconnection (Fawcett & Keynes, 1990). One protein responsible for Schwann cell sorting and

organization during nerve repair is Sox2. This transcription factor modifies glial cell behavior to promote the formation of the cellular channels that guide regrowing axons (Parrinello et al., 2010).

2.3.4. Sox2

Sox2 belongs to the family of high-mobility group transcription factors (SRY-related HMG-box). Sox2 together with Sox1 and Sox3, in mammals, form the family of SOXB1 proteins which have high biochemical and functional similarity (Wegner & Stolt, 2005). Sox2 is important for the maintenance of stem cell renewal during development and in the adult stem cell niches (Arnold et al., 2011). It is expressed in the inner cell mass of the blastocyst (Avilion et al., 2003). Sox2 downregulation impairs the maintenance of epiblast in an undifferentiated state and induces its differentiation to trophectoderm or extraembryonic ectoderm causing the lethality of mouse embryo (Avilion et al., 2003). Additionally, in adult, Sox2 is responsible for the maintenance of stem cell niches (e.g. glandular stomach, esophagus, forestomach, anus and testis in mice) and its deletion affects stem cell proliferation disturbing tissue homeostasis (Arnold et al., 2011). Moreover, Sox2 together with Oct3/4, Klf4 and c-Myc (or other combinations) can reprogram differentiated cells into a pluripotent state (Chambers & Tomlinson, 2009).

2.3.4.1. *Role of Sox2 in the nervous system*

Sox2 is one of the first regulators of early specification of the neuroectoderm during vertebrate gastrulation (Graham et al., 2003; Kishi et al., 2000). In the CNS, Sox2 maintains the self-renewal of neural stem cells avoiding their differentiation. For example, during CNS development in mice, knockout of Sox2 impairs hippocampal development and results in the absence of the dentate gyrus at P7 (Arnold et al., 2011). In adults, Sox2 is highly expressed in the neurogenic regions of the brain, the subventricular zone of the lateral ventricles and in the subgranular zone in the dentate gyrus of the hippocampus (Wegner & Stolt, 2005). However, Sox2 is also expressed in a small proportion of postmitotic neurons, among them, pyramidal cells in the

cerebral cortex, striatal neurons and thalamic neurons (Ferri et al., 2004; Wegner & Stolt, 2005).

Very little is known about the role of Sox2 in the PNS during adulthood. Sox2 is downregulated in neural crest cells during the closure of the neural tube. Sox2 is completely absent in migratory neural crest cells. Its overexpression impairs the migratory capacity of these cells (Wakamatsu et al., 2004). Later during PNS development, Sox2 is restricted to glial cells. It is expressed in immature Schwann cells and acts as a repressor of myelination, keeping Schwann cells in the immature stage and promoting their proliferation (Le et al., 2005). Sox2 is down-regulated postnatally and it is only localized in the adult rat sensory system particularly in satellite glial cells, non-myelinated Schwann cells (low expression) and in many perisynaptic Schwann cells (Koike et al., 2014). Its exact role in the different glial cell types is still not well understood. During the regeneration of the PNS, Sox2 plays an important role acting as a repressor of myelination and modulating Schwann cell behavior after nerve injury (Parrinello et al., 2010).

2.3.5. Molecular changes in Schwann cells during nerve repair

In regenerative nerve, axons influence Schwann cells by the secretion of trophic molecules like Neuregulin that promotes proliferation and migration of the glial cells (S. Heermann et al., 2011; Namgung, 2015; Wakatsuki et al., 2014). The loss of contact between Schwann cells and the axons and the downregulation of myelinated genes promote the adoption of a repair state characterized by the up-regulation of transcription factors such c-Jun and Sox2 by Schwann cells (K. Jessen & Mirsky, 2016). c-Jun controls Schwann cells status inducing the repair phenotype (an elongated bipolar morphology that influences the formation of the band of Büngner). It promotes the up-regulation of trophic factors and cell surface proteins to support axon growth. It Downregulates myelin genes and influences the immune response to injury promoting the recruitment and activation of macrophages (Arthur-Farraj et al., 2012). Repair Schwann cells express neurotrophic factors that act as chemoattractant for the growing axons, including NGF (decreased in the injured axon), BDNF, NT-4, GDNF and IGF-1. Particularly BDNF and GDNF were

described as direct targets of c-Jun (Arthur-Farraj et al., 2012; K. Jessen & Mirsky, 2016).

Sox2 is the other important regulator of the repair Schwann cell phenotype. Sox2 maintains the glial cells in a non-differentiated state, suppresses the expression of myelin genes and changes Schwann cells behavior to favor the formation of the band of Büngner (Kristján R Jessen et al., 2015). Sox2 expression in Schwann cells is induced by fibroblasts through ephrin-B/EphB2 signaling, a family of receptor tyrosine kinases. Fibroblasts express ephrin-B ligand and bind to the EphB2 receptor in Schwann cells. This first signal induces Schwann cells sorting. Sox2 expression modifies glial cells behavior from repulsion to adhesion. Sox2 up-regulation induces a relocalization of the cell-cell adhesion protein N-cadherin, from the cytoplasm to the cell-cell contacts in Schwann cells, which help to maintain the chain of glial cells important for axon guidance (Parrinello et al., 2010). However, the specific mechanism of how Sox2 induces N-cadherin relocalization and how Sox2 modifies Schwann cell behavior is not completely understood.

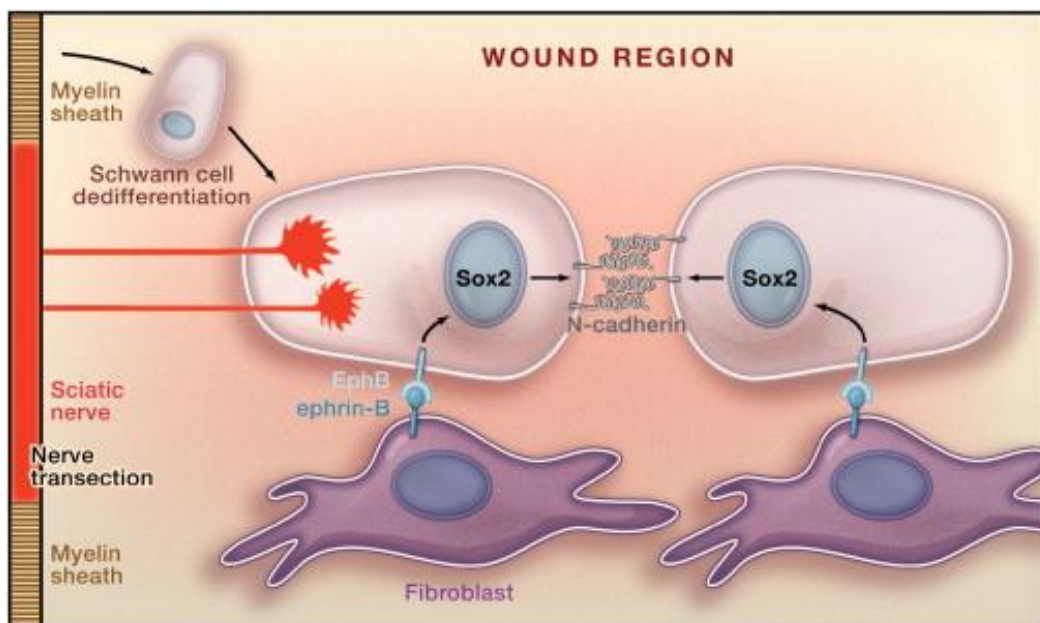


Figure 3. Sox2-dependent Schwann cells sorting during PNS regeneration. After an injury, fibroblasts induce Sox2 expression in Schwann cells through ephrin-B/EphB signaling. Sox2 promotes N-Cadherin relocalization inducing

Schwann cell-cell junction (Reprinted from Klein, 2010 and reproduced with permission from Elsevier).

2.4. Extracellular matrix in the peripheral nerves

A main component of the cellular microenvironment is the extracellular matrix. The ECM is a dynamic structure able to respond rapidly to environmental changes and essential for mediating appropriate cellular responses. Cells communicate efficiently using molecular and mechanical cues present in the ECM to trigger adhesion, migration, proliferation and differentiation during important processes such as morphogenesis and wound healing (Bonnans et al., 2014; Sakai et al., 2003). In the PNS, the ECM is composed of glycoproteins, proteoglycans and non-proteoglycan polysaccharides, which are found in the perineurium and in the endoneurium (Gonzalez-Perez et al., 2013). The ECM proteins found in the endoneurium are located in the basal lamina produced by the glial cells and endoneurial cells, fibroblasts do not produce a basal lamina (Bunge et al., 1989). Collagen fibrils of type I and III are mainly located in the perineurium and the endoneurium around Schwann cell-axon units. Perineurial cells produce collagen type IV and V, laminins, nidogen and heparan sulfate proteoglycans. Schwann cells produce collagen type IV, laminins, FN, heparan sulfate proteoglycans and nidogens (Bunge et al., 1989; Gonzalez-Perez et al., 2013; Peters et al., 1996).

2.4.1. ECM during regeneration of the PNS

During the regeneration of the PNS, the ECM acts not only as an adhesive scaffold, but it also constitutes a dynamic matrix that modulates signaling pathways to drive regeneration, influencing glial cells behavior and promoting growth and orientation for the migrating axons (Gonzalez-Perez et al., 2013). The basal lamina surrounding Schwann cell-axon units plays a crucial role during the process of regeneration. After crush injury the maintenance of the basal lamina in the endoneurial tubes favors regeneration since axons can follow their original path (Kristján R Jessen et al., 2015). In case of neurotmesis, Schwann cells organize themselves and increase the production of ECM proteins that contributes to the formation of the basal lamina

that guide the axons throughout the formation of the band of Büngner (Gonzalez-Perez et al., 2013; Kristján R Jessen et al., 2015). Many studies have demonstrated the relevance of the basal lamina and its ECM components for PNS regeneration. Decellularized nerve grafts, where Schwann cell-basal lamina remains, promote neurite growth (Bunge et al., 1989). However, regeneration is more efficient when Schwann cells are present, probably due to the contribution of trophic factors but also because Schwann cells act as a permissive surface (Bunge et al., 1989). Moreover, the growth of some neurons from the CNS (from rat cortex, locus coeruleus and olfactory bulb) can be stimulated by the presence of Schwann cells-derived ECM (Bunge et al., 1989), which reinforce the importance of the basal lamina and the ECM produced by Schwann cells.

ECM proteins, such as laminin, collagen and FN, have been applied to tubular structure, used to reconnect the cut ends of the nerve, to improve regeneration by mimicking Schwann cell-basal lamina (X. Gu et al., 2014; S. Klein et al., 2016). Nevertheless, in order to have a successful reconnection of the growing axons, the tubular structure has to simulate the microenvironment present *in vivo* in a regenerative nerve (William Daly et al., 2012). For this reason, it is necessary to have a better understanding of the physiology and molecular pathways that influence the ECM production during the regeneration of peripheral axons. This will improve the design of bioengineered materials for reconstructive surgery after peripheral lesions. Besides, insights from the mechanisms regulating the regeneration of the PNS could be applied to the central nervous system.

2.4.2. Fibronectin

One of the main components of the basal lamina, essential for axonal growth and Schwann cells proliferation and migration, is fibronectin (FN) (Webber & Zochodne, 2010). FN is highly expressed during development. In the developing peripheral nerves, FN is present along axon bundles and correlates with the expression of the integrin receptor $\alpha 5\beta 1$, their interaction probably modulates matrix formation (Lefcort et al., 1992; Peters & Hynes, 1996). In adulthood, FN expression in the PNS is decreased but up-regulated again

the type III repeats, one is located between repeats III₇ and III₈ defined as EIIIB, or EDB in humans, the second one EIIIA or EDA located between repeats III₁₁ and III₁₂ (White & Muro, 2011). These two domains can be included or completely excluded by exon skipping. Third, the V or IIICS domain called type III connecting segment between repeats III₁₄ and III₁₅, and it can be complete or partially included (White et al., 2008). These spliced domains are cell and tissue specific. EIIIA and EIIIB are always absent in plasma FN, on the contrary, cellular FN can have both or only one. The V domain can be included in both types of FN and particularly in plasma FN where it is present only in one subunit. The combination of the spliced domains gives, as a result, a total of 20 and 12 isoforms in human and rodents respectively. The roles of the spliced domains, specifically EIIIA and EIIIB, are not completely understood (White et al., 2008; White & Muro, 2011). The inclusion of the spliced regions is higher during development with roles in angiogenesis, cell migration and cell differentiation and for example deletions of EIIIA and EIIIB together lead to embryonic lethality (Peters & Hynes, 1996; White et al., 2008). In adulthood, the presence of these regions increases during tissue repair, fibrosis and angiogenesis (Peters et al., 1996; White & Muro, 2011). After peripheral nerve injury EIIIA, EIIIB and V spliced regions are highly expressed and studies based on *in situ* hybridization and PCR showed that Schwann cells expressed the different spliced isoforms (Mathews & Ffrench-Constant, 1995; Vogelesang et al., 1999), however, their role in the regenerative PNS is not clear.

2.4.2.2. *FN receptors: the integrins*

Integrins are the main receptors of FN, these are trans-membrane receptors composed of two subunits noncovalently bound, α and β . In vertebrates there are 24 heterodimers in the integrin family depending on the $\alpha\beta$ combination (R. O. Hynes, 2002). They can interact with the ECM molecules and drive specific downstream signaling influencing the actin cytoskeleton, except of $\alpha6\beta4$ that links to intermediate filaments through the $\beta4$ long cytosolic domain (Moser et al., 2009). Each subunit consists of a long extracellular domain that interacts with the ligand, a single transmembrane domain and a short cytoplasmic tail. Integrins undergo a conformational change that induces

their activation from a low- to a high-affinity state (Moser et al., 2009). This change depends on the binding of the proteins Talins and Kindlins to integrin tails. This binding causes a separation of α and β transmembrane domain, originally interacting (Moser et al., 2009). After Talin and Kindlins binding, the affinity state of the integrins changes from a bent conformation to an extended conformation, finally leading to their activation (Moser et al., 2009). There are nine heterodimer integrins that can bind to FN, the main ones are $\alpha5\beta1$ and $\alphaV\beta1$ integrins. They two recognize the Arg-Gly-Asp (RGD) motif present in repeats III₉₋₁₀ important for cell adhesion and matrix assembly (To & Midwood, 2011).

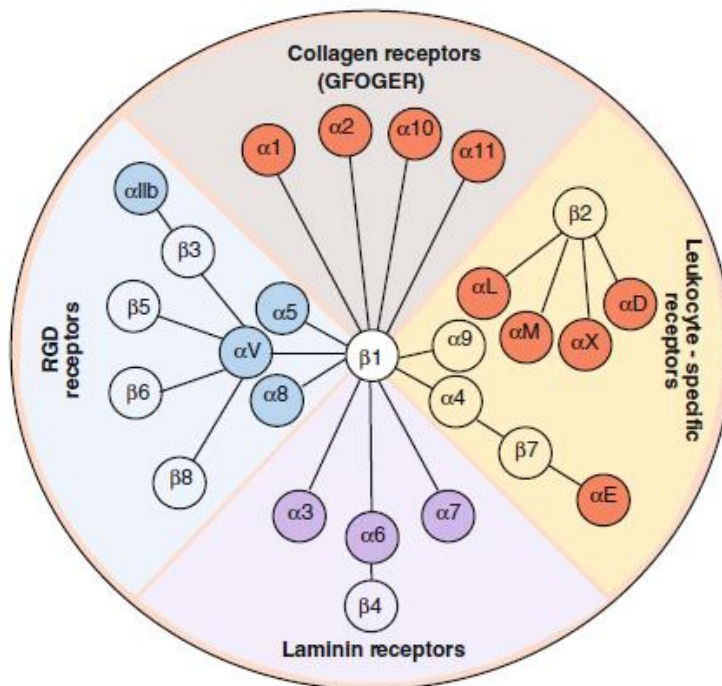


Figure 5. The Integrin receptor family.

Representation of the $\alpha\beta$ associations in mammals and their ligand specificity.

Modified from Barczyk et al (Barczyk et al., 2010)

2.4.2.3. FN activation

The assembly of FN into the fibrillar matrix (fibrillogenesis, Figure 5) is a cell-mediated process and it occurs when FN binds to integrins conducting to a conformational change that exposes FN-FN binding sites, and this association between FN molecules leads to the fibril formation (Mao & Schwarzbauer, 2005). Specifically, FN is secreted in a folded conformation unable to undergo fibril assembly. The first step implied the interaction with cell surface receptors,

normally the integrins $\alpha5\beta1$ or $\alpha v\beta1$, which recognize the cell-binding sequence, RGD, present within the 70-kDa N-terminal domain of FN (Figure 4) (To & Midwood, 2011). This first interaction occurs in the focal adhesion sites (2D models) where there is an accumulation of downstream signaling molecules like Paxillin, Focal adhesion Kinase (FAK), phosphotyrosines and integrins. Integrins, accumulated in focal adhesions, change to their active form increasing the affinity for FN and influencing the actin cytoskeleton. This results in a mechanical force due to cell contractility during migration. Ligated FN fibers to integrins in the focal adhesion sites are pulled from the edges of the cell to the cell center along actin stress fibers resulting in maturation to fibrillar adhesion. This mechanical force modifies FN structure from the folded conformation to the extended conformation and subsequently induces the exposure of FN-FN binding sites. Finally, FN molecules interact between each other and are incorporated into fibrils in the ECM (Mao & Schwarzbauer, 2005; To & Midwood, 2011; Wierzbicka-Patynowski & Schwarzbauer, 2003).

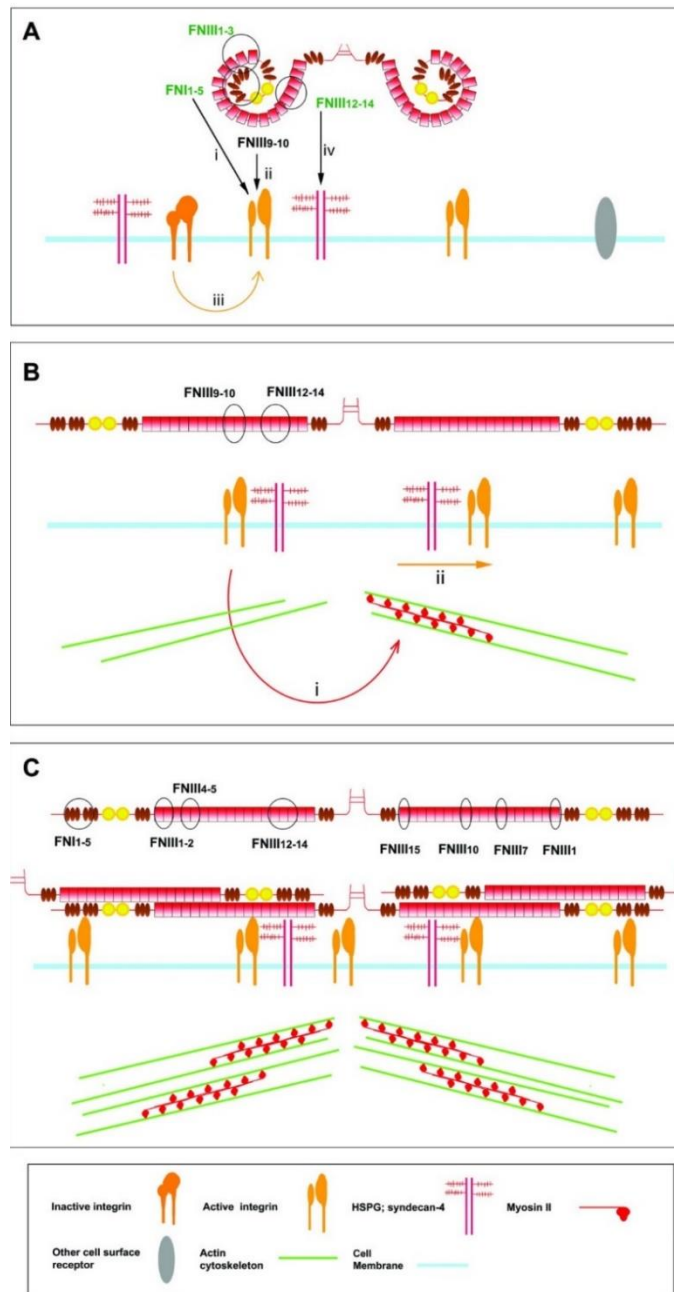


Figure 6. FN fibrillogenesis formation. (A) Folded FN binds to cell surface receptors, 70kDa FN domain binds to active integrins. (B) FN changes to an unfolding conformation, influences actin cytoskeleton and induces myosin-II dependent contractility. Integrins and other molecules are clustered in the site of adhesion. (C) Unfolded FN exposes FN-FN binding sites for intermolecular interactions resulting in the fibril assembly. (To & Midwood, 2011)

2.4.2.4. FN during PNS regeneration

After a peripheral nerve injury, FN fibrils increase at the injury site, supporting cellular adherence and promoting migration and proliferation of Schwann cells to favor axonal growth (Lefcort et al., 1992; Wakatsuki et al., 2014). After neurotmesis, FN is the main ECM component which fills the bridge space upon PNS regeneration (Cattin et al., 2015). An increment in FN is also observed in Schwann cell-basal lamina after injury (Lefcort et al., 1992). Different studies showed that the use of FN for coating synthetic tubes promotes Schwann cell migration and axon regrowth in similar levels that nerve grafts, however, functional recovery was still poor (Mottaghitlab et al., 2013; Whitworth et al., 1995). Furthermore in FN-depleted nerve graft, Schwann cells and fibroblasts migration is decreased and axon regrowth is impaired (Wang et al., 1992).

These evidences demonstrate the importance of the ECM and particularly FN for Schwann cell behavior and nerve repair. For this reason, it is necessary to acquire a deeper knowledge on how Schwann cells modulate their ECM production and the specific role of the ECM proteins during each step of PNS regeneration. In the case of FN, its regulation in Schwann cells remained unclear as well as whether Schwann cells can produce their own FN *in vivo* or if it is acquired from external sources and incorporated into the glial basal lamina. Addressing these questions are essential for a better understanding of the ECM dynamics during nerve repair and will provide new mechanisms that can be exploited to promote a better functional recovery in patients after nerve trauma.

2.5. Aim of the thesis

A proper understanding of the mechanism that regulates peripheral nerve regeneration is crucial to improve functional recovery. Functionality is given by the proper reinnervation of the original neuronal targets which mean first an accurate guidance of the axons during their elongation across the injured area and the distal stump, and second a correct recognition of the targets. As it was mentioned before, Schwann cells are major players in axon guidance thought

the Band of Büngner. These cells and their ECM present in the basal lamina guide the axons to reach their original targets. Regulation of Schwann cell ECM, and particularly FN, is not completely understood. In other models such as human cancer, FN is controlled by Sox2 to induce invasion and metastasis of ovarian tumor cells (Lou et al., 2013). Considering that Sox2 is an important modulator of the repair Schwann cell phenotype, an open question was if Sox2 can control ECM expression in Schwann cells to modify cell behavior.

The overall aim of this work was to unravel the role of Sox2 in Schwann cell behavior and its implication on Schwann cell ECM dynamics during the regeneration of peripheral neurons. The working hypothesis of this doctoral thesis was that Sox2 controls Schwann cells behavior through the modulation of ECM proteins. To test this hypothesis, the following objectives were proposed:

1. To develop an *in vitro* model system that allows to study the role of Sox2 expression in repair Schwann cells and its implications for neuronal regeneration.
2. To identify potential ECM-related genes and pathways downstream of Sox2 and involved in the repair Schwann cell phenotype.
3. To assess the impact of the genes and pathways, identified in Sox2 expressing Schwann cells, on growing axons.
4. To evaluate the relevance of Sox2-dependent Schwann cell behavior in human induced pluripotent stem cell (iPSC)-derived neurons.
5. To validate the findings *in vivo* during regeneration of the posterior lateral line in zebrafish and after sciatic nerve transection in adult rats.

3. Results

3.1. Sox2 overexpression modify Schwann cell behavior

3.1.1. Development of an *in vitro* model to study the role of Sox2 in Schwann cells

The Schwann cell line RSC96 was transduced with a plasmid encoding the Sox2 gene to induce the glial cells to a repair state (Figure 7A). This glial cell line is a spontaneously immortalized Schwann cell line derived from a long-term culture of primary rat Schwann cells and it has been widely used to study different aspects of the Schwann cell biology (Badache & De Vries, 1998; Chang et al., 2013; Ji et al., 2012). In culture, RSC96 Schwann cells (SC) grow as a monolayer and display contact inhibition of locomotion. Sox2 overexpression induced a change in SC behavior, from cell-cell repulsion to cell-cell adhesion and the formation of cellular aggregates (Figure 7B).

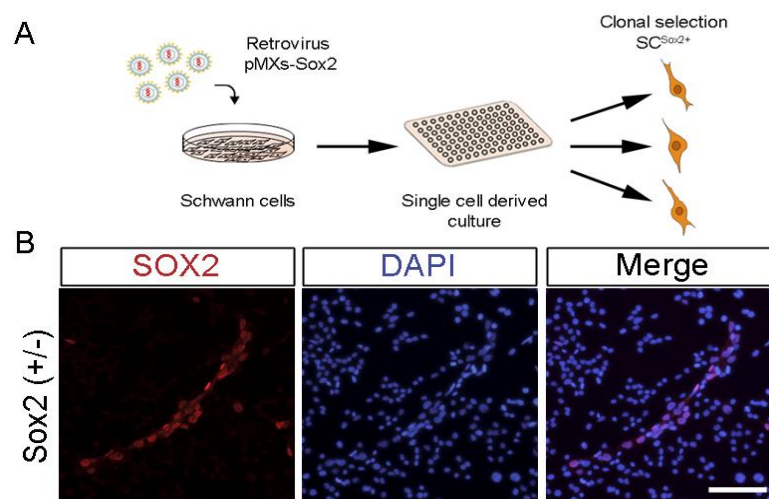


Figure 7. Creation of the Sox2-overexpressing Schwann cell line. A) Schematic representation of the protocol used to derive Sox2-positive clones from the rat Schwann cell line RSC96 transduced with Sox2 retrovirus. B) Immunofluorescence images of SOX2 (red) in the mixed population (Sox2(+/-)) of Schwann cells, nuclei were counterstained with DAPI (blue). Scale bar, 200 μm .

Sox2-positive Schwann cell clones (SC^{Sox2+}) were selected after a single cell derived culture (Figure 7A and 8A) and the overexpression of Sox2 was confirmed by Western Blot (Figure 8B). Interestingly, SC^{Sox2+} clones showed cell-cell adhesion and the formation of cellular channels (Figure 8A) as previously reported (Parrinello et al., 2010).

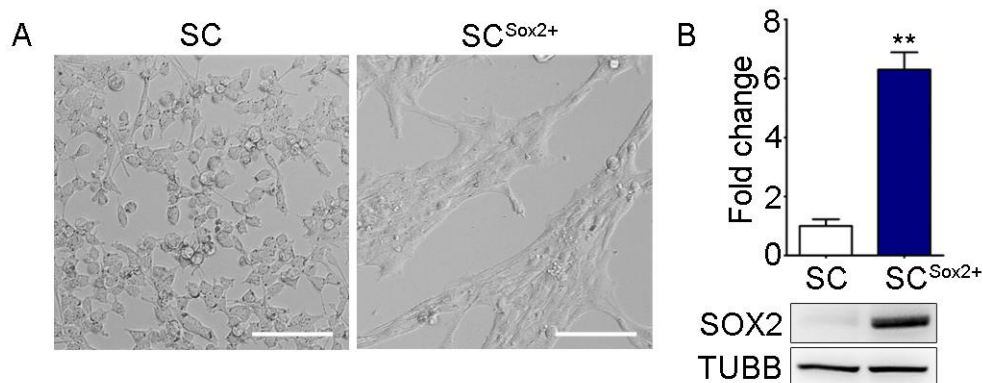


Figure 8. Sox2 overexpression changed Schwann cell phenotype. A) Phase contrast images of SC and one derived clone, SC^{Sox2+}, after Sox2 transduction. Scale bar, 100 μ m. B) Western Blot analysis of total Sox2 protein levels in the whole lysate of SC and SC^{Sox2+}. TUBB was used as a loading control (N=3). Graph shows mean value \pm s.e.m. Student's t-test, **p=0.0011.

3.1.2. Sox2 overexpression promotes the repair Schwann cell phenotype *in vitro*

Gene expression profiling of the distinct Schwann cell states during development and repair have been well characterized (K. R. Jessen & R. Mirsky, 2005; Kristján R Jessen et al., 2015). To characterize the SC stage after Sox2 overexpression, I analyzed different Schwann cell markers by semiquantitative RT-PCR (Figure 9). *c-Jun*, and key regulator of pro-regenerative Schwann cells during PNS regeneration (Arthur-Farraj et al., 2012), did not change after Sox2 overexpression. *Gap43* was up-regulated after Sox2 overexpression. The Glial fibrillary acidic protein encoded by the *Gafp* gene was up-regulated, this is a specific cytoskeleton constituent of Schwann cells and it is one regulator of cell proliferation specifically after nerve damage.

GFAP interacts with integrin $\alpha v\beta 8$ which induces glial cell mitosis (Triolo et al., 2006). Additionally, *Nestin* was significantly up-regulated in SC^{Sox2+}, this gene is normally expressed in myelinated Schwann cells but also upregulated in Schwann cells of degenerated nerves (Hockfield & McKay, 1985; Weiss et al., 2016). Regarding the transcription factors *Krox24* and *Krox20*, no differences in mRNA levels were found between SC and SC^{Sox2+}. However, *Krox24* expression in both cell types was higher than the one of *Krox20*, suggesting a non-myelinated and proliferative stage of the Schwann cells (Topilko et al., 1997). The expression of *S100 β* , a marker of immature Schwann cells and adult Schwann cells, remained at low levels after Sox2 expression, indicating that Schwann cells are not reverted to an immature state (Kristjan R Jessen & Rhona Mirsky, 2005; Ji et al., 2012). Finally *Sox10*, a key regulator of different stages of Schwann cell differentiation and an inducer of myelination (Bremer et al., 2011), was not detected in both populations (Figure 9), probably its expression was lost during the process of immortalization of the primary Schwann cells. In summary, this expression pattern in SC^{Sox2+} confirmed the undifferentiated stage in the *in vitro* model and the similarities with the repair Schwann cells phenotype observed *in vivo*.

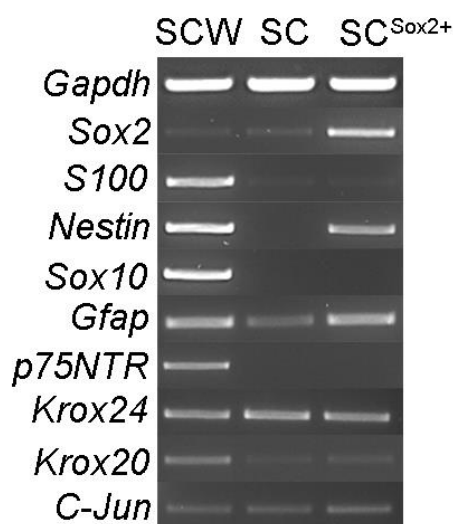


Figure 9. Sox2 transduction induced the expression of genes relates with nerve repair. Representative image of the semiquantitative RT-PCR analysis of Schwann cell markers in SC and SC^{Sox2+}, the Schwannoma cell line RT4D6P2T (SWC) was used as a positive control. *Gapdh* was used as a reference gene.

3.1.3. Schwann cells proliferation remains at the same levels after Sox2 overexpression

Sox2 have been widely implicated in the maintenance of stem cell renewal. Hence, I evaluated proliferation in the Schwann cells before and after Sox2 transduction, by immunofluorescence staining using the phospho-histone3 marker (Phospho-H3). After Sox2 overexpression, non-significant (n.s.) differences in the number of positive phopho-H3 cells were found between SC and SC^{Sox2+} (Figure 10A and 10B). This result showed that in the developed *in vitro* system Sox2 did not influence the proliferation of the Schwann cell line. However, RSC96 is an immortalized cell line highly proliferative which could cover any additional Sox2 effect on proliferation.

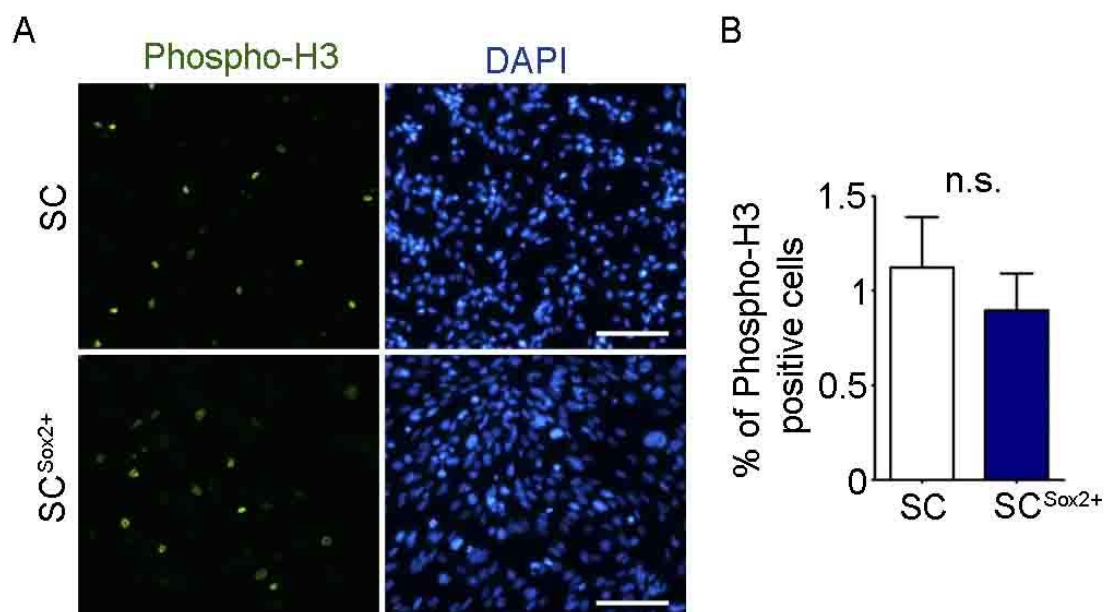


Figure 10. Proliferation did not change in Sox2-positive Schwann cells. A) Immunofluorescence staining and B) quantification of the mitosis marker Phospho-H3 (green) in SC and SC^{Sox2+}. Nuclei were counterstained with DAPI (blue). Scale bar, 100 μ m. Unpaired t-test with Welch's correction, non-significant, $p=0.5223$ (n.s.).

3.1.4. Sox2 induces Schwann cell organization and directional migration

A distinctive aspect of the repair Schwann cells is their capacity of collective migration and the formation of the band of Büngner after nerve damage. In order to study the effect of Sox2 on cell organization and migration, I evaluated the F-Actin bundles anisotropy and persistence of SC and SC^{Sox2+} as measurements of cell organization and directional migration respectively. Anisotropy was calculated in various areas (where several cells were located) of same size of the confocal images using the FibrilTool (ImageJ plug-in). Values close to one represented a perfect alignment of the filaments. SC resulted in a low actin filament anisotropy compared to SC^{Sox2+}, where a significant increase of actin filament alignment was observed, demonstrating that Sox2 overexpression increased Schwann cells organization (Figure 11A and 11B).

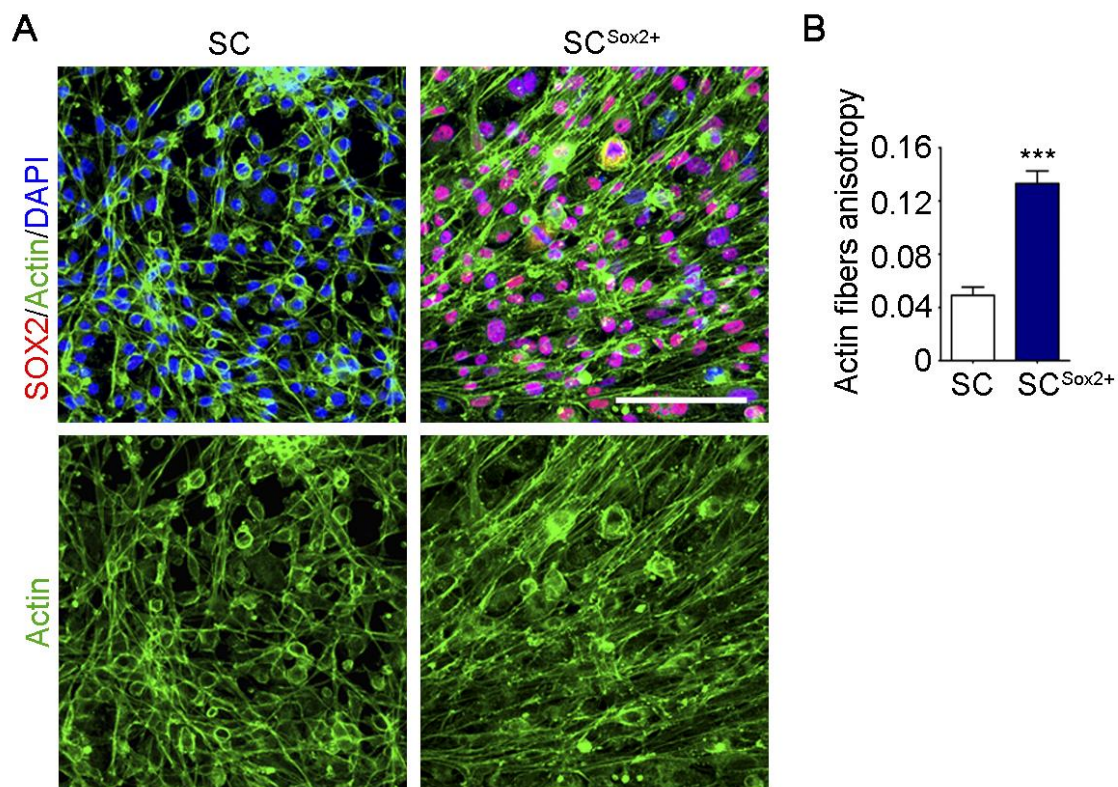


Figure 11. Sox2 expression increased Schwann cell organization *in vitro*. A) Representative immunostaining confocal images of SOX2 (green) and Actin fibers (red) of SC and SC^{Sox2+} in FBS-supplemented medium. Nuclei were counterstained with DAPI (blue). Scale bar, 100 μ m. B) Quantification of actin fiber anisotropy by F-actin staining of SC and SC^{Sox2+}. Graph shows mean value \pm s.e.m. Student's t-test, *** $p < 0.0001$. (N=3, $n \geq 16$ areas).

To better decipher the cell behavior leading to the Schwann cell alignment observed in fixed cells, time-lapse images of live cells were acquired every 25 minutes for a time period of 85 hours. Analysis of the images showed that SC move randomly and in a repulsive manner, whereas SC^{Sox2+} aggregate to form a continuous cellular flow with directionality (Figure 12A). To quantify the level of directionality, I tracked 10 cells during the last 42 hours. Persistence (a parameter to evaluate directionality) was calculated as the displacement divided by the total distance travelled by the cell. SC^{Sox2+} showed a significant increase in persistence with a 3-fold change compared to SC, demonstrating their higher capacity to maintain the direction of motion in contrast to the traveled distance, which was the same in both cell populations (Figure 12B and 12C).

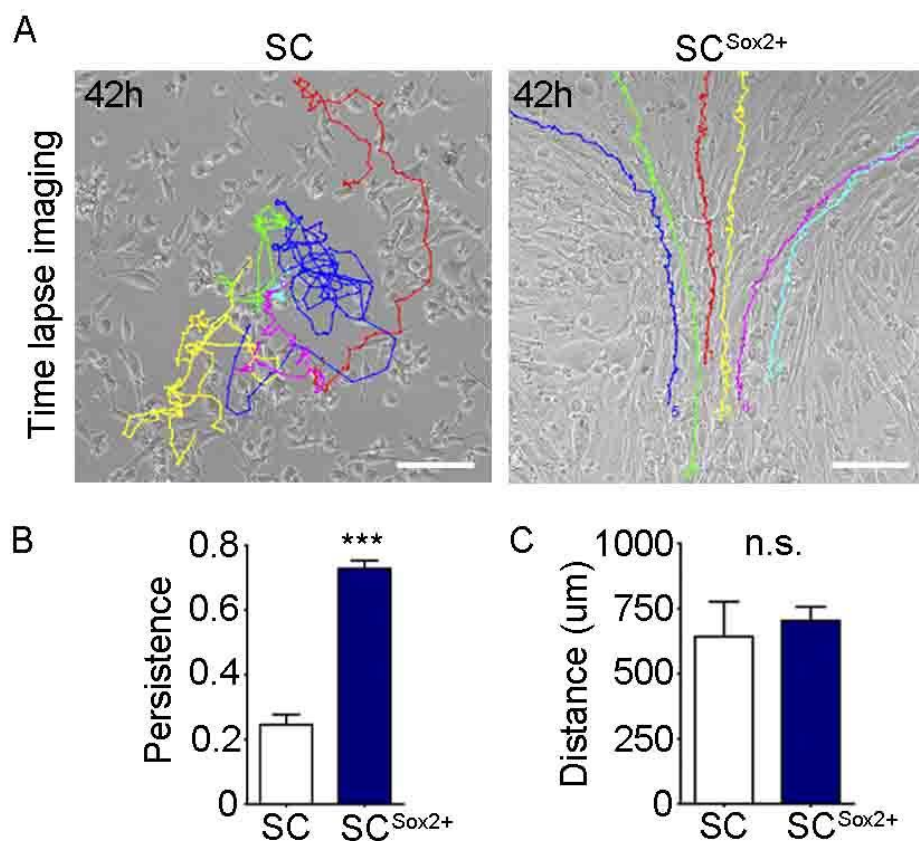


Figure 12. Sox2 induced persistent Schwann cell migration. A) Representative time-lapse images showing the cell tracking of SC and SC^{Sox2+}. Color lines show the single-cell tracks of the Schwann cells for 42 hours. Scale bar, 100 μ m. B) Quantification of persistence and traveled distance of SC and SC^{Sox2+}. (n=10 cells). Graph shows mean value \pm s.e.m. Unpaired t-test with Welch's correction, *** $p < 0.0001$ and $p = 0.6790$ (n.s.).

3.2. Identification of genes and pathways downstream of Sox2, important for Schwann cell behavior

Sox2 overexpression induced Schwann cell aggregation and orientation. To identify genes and pathways responsible of this phenotype, I took a broad expression profile approach using microarray data of total RNA extracted from clones expressing distinct levels of Sox2. The data analysis was performed in collaboration with Dr. Dietrich Trümbach, from the bioinformatic department of the Institute of Developmental Genetic at the Helmholtz Zentrum München.

3.2.1. ECM- and cell adhesion-related genes are significantly up-regulated in Sox2-positive Schwann cells

We created a hierarchical clustering represented with a heat map where we identified the top 10 up- and down- regulated ECM related genes in two Sox2-expressing clones (Figure 13). To identify differentially regulated processes that could be important for the Schwann cell phenotype observed after Sox2 expression, we derived six clusters and studied the subtrees of the row dendrogram with similar gene expression profiles as a result of the hierarchical clustering to biological function. We found that in cluster one, response to wounding was significantly up-regulated ($p=4,07e^{-06}$, FDR=0.0013) and the second biological process was the regulation of cell migration ($p=8,74e^{-05}$, FDR=0.013). Interestingly, in cluster two (which includes the biggest set of genes in the heat map) the most significant biological process was related to ECM organization ($p=7.27e^{-07}$, FDR=0.0007) and the second process was cell adhesion ($p=2,06e^{-06}$, FDR=0.0010) (Figure 13). In cluster three, relaxation of cardiac muscle was the first significant biological process ($p=2.67e^{-04}$, FDR=0.0343). In cluster four, the main significant process was sodium ion transmembrane transport ($p=3.35e^{-05}$, FDR=0.0296). In cluster five, cell surface receptor signaling pathway was the most significant biological process ($p=4.79e^{-05}$, FDR=0.0406) and finally in cluster six, no biological process could be identified as significant.

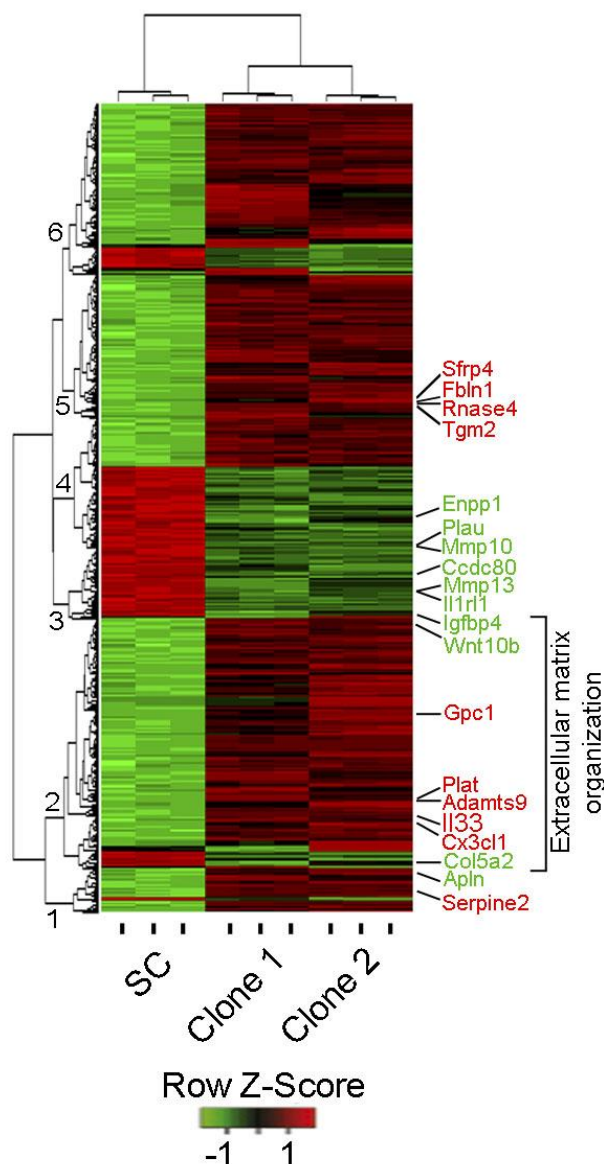


Figure 13. mRNA Expression profile across two clones and the control. Heat map of the normalized overlapping genes differentially expressed in two selected Sox2-positive Schwann cell clones (SC^{Sox2+}) compared to the wild-type (SC). The top significantly up- (in red) and downregulated (in green) ECM-related genes together with the main biological process from cluster two are highlighted.

Then, we constructed a Venn diagram with the genes significantly up- and down-regulated in the two Sox2-positive clones and found 692 common genes significantly regulated in the two Sox2-positive clones compared to wild type cells, 484 genes up-regulated and 208 genes down-regulated (Figure 14). We next performed enrichment analysis of the common genes significantly up-regulated identified in the Venn diagram in the two SC^{Sox2+} clones. We considered only the common genes in the study to avoid differences within the cell populations due to clonal selection or to the Sox2 expression level. The enrichment showed that, looking at gene ontology categories 'biological

processes' and 'cellular components', cell adhesion and cell migration as well as ECM components, were significantly overrepresented in the Sox2-positive clones (Figure 15A and 15B). Additionally, we identified the top up-regulated genes involved in cell adhesion and ECM from the common set of genes and validated them by semiquantitative RT-PCR (Figure 16A and 16B).

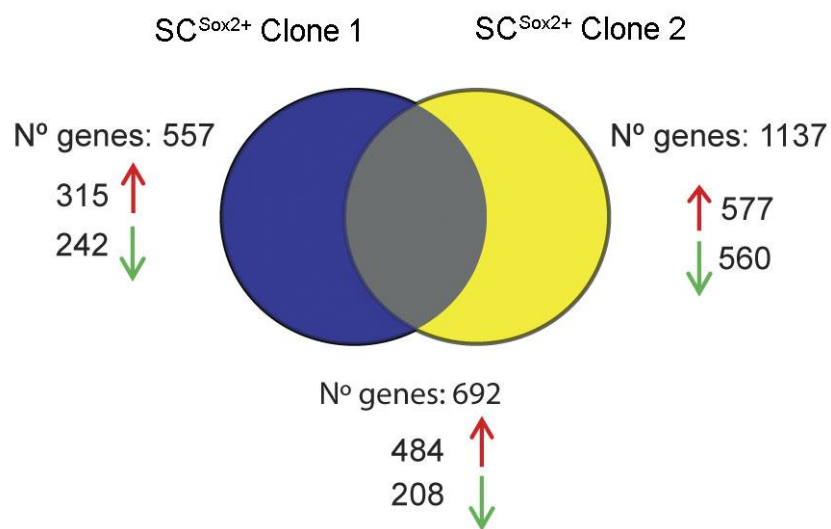


Figure 14. Venn diagram of significantly regulated genes in Sox2 clones. Probes with a p -adjusted < 0.002 and $2 < FC < -2$ were considered for the analysis. The higher expression of Sox2 was in clone 1.

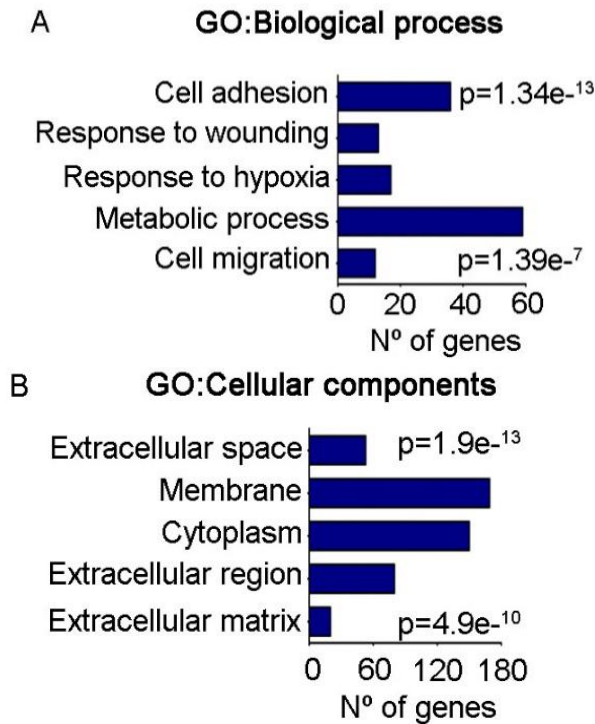


Figure 15. Gene ontology enrichment analysis for biological process and cellular components for the up-regulated overlapping genes in two clones of SC^{Sox2+}. Cell adhesion- and ECM-related genes were significantly overrepresented in the analysis.

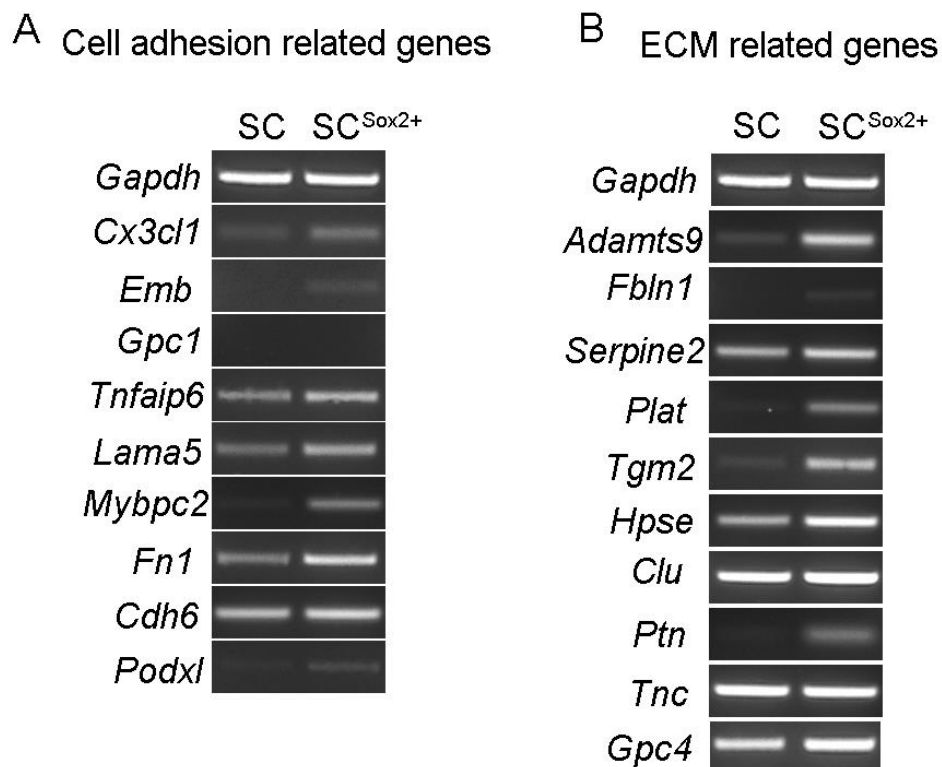


Figure 16. Top genes significantly up-regulated in both clones. A) and B) Validation of cell adhesion- and extracellular matrix-related genes significantly up-regulated in the microarray assay by semiquantitative RT-PCR in SC and SC^{Sox2+}.

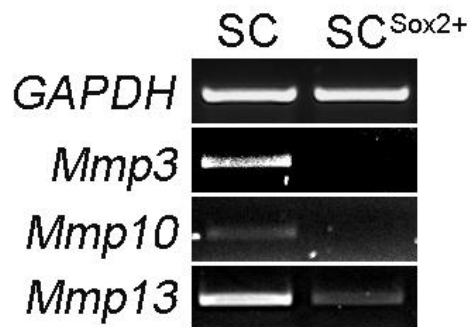


Figure 17. Significantly down-regulated matrix metalloproteases in Sox2-positive Schwann cells. Validation of matrix metalloproteases genes significantly down-regulated in the microarray assay by semiquantitative RT-PCR in SC and SC^{Sox2+}.

Finally, to identify key Sox2-regulated ECM genes in SC^{Sox2+} clones, we took the top 118 differentially expressed ECM genes related to cell adhesion and migration from the common set and created a literature-derived network based on sentence level co-citations. As shown in Figure 18, *Fn1* was identified as a highly interconnected gene which suggested that FN represents a putative key regulator within the network and a possible downstream effector of Sox2 to control and modulate Schwann cell adhesion and migration.

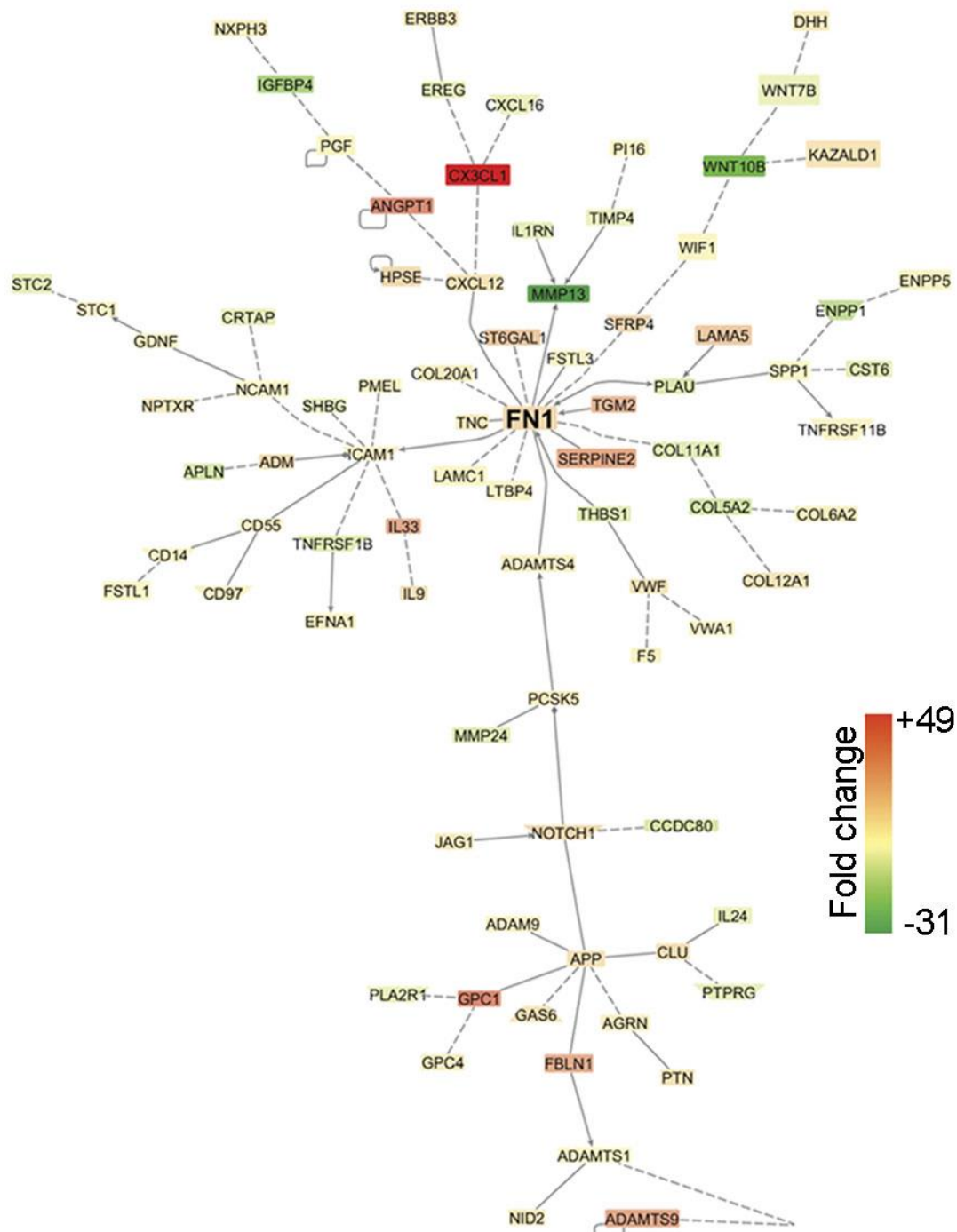


Figure 18. Literature-derived network of ECM related genes involved in cell adhesion and migration. *Fn1* was the highest interconnected gene within the network. Dashed line connects genes associated by experimental validation. Continued line connects genes associated by expert-curation (experts reviewing the original literature, data base version 2.6). Arrow line represents that gene A activates gene B. Line with a square and a vertical line at the end represents that gene A inhibits gene B.

3.2.2. Sox2 induces FN up-regulation and fibrillogenesis in Sox2-positive Schwann cells

From the microarray data analysis, FN was identified as a candidate gene regulated by Sox2 that could influence Schwann cell behavior. *Fn1* up-regulation in SC^{Sox+} was confirmed by semiquantitative RT-PCR, as shown in section 3.2.1, Figure 15A. To evaluate FN protein levels in SC^{Sox2+} and its implication for Schwann cell behavior, I first assessed FN levels in different culture media. Plasma FN is one component of the FBS which is used to supplement the medium, and cells can take soluble FN from this exogenous source and incorporate it into their ECM. To avoid external sources of FN, I compared the FN levels in the DMEM maintenance medium supplemented with 10% FBS (FBS DMEM) (i), with the same medium but supplemented with 10% FBS after the FN depletion protocol (FndFBS DMEM) (ii) and with KSR medium supplemented with 10% knock-out serum replacement (KSR DMEM) (iii). Lower levels of FN were confirmed by western blot in KSR medium (iii) compared to DMEM medium 10% FBS FN-depleted FBS protocol (ii), making the cell culture in KSR medium the best suitable conditions for the studies of FN dynamics (Figure 19).

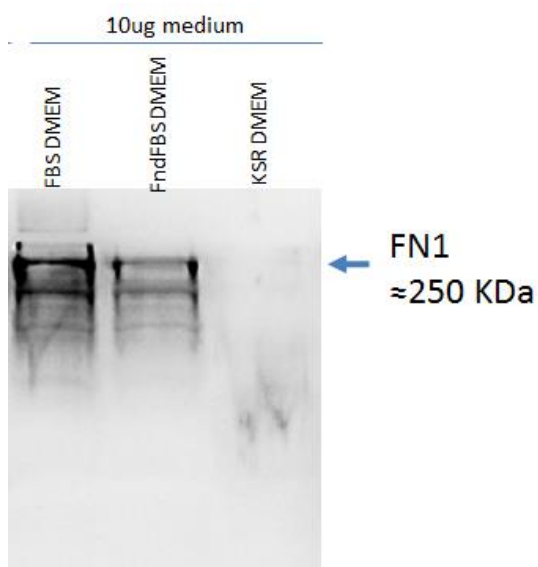


Figure 19. FN protein levels in the cell culture media. The first line corresponds to the DMEM maintenance medium (FBS DMEM), the second line to the DMEM maintenance medium supplemented with 10% FBS after FN depletion protocol (FndFBS DMEM) and the third line to KSR medium supplemented with 10% KSR serum replacement medium (KSR DMEM).

Once the best conditions were set for FN studies, I cultured the Schwann cells in KSR medium for 72 hours and evaluated FN protein levels by immunostaining, qPCR and Western Blot in SC and SC^{Sox2+}. As it was mentioned in the introduction, cellular FN can contain distinct spliced domain. Here I evaluated *Fn1* mRNA levels of the canonical form and the presence of the spliced domain EIIIA and EIIIB (only expressed in cellular FN) by qPCR. The results confirmed the up-regulation of *Fn1* but also the high expression of *Fn1* containing the spliced domains EIIIA and EIIIB upon Sox2 overexpression (Figure 20A). Quantification of protein levels in the whole lysate by Western Blot confirmed that FN was significantly up-regulated in SC^{Sox2+} compared to SC (Figure 20B). Confocal images showed that in SC^{Sox2+}, FN is localized at the edges and towards the cell center (Figure 20C, arrows), a characteristic of fibrillar adhesion, in contrary to SC, where FN was localized only at the cell edges, typical of nascent adhesions (Figure 20C, Head arrows).

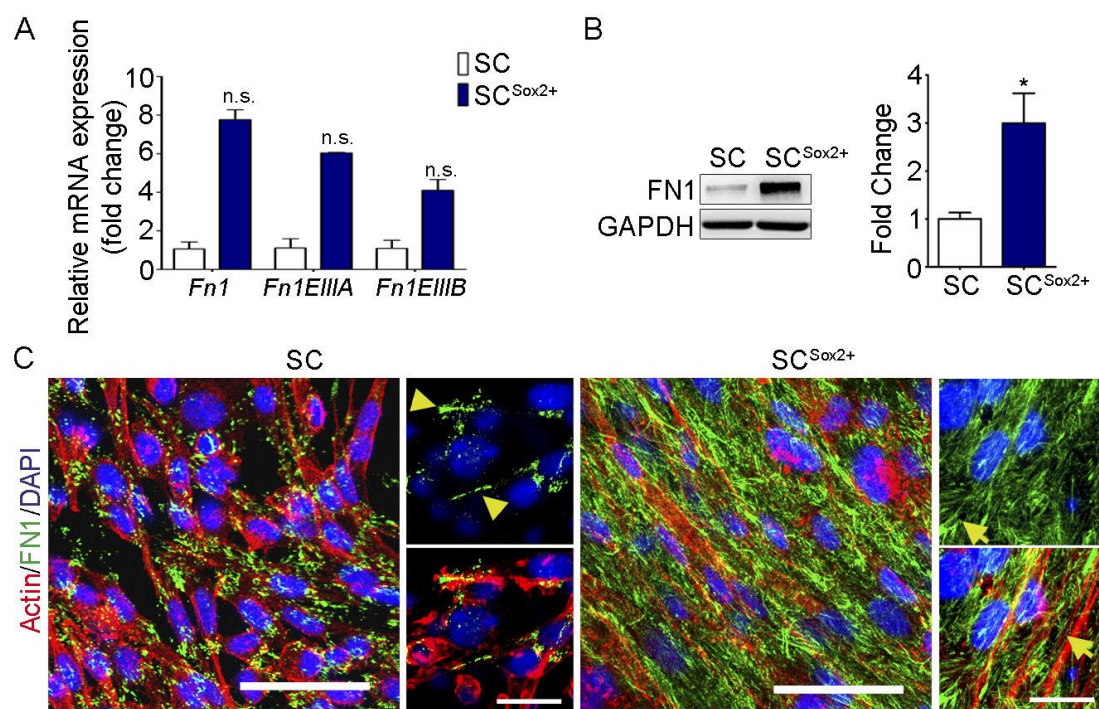


Figure 20. Sox2 induces FN fibrillogenesis in Schwann cells. A) Graph shows RT-qPCR measurements of *Fn1*, *Fn1* containing the spliced domain EIIIA and EIIIB in SC and SC^{Sox2+} after 3 days in culture. *Gapdh*, *Ankrd27* and *Rictor* were used as reference genes, values are relative expression to SC. (N=3) Graphs show mean value \pm s.e.m. Mann-Whitney test, n.s. B) Western

blot analysis and quantification of total FN1 protein in the whole lysate of SC and SC^{Sox2+}. GAPDH was used as a loading control. (N=4). Graphs show mean value \pm s.e.m. * $p < 0.05$. C) Representative confocal images of Actin fibers (red) and FN1 (green) immunostainings of SC and SC^{Sox2+} showing focal adhesion areas in SC (arrow head) compare to fibrillar adhesion in SC^{Sox2+} in FN-free medium (arrows). Nuclei were counterstained with DAPI (blue). Scale bars, 50 μ m and 25 μ m (amplified pictures).

To confirm the expression of the main FN receptors in Schwann cells, integrins $\alpha 5\beta 1$ and $\alpha v\beta 1$, I evaluated the gene expression of each subunit by semiquantitative RT-PCR (Figure 21). Non-significant differences were found between SC and SC^{Sox2+}. Additionally, I also evaluated the expression of the subunits $\beta 8$ and $\beta 3$ that were reported to be important for Schwann cell migration (Milner et al., 1997). I found the subunit $\beta 8$ significantly up-regulated in SC^{Sox2+} but no expression of the subunit $\beta 3$ in either of the cell lines. The rat schwannoma cell line (SCW) was used as a positive control for $\beta 3$ expression (Figure 21). Further studies at the protein levels are required to evaluate the possible combination of integrin subunits and their activation state.

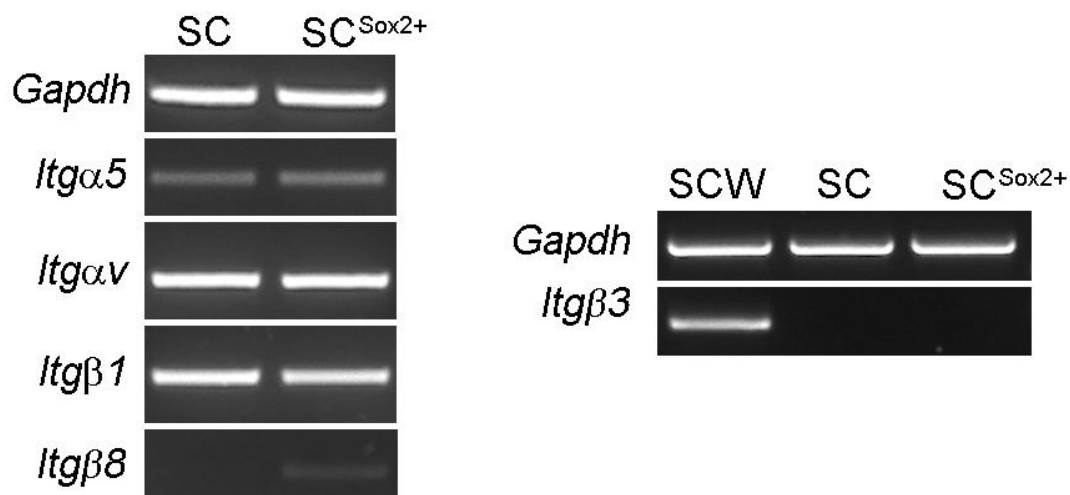


Figure 21. Evaluation of mRNA expression of integrins in Schwann cells. Semiquantitative RT-PCR of mRNA expression levels of integrins in SC and SC^{Sox2+}. *Gapdh* was used as a reference gene. SCW cell line was used as a positive control for primer amplification.

3.2.3. FN fibrillogenesis is present in Sox2-positive primary rat Schwann cells

In order to study if primary Schwann cells also co-expressed Sox2 and FN, I extracted primary rat Schwann cells and fibroblasts from adult sciatic nerves and cultured them for 20 days according to the protocol described by Kaewkhaw et al, (R. Kaewkhaw et al., 2012) but with normal DMEM medium to maintain the fibroblasts population. Schwann cells were kept with primary fibroblasts from sciatic nerves to induce Sox2 expression as was previously shown by Parrinello et al. (Parrinello et al., 2010). As shown in Figure 22, and similar to previous studies, fibroblasts and Schwann cells did not intermingle and Sox2-positive Schwann cells formed groups of cells where co-expression of Sox2 and FN fibrillogenesis was identified by immunostaining. These results suggested that Sox2 could induce FN fibrillogenesis in primary Schwann cells. However, in the mentioned co-culture condition, both the fibroblasts and the medium are exogenous sources of FN that could also influence and induce the process of fibrillogenesis in Schwann cells.

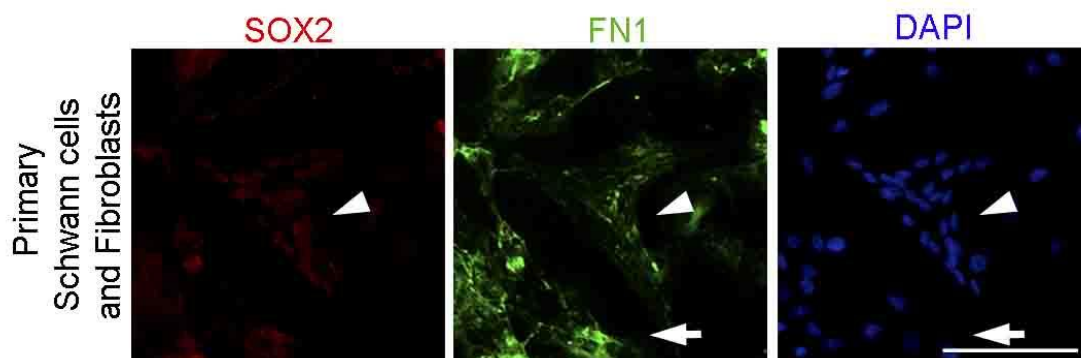


Figure 22. Sox2 and FN expression in primary rat Schwann cells from adult sciatic nerves. Representative immunofluorescence images of FN1 (green) and SOX2 (red) of primary co-culture of Schwann cells and fibroblast extracted from adult rat sciatic nerves and cultured for 20 days. Nuclei were counterstained with DAPI (blue). Scale bar, 100 μ m.

3.2.4. Cell-Matrix adhesions are modified upon Sox2 overexpression

The formation of cell-matrix adhesions is a dynamic process that changes from nascent adhesion, focal adhesion to fibrillar adhesion. Focal adhesion is characterized by an increased in the expression of proteins like FAK and Paxillin and their phosphorylation state. In contrast, fibrillar adhesion has reduced levels of FAK and Paxillin. These proteins are important components of the integrin-regulated signaling pathway downstream of FN and differentially recruited in the adhesion structures (Berrier & Yamada, 2007). To study the capacity of Schwann cells to form focal and fibrillar adhesions upon Sox2 expression, I evaluated by immunostaining and Western Blot the localization and the protein levels of Paxillin and FAK, and their phosphorylation state, in SC and SC^{Sox2+}, in the developed *in vitro* system using FN-depleted medium conditions.

The analysis of protein expression by immunostaining showed that in SC, phosphoPaxillin (pPaxillin) and Paxillin are located in the peripheral region of the cell forming structures similar to nascent adhesions, contrary to SC^{Sox2+}, where these proteins formed larger structures typical of focal adhesion (Figure 23A and 23B). The differences between SC and SC^{Sox2+} regarding the type of structures formed by Paxillin and pPaxillin, were quantified by high content analysis of the confocal images. This was done in collaboration with Dr. Kamyar Hadian and Dr. Jara Brenke from the Assay Development and Screening Platform at the Helmholtz Zentrum München. We evaluated two parameters, the width and the length of the structures and represented them as the ratio width to length. This was used as a measurement of the type of structure. Values close to one represented a circular shape (nascent adhesions) and close to zero represented an elongated form (focal adhesion). SC^{Sox2+} showed a significant increase in the formation of focal adhesion structures compared to SC (Figure 23C-23F). However, FN fibrillogenesis was also observed in SC^{Sox2+} (Figure 20C) suggesting an increase or transition from focal to fibrillar adhesion after Sox2 overexpression.

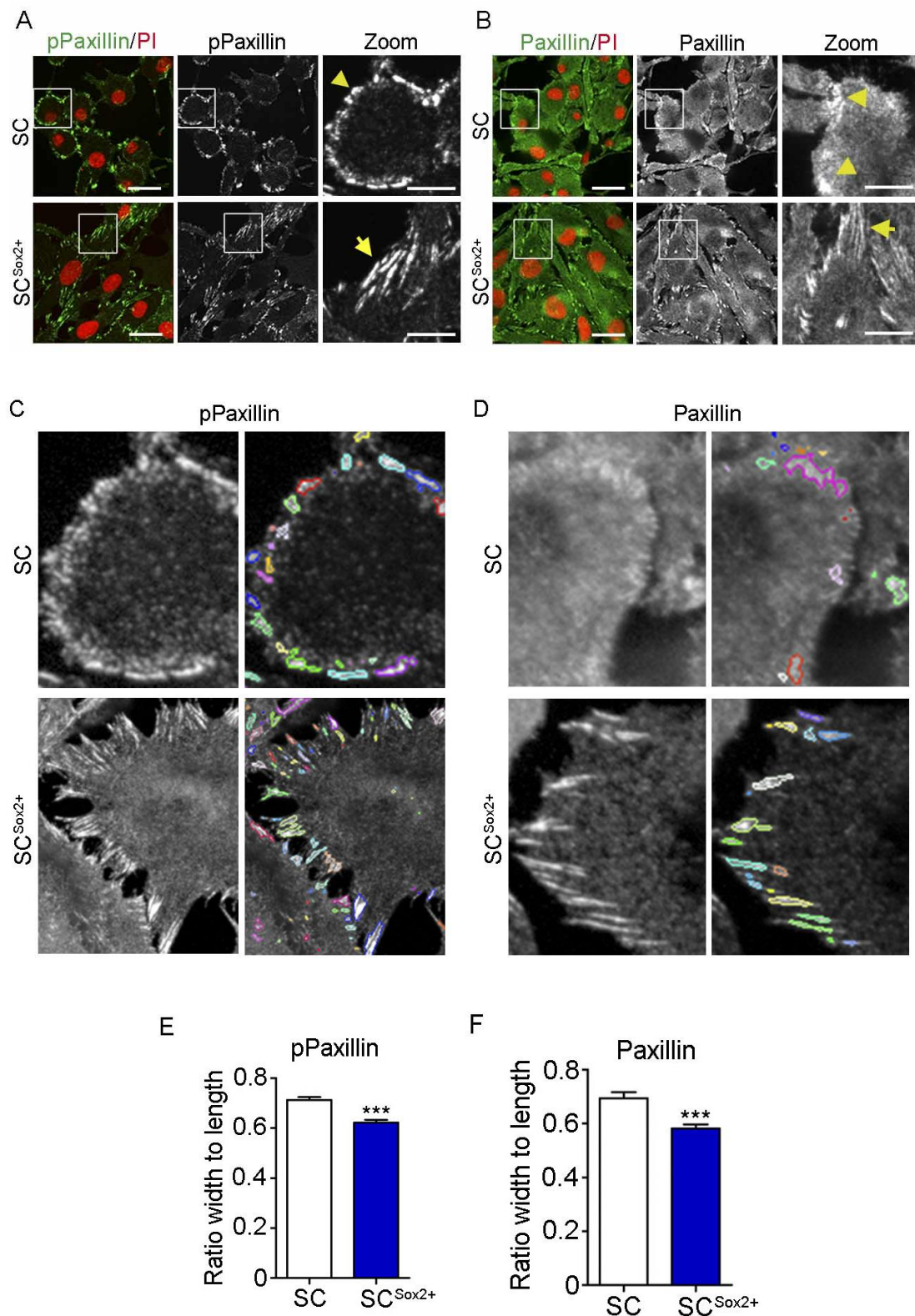


Figure 23. Sox2 overexpression induces a transition from focal complexes to focal adhesions. A) and B) Representative confocal images of pPaxillin (Tyr 118, green) and total Paxillin (green) immunostainings of SC and SC^{Sox2+}. Arrow heads show nascent adhesions in SC and arrows show fibrillar adhesions in SC^{Sox2+}. Nuclei were counterstained with Propidium Iodide, PI (red). Scale bars,

25 μm and 10 μm (zoom). C) and D) Representative images of the shape analysis performed for pPaxillin and Paxillin staining in SC and SC^{Sox2+} E) and F) Graphs showing the quantification of pPaxillin and Paxillin staining pattern from the shape analysis. The ratio width to length is presented as the mean of different picture areas \pm s.e.m. pPaxillin was analyzed using a Student's t-test *** $p < 0.0001$ and Paxillin using a Unpaired t-test with Welch's correction *** $p = 0.0010$.

Furthermore, pFAK showed a similar staining pattern compared to pPaxillin and Paxillin. In SC, pFAK was localized only in the periphery of the cells, meanwhile in SC^{Sox2+} was localized in the periphery and toward the cell center (Figure 24A). This reinforced the evidences of an increase in the formation of focal adhesions structures in SC^{Sox2+}. FAK immunostaining showed only round structures in the periphery of both cell type, SC and SC^{Sox2+} (Figure 24B).

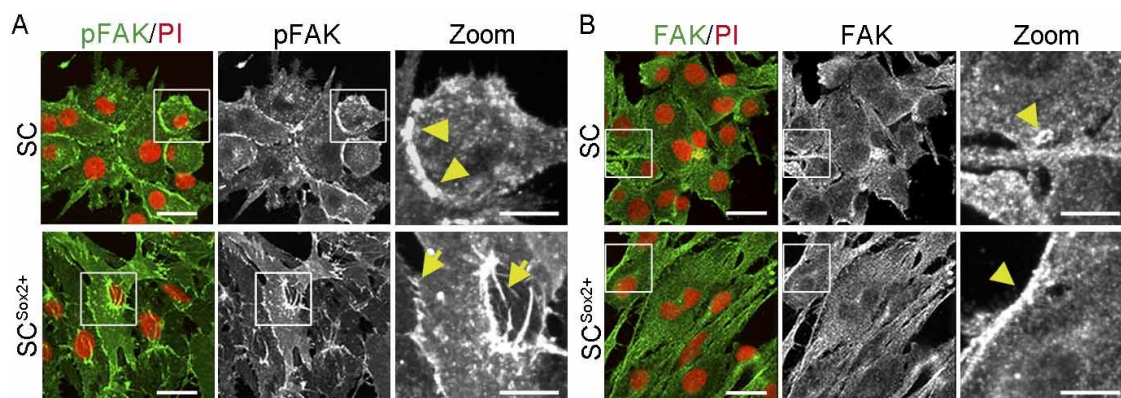


Figure 24. Focal adhesion is increased in SC^{Sox2+}. A) Representative confocal images of pFAK (Tyr 397, green) and B) total FAK (green) immunostainings of SC and SC^{Sox2+}. Nascent adhesions are indicated by arrow heads and focal adhesion by arrows. Nuclei were counterstained with Pridium Iodide, PI (red). Scale bar, 25 μm .

Additionally, I evaluated by Western Blot the total protein levels of Paxillin, FAK and their phosphorylation state in SC and SC^{Sox2+}. Although nonsignificant differences were found between both cell types, there was a tendency that in SC^{Sox2+}, pPaxillin and Paxillin expression were decreased compared to their expression in SC (Figure 25A). The proportion of pFAK and

FAK showed lower levels in SC^{Sox2+} compared to SC (Figure 25B), suggesting a transition to fibrillar adhesions. According to previous studies, pPaxillin recruits FAK into the adhesion sites (Zaidel-Bar et al., 2007). In SC^{Sox2+} the ratio pPaxillin:Paxillin was higher in comparison to SC, which could lead to an increase in total FAK levels, potentially explaining the slight increase in total FAK levels observed in SC^{Sox+} (Figure 25A and 25B). These results suggested that Sox2 overexpression induced the formation of focal adhesion and the maturation into fibrillary adhesion structures.

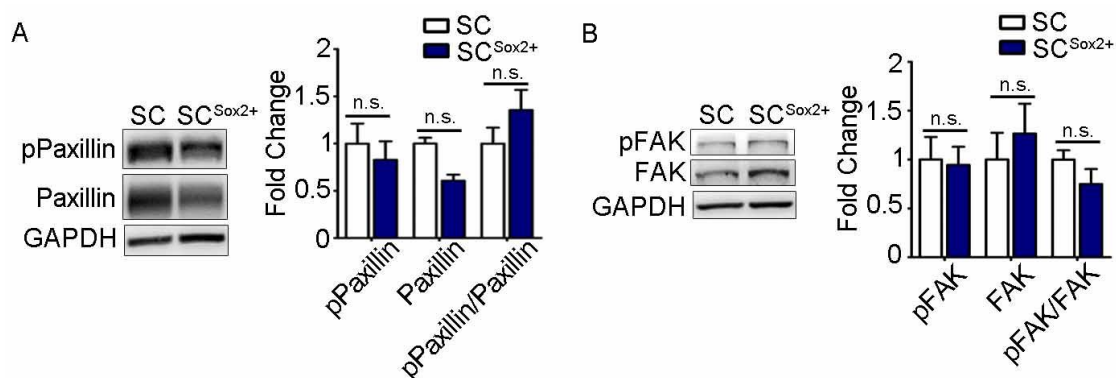


Figure 25. Sox2 induced the transition from nascent adhesion to focal adhesion. A) Western blot analysis and quantification of pPaxillin and total Paxillin protein levels by western blot in the whole lysate of SC and SC^{Sox2+}. B) Western blot analysis and quantifications of pFAK and total FAK protein levels in the whole lysate of SC and SC^{Sox2+}. GAPDH was used as a loading control. (N=3) Graphs show mean value \pm s.e.m. Mann-Whitney test pPaxillin p=0.4 (n.s.), Paxillin p=0.1 (n.s.), pPaxillin/Paxillin p=0.4 (n.s.), pFAK p=1 (n.s.), FAK p=1 (n.s.), pFAK/FAK p=0.4 (n.s.).

3.2.5. Sox2 directly controls FN expression in Schwann cells

After confirming that Sox2 induced the up-regulation of FN, the next question was if Sox2 could directly control FN expression in Schwann cells. *In silico* promoter analysis of the rat *Fn1* promoter region displayed several potential binding regions in the rat *Fn1* promoter that can be recognized by the SOXB family, V\$SORY (Figure 26A and 26B). Specifically, two Sox2 binding sites and one Sox3 binding site were identified. However, considering the high

level of similarity between the core sequences (Capital letters, Figure 26B), it is possible that Sox2 also recognizes the Sox3 binding site region.

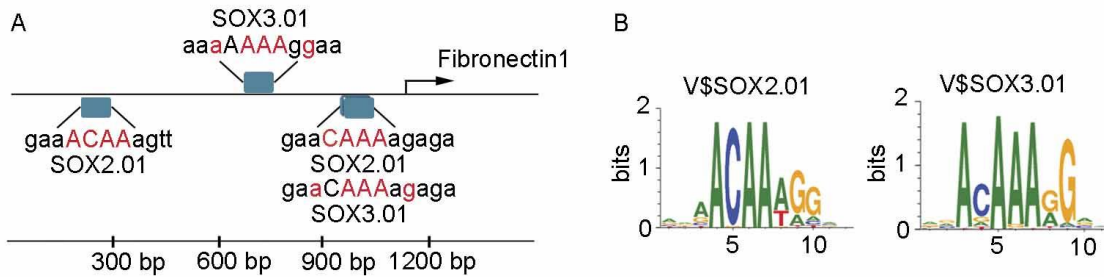


Figure 26. Potential binding sites of Sox2 in the *Fn1* rat promoter. A) *In silico* promoter analysis of V\$SORY family binding sites within the promoter sequences of the rat *Fn1* gene. bp mark in red appear in a position where the matrix exhibits a high conservation profile, while capital letters denote the core sequence. B) Representation of Sox2 and Sox3 binding sites, showing the similarity between the sequences recognized by the two transcription factors.

To validate the *in silico* results, I performed a Chromatin Immunoprecipitation (ChIP) of Sox2 and evaluated the promoter region of *Fn1* (P1 and P2, Figure 23A) together with a non-relevant region about 2000 bp upstream of the transcription starting site (TSS), as a negative control (P3, Figure 27A). The ChIP results showed that Sox2 binds to the promoter region of the rat *Fn1* gene. However, since the size of the amplicon was about 300 bp and the chromatin size after sonication between 100 and 1000 bp, it was not possible, by semiquantitative RT-PCR, to decipher if there was a preference for one of the Sox binding sites (Figure 27B).

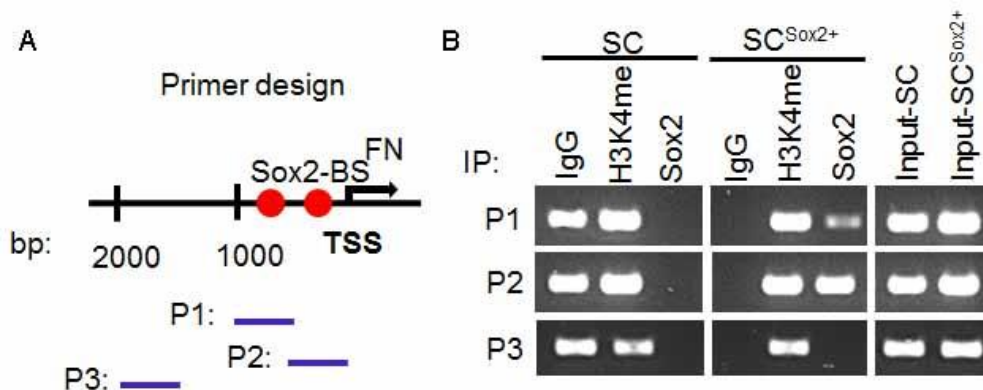


Figure 27. Sox2 bound to the rat *Fn1* promoter. A) Schematic representation of the primer design to amplify the Sox2 binding regions and a non-relevant region 200 bp upstream the TSS. B) ChIP analysis of Sox2 binding site in the rat *Fn1* proximal promoter, H3K4me and IgG were used as positive and negative IP controls respectively.

In collaboration with Dr. Trümbach, we evaluated the relevance and conservation of the Sox2 binding sites in the *Fn1* promoter region of various species. We found that the binding site located -200 nucleotides upstream of TSS in the rat *Fn1* promoter was conserved across 8 of 9 species including humans (Figure 28), in which the potential Sox2 binding site was located -225 nucleotides upstream of the TSS. *E. caballus* (Horse) was the only species in the study that did not show the conserved binding site. These results also suggested that Sox2 could have preference for the binding site close to the TSS, however, more details studies are needed to confirm this hypothesis.

alignment position		501.....	511.....	521.....	531.....	541.....
GXP_106290(FN1/human) (FN1)	374	GCGGGCCATC	AGCATCTCTT	TTGTTGCGCT	GCGAACCCACA	GT---CCCCC
GXP_1045519(FN1/rhesus_monkey) (FN1)	403	GCGGGCCATC	AGCATCTCTT	TTGTTGCGCT	GCGAACCCACA	GT---CCCCC
GXP_5899143(FN1/chimp) (FN1)	401	GCGGGCCATC	AGCATCTCTT	TTGTTGCGCT	GCGAACCCACA	GT---CCCCC
GXP_223655(FN1/mouse) (FN1)	394	GCGGGAGATC	AGCATCTCTT	TTGTTGCGGG	GCGAACCCACC	GT---ACCCC
GXP_241420(FN1/rat) (FN1)	394	GCGGGAGATC	AGCATCTCTT	TTGTTGCGGG	GCGAACCCACC	GT---ACCCC
GXP_1651307(FN1/horse) (FN1)	162	GCGGGCGATC	AGCATCTCTT	TTGATCGCGG	GCGAACCCACA	GT---CCCCC
GXP_3882392(FN1/cow) (FN1)	389	GCGGGCGATC	AGCATCTCTT	TTGTTCAAGG	GCGAACCCACA	GT---TCCCC
GXP_3541955(FN1/pig) (FN1)	408	GCGGGCGATC	AGCATCTCTT	TTGTTGCGCT	GCGAACCCACA	GT---CCTCC
GXP_951696(FN1/opossum) (FN1)	296	GCCCGCGATC	AGCATCTCTT	TTGTTAGCGG	Cc c g g c a c a g c c t t c C T C C	

Figure 28. Sox2 binding site in the *Fn1* promoter is conserved across species. *In silico* promoter analysis of the V\$SORY family showed a binding site in *Fn1* promoter which was conserved in different mammalian species. Matrix Family Library Version 9.3 (March 2015). Rat TSS located in the alignment position 744.

Finally, to test the functionality of the Sox2 binding site in Schwann cells, I evaluated the regulatory activity of Sox2 on FN in SC and SC^{Sox2+}. I used the expression of the Lucia luciferase synthetic gene as a reporter assay of the human FN promoter which only contains one Sox2 binding site, identified by *in silico* promoter analysis. The reporter plasmid pDRIVE5Lucia-hFibronectin (hFn1), contains a fragment of 786 bp corresponding to the human *Fn1*

promoter. Sox2 binding site in the reporter plasmid was analyzed *in silico* to identify the binding region. Using a site directed mutagenesis protocol, the core-sequence was modified to avoid the possible binding of Sox2 (hFn1_mut) (Figure 29A). Comparisons were done between the same cell lines to avoid differences regarding the transfection efficiency. Lucia luciferase activity induced by Sox2 was significantly increased in SC^{Sox2+} compared to the control plasmid (without the promoter, Figure 29B). In SC, an increase in the activity of the reporter was observed but it was not significant when it was compared to the control plasmid (Figure 29B) showing the low expression of FN in SC. Then, using the hFn1_mut plasmid, I confirmed that the Lucia luciferase signal observed was through the direct regulation of Sox2. SC^{Sox2+} showed a significant reduction of the reporter expression to below the basal levels and a similar trend was observed in SC, where the activity of the reporter was decreased to similar values as the control. These results suggested that the low expression levels of FN expression in SC is also due to the binding of Sox2 to the FN promoter. The mouse NIH/3T3 fibroblast line was used as a control of the assay. This cell line has high levels of FN expression but no expression of Sox2. As expected, a significant increase in the Lucia luciferase signal was observed, but no differences after the mutation of the Sox2 binding site (Figure 29B). These results confirmed that Sox2 acts as a strong transcriptional activator of FN expression and fibrillogenesis in Schwann cells.

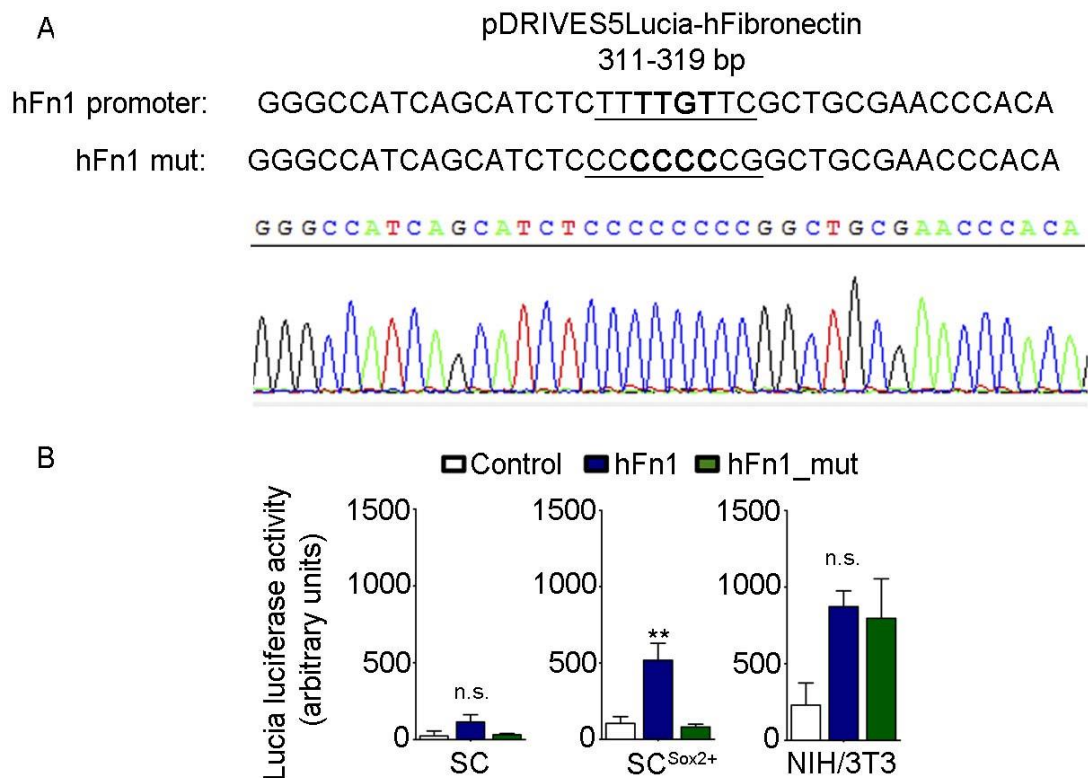


Figure 29. Sox2 directly controlled FN expression in Schwann cells. A) Site-directed mutagenesis of Sox2 binding site of the human FN promoter located in the reporter plasmid pDRIVE5Lucia-hFibronectin for the Lucia luciferase reporter assay. Image shows the substitution of 8 bp of the Sox2 binding sequence (hFn1_mut). B) Reporter assay showing Lucia luciferase activity 48h post transient transfection of SC and SC^{Sox2+} with the pDRIVE5Lucia-hFibronectin plasmid containing the human *Fn1* promoter region (hFn1), the human *Fn1* promoter with a mutation in the Sox2 binding site (hFn1_mut) and the control plasmid without the *Fn1* promoter region (control). (N=5). Graphs show mean value \pm s.e.m. SC samples were analyzed with the Kruskal-Wallis test, $p=0.0534$ (n.s.), SC^{Sox2+} samples were analyzed with ANOVA ** $p=0.0008$, SC samples were analyzed with the Kruskal-Wallis test, $p=0.0581$ (n.s.).

3.3. FN is important for Schwann cell organization and directional migration

The results suggested that FN could play a major role in Schwann cell behavior. Previous studies showed that *in vivo* FN is present in Schwann cells basal lamina and up-regulated during nerve repair. In order to decipher the

specific role of FN in repair Schwann cells, I knocked-out (KO) FN from the SC^{Sox2+} using the CRISPR/Cas9 technology and evaluated Schwann cell behavior.

3.3.1. Generation of the *Fn1* knock-out rat Schwann cell line using CRISPR/Cas9 genome-editing system

A sgRNA sequence was designed to target the intron between exons 13 and 14, a region present in all FN spliced variants (Figure 30A). FN KO clones of SC^{Sox2+} were selected from a single cell-derived culture and FN expression was verified by qPCR, Western blot and immunostaining (Figure 30B-D). One clone was sequenced in order to confirm the genomic deletion of the targeted sequence. The first sequence analysis showed the presence of two different deletions in the alleles of the gene. To confirm this, a primer set positioned at both sides of the intended breakpoints was designed and the PCR product was used for subcloning and sequence analysis. 10 bacterial colonies were analyzed by sequencing and the results showed two distinct PCR products corresponding to the mutant alleles. The sequence analysis confirmed that the deletion in allele 1 occurred in between the expected cleavage site of Cas9, 3 bp upstream of the PAM sequence and deleting 16 bp. In allele 2, the deletion was bigger with a total of 40 bp including the PAM sequence (Figure 30E). Taken together, using the CRISPR/Cas9 genome-editing system, a frame shift was created in the *Fn1* gene resulting in a FN KO Sox2-positive Schwann cell line, SC^{Sox2+/Fn1-/-}.

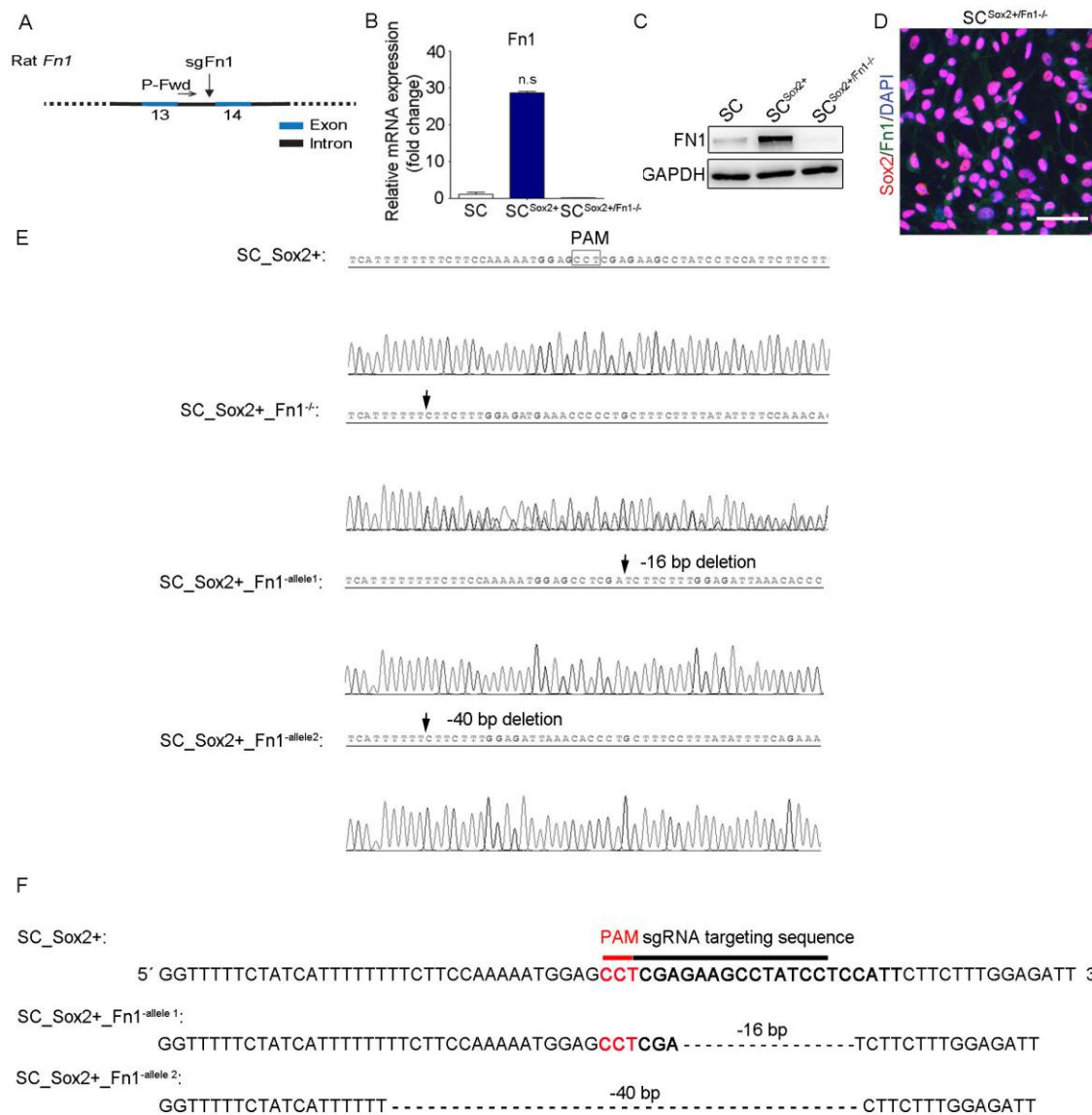


Figure 30. Generation of a FN KO cell line from the SC^{Sox2+} using the CRISPR/Cas9 system. Related to Figure 3. A) sgRNA design (sgFn1) to induce a frame shift in the rat *Fn1* gene. sgFn1 targets between exons 13 and 14 of *Fn1*. P-Fwd represents the primer used for sequencing. B) Graph shows RT-qPCR measurements of *Fn1* mRNA levels from SC and SC^{Sox2+} *in vitro* after 3 days in culture. *Gapdh*, *Ankrd27* and *Rictor* were used as reference genes, values are relative expression to SC. (N=3) Graphs show mean value \pm s.e.m. Mann-Whitney test, n.s. C) Western Blot analysis of FN1 protein levels in the whole lysate of SC, SC^{Sox2+} and SC^{Sox2+/Fn1-/-}. GAPDH was used as a loading control. D) Representative confocal image of FN1 (green) and Sox2 (red) immunostaining of one *Fn1* KO clone (SC^{Sox2+/Fn1-/-}). Nuclei were counterstained with DAPI (blue). Scale bar, 100 μ m. E) Sequence analysis of cloned PCR products of the *Fn1* gene from the SC^{Sox2+/Fn1-/-} cells, indicating the deletion of 16 bp and 40 bp within the sgRNA target region in each of the two alleles of the KO clone.

3.3.2. FN fibrillogenesis induces Schwann cell aggregation and organization

FN expression is important for cell adhesion and migration. To confirm its implications in repair Schwann cells, I first evaluated cell organization through the anisotropy of the actin fibers. 72 hours post seeding, F-Actin was labelled and analyzed in SC, SC^{Sox2+} and FN knock-out line SC^{Sox2+/Fn1-/-} together with the immunostaining of Sox2 and FN. The results showed that after 3 days in culture, FN ablation in SC^{Sox2+} led to a loss of Schwann cells organization as seen in Figure 31A. Confocal images showed that SC^{Sox2+/Fn1-/-} are disorganized in a similar way to SC (Figure 31A). To evaluate if the cells aligned along FN fibers, I measured different areas of the confocal images and calculated the angle of orientations of actin fibers together with FN fibers, using the fibrilltool plug-in for ImageJ. A correlation analysis of the direction of both types of fibers showed that Schwann cells were oriented along the FN fibrils (Figure 31B and 31C). Looking at the anisotropy of FN fibers, I found that organization of the FN matrix is significantly increased in SC^{Sox2+} compared to SC. Actin bundles anisotropy was also significantly higher in SC^{Sox2+} compared to SC^{Sox2+/Fn1-/-}, where anisotropy of Actin was completely lost reaching values similar to SC (Figure 31D and 31E). These results demonstrated the importance of FN fibrillogenesis in Schwann cell alignment.

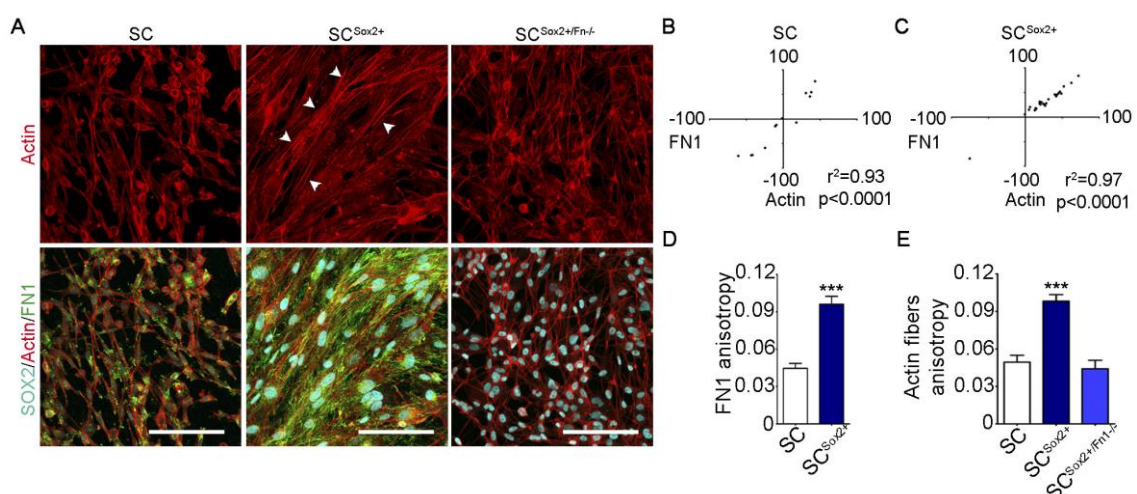


Figure 31. Sox2-induced FN fibrillogenesis is responsible for Schwann cell organization. A) Representative confocal images of SOX2 (cyan), Actin fibers (red) and FN1 (green) immunostainings of SC, SC^{Sox2+} and SC^{Sox2+/Fn1-/-}.

Arrow heads show the organization of the actin fibers in the SC^{Sox2+} cells. Scale bar, 100 μ m. B) and C) Correlation of FN1 fiber angles with the orientation of actin fibers of SC, SC^{Sox2+} and SC^{Sox2/Fn1-/-}. D) and E) Quantification of FN1 anisotropy of SC and SC^{Sox2+} and actin fibers of SC, SC^{Sox2+} and SC^{Sox2/Fn1-/-}. Graphs show the mean \pm s.e.m. FN1 anisotropy was analyzed using a Unpaired t-test with Welch's correction *** $p < 0.0001$. Actin fibers anisotropy was analyzed using ANOVA *** $p < 0.0001$.

Additionally, FN expression also influenced Schwann cell adhesion to the culture dish. When Schwann cells were cultured in gelatin with KSR medium, the adherence capacity of SC and SC^{Sox2+/Fn1-/-} were lower compared to SC^{Sox2+} and a similar behavior was observed in laminin-coated dishes when Laminin was used at concentrations lower than 2 μ g/ml. These results suggested that high levels of FN were also necessary for Schwann cell adhesion *in vitro* (Figure 32).

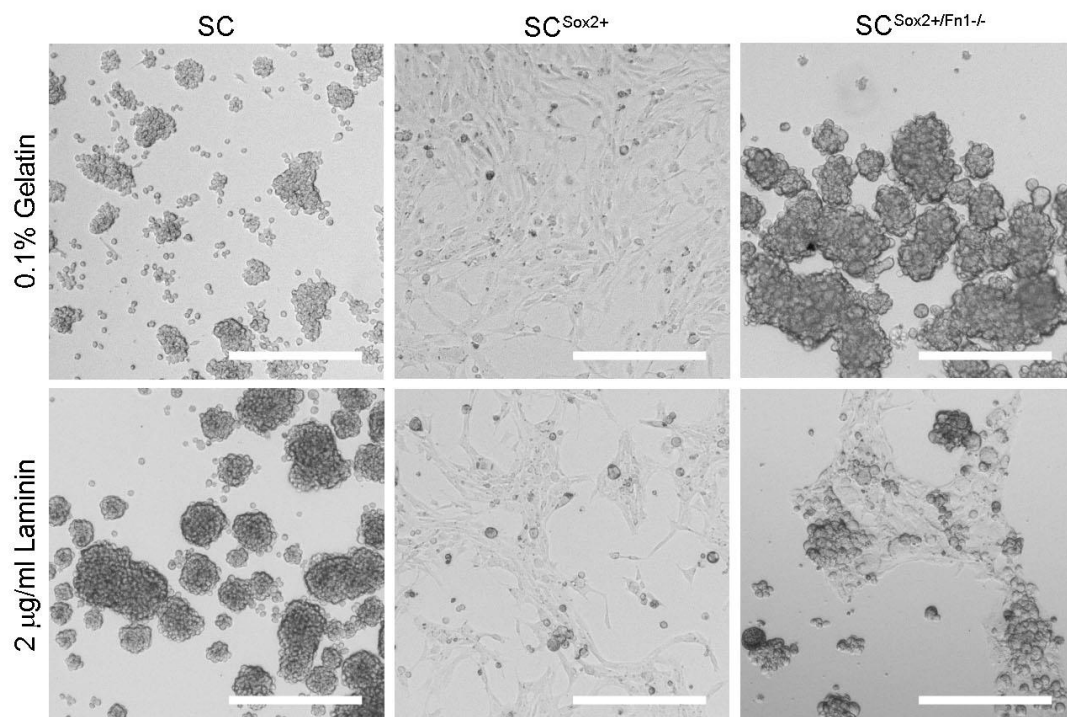


Figure 32. Adhesion to the substrate is dependent on the expression of FN by Schwann cells. Phase contrast images of SC, SC^{Sox2+} and SC^{Sox2+/Fn1-/-} cultured with different coating conditions. Low FN expression in SC or no expression in SC^{Sox2+/Fn1-/-} impairs Schwann cell adhesion. Scale bar, 250 μ m.

3.3.3. Directional migration of Schwann cells is dependent of FN expression

To better visualize and understand cellular organization, I performed time-lapse imaging of SC^{Sox2+/Fn1-/-}, SC^{Sox2+} and SC over 3 days. Live imaging showed that Schwann cells with low FN (SC) or no Fn1 (SC^{Sox2+/Fn1-/-}) exhibit random movement in contrast to SC^{Sox2+} which aggregated and migrated collectively (Figure 33A). To quantify the persistence of migration, I tracked 10 cells from each condition for a time period of 42 hours. Persistence and distance analysis showed that the capacity to maintain the direction of motion was lost upon FN knockout independently of the distance travelled which was increased in this condition (Figure 33B and 33C). These results demonstrated that Sox2-dependent FN expression is required for Schwann cells directional migration *in vitro*.

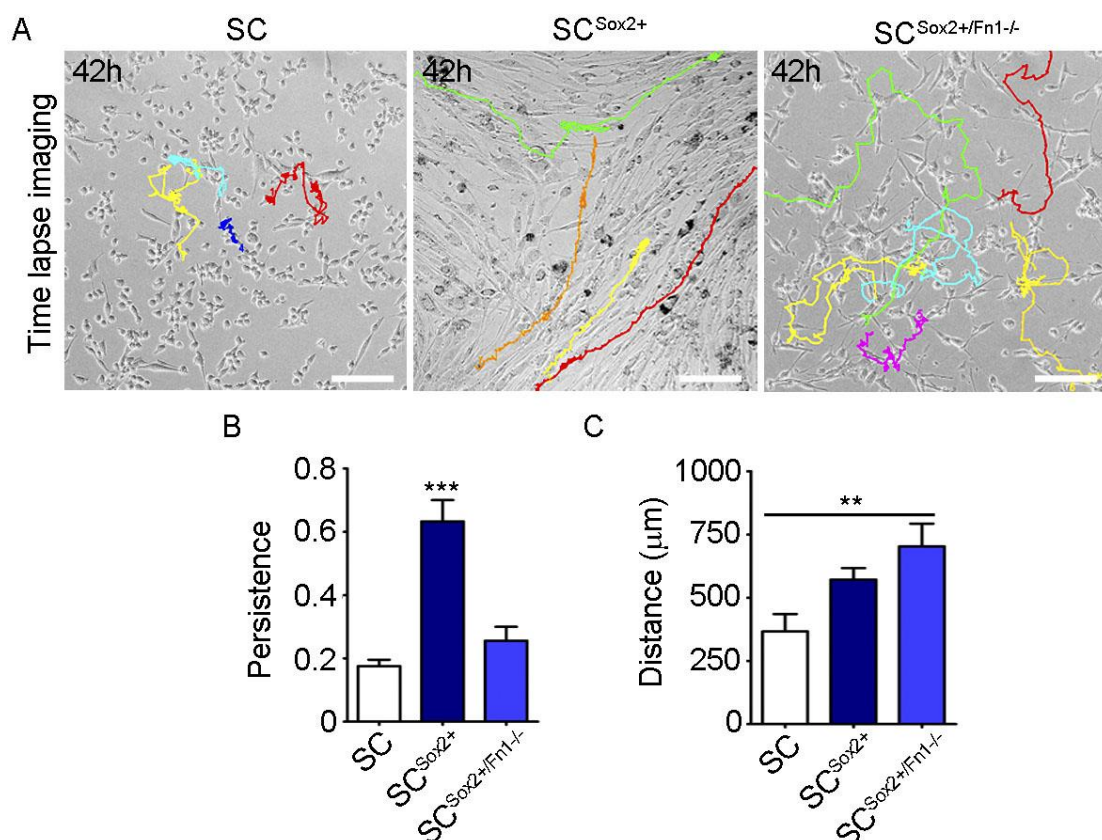


Figure 33. FN fibrillogenesis is important for persistent Schwann cell migration. A) Representative time-lapse images showing the cell tracking of SC, SC^{Sox2+} and SC^{Sox2+/Fn1-/-} respectively in KSR medium (FN-free). Color lines

show the single-cell tracks of the Schwann cells for 42 hours. Scale bar, 100 μm . B) and C) Quantification of the distance and persistence of SC, SC^{Sox2+} and SC^{Sox2/Fn1-/-} migration in KSR medium. (n=10 cells). Graphs show the mean \pm s.e.m. ANOVA **p=0.0081, ***p<0.0001.

3.3.4. Schwann cell-cell adhesion is independent of FN expression

In Schwann cells 2D cultures, Sox2 mediates cell clustering via the formation of N-Cadherin junctions, controlled by ephrin-B/EphB2 signaling (Parrinello et al., 2010). Cadherin-mediated cell-cell adhesion is a general mechanism by which multicellular structures form during morphogenesis and regeneration, acting in coordination with integrin-mediated cell-ECM adhesion (Lefort et al., 2011). To address the question whether FN loss influences N-Cadherin mediated Schwann cell-cell adhesion, I evaluated the protein expression levels of N-Cadherin in SC, SC^{Sox2+} and SC^{Sox2+/Fn1-/-} by immunostaining. I confirmed that N-cadherin is localized at the membrane of SC^{Sox2+} and SC^{Sox2+/Fn1-/-} in cell-cell junctions, independent of FN expression (Figure 34). However, there was an increase in the formation of N-Cadherin adherent junctions in SC^{Sox2+}, suggesting that FN fibrillogenesis facilitates the formation of adherent contacts between Schwann cells during their migration (Figure 34). These results suggested that N-Cadherin expression is important for cell-cell adhesion as it was previously reported but not for the organization of Schwann cells which is, according to our results, dependent on FN.

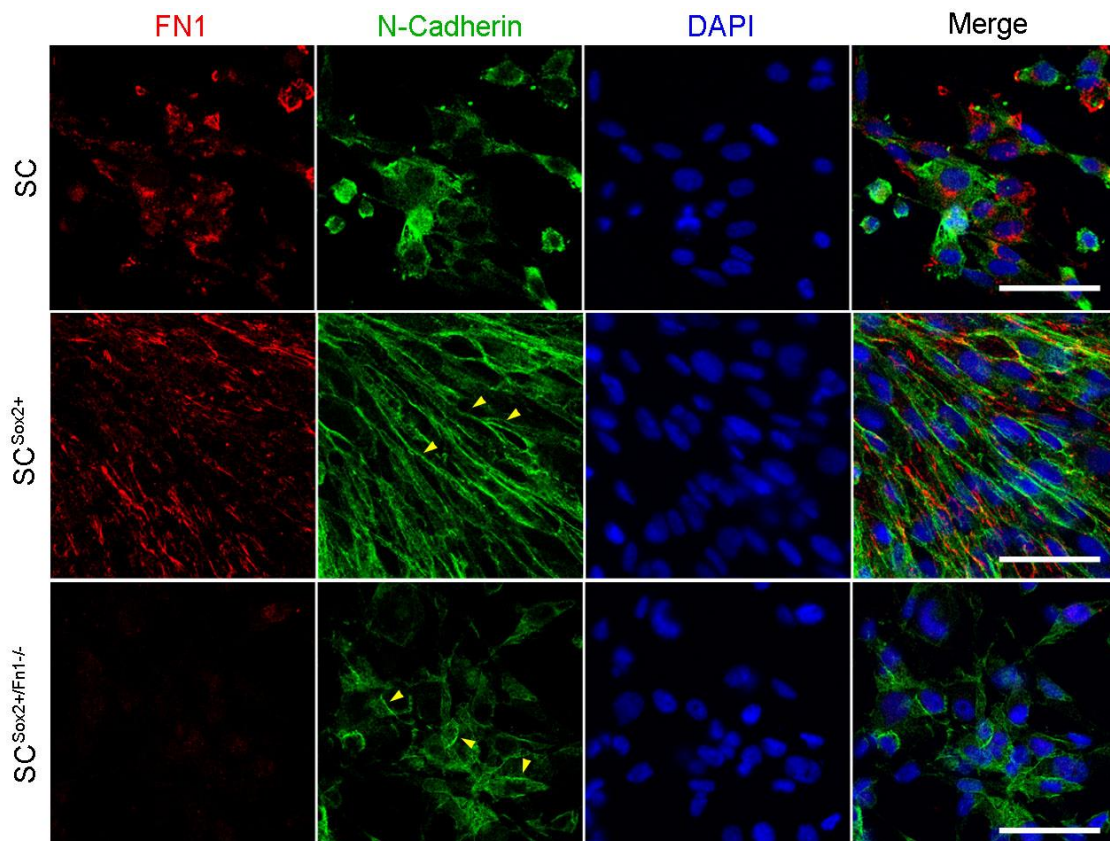


Figure 34. N-Cadherin expression in Schwann cells. Representative confocal images of FN1 (red) and N-cadherin (green) in SC, SC^{Sox2+} and SC^{Sox2/Fn1-/-} in KSR medium (FN-free). Nuclei were counterstained with DAPI (blue). Arrow heads show the localization of N-Cadherin in cell-cell adherent junctions. Scale bar, 50 μ m.

3.4. FN-dependent Schwann cell organization is necessary for axon guidance

After nerve injury, the regeneration process depends on the capacity of axons to regrow in an organized way to facilitate an accurate reinnervation of the original target. Bands of Büngner made of Schwann cells are key players in this process. In order to test whether FN fibrillogenesis-dependent Schwann cell aggregation and directional migration might be responsible for directing organized axon guidance, I established co-culture systems of neurons on the Schwann cell lines: SC, SC^{Sox2+} and SC^{Sox2+/Fn1-/-} (Figure 35A). The glial cells were cultured first as a monolayer on which neurons were co-culture for 48

hours. All the different conditions were analyzed for axons anisotropy as a measurement of guided growth

3.4.1. Axons from dorsal root ganglion neurons follow Schwann cell orientation

The first co-culture system studied was between dissociated neurons from adult mouse dorsal root ganglion (DRG) (neurons from the sensory system) and the Schwann cell lines: SC, SC^{Sox2+} and SC^{Sox2+/Fn1-/-} (Figure 35A). This particular type of neurons when in culture, do not form dendrites, they only generate axons. Interestingly by immunostaining of FN and one pan-neuronal marker (β3-Tubulin, TUBB3), I observed that axonal processes follow the orientation of the SC^{Sox2+}, but they were not oriented when plated on SC or SC^{Sox2+/Fn1-/-} (Figure 35B). When FN fibers angles and the orientation of axons were analyzed using the TUBB3 staining, I found a significant correlation of the angles between FN and axons only in the presence of SC^{Sox2+} and not when neurons were cultured with SC (Figure 35C and 35D). Suggesting that axons aligned along Schwann cells and FN fibers orientation. To confirm this observation, I analyzed the anisotropy of FN fibers and axons in the different co-culture conditions. The anisotropy values of SC^{Sox2+} were again significantly higher compared to SC (Figure 35E), and the axonal anisotropy showed that neurons are able to regrow in an organized way (axons parallel to one another) only when they are co-cultured with SC^{Sox2+} (Figure 35F). Axonal anisotropy values of SC^{Sox2+/Fn1-/-} were similar to the condition when neurons are co-cultured with SC. These data suggested that FN-dependent Schwann cell alignment, controlled by Sox2, is necessary for axon guidance.

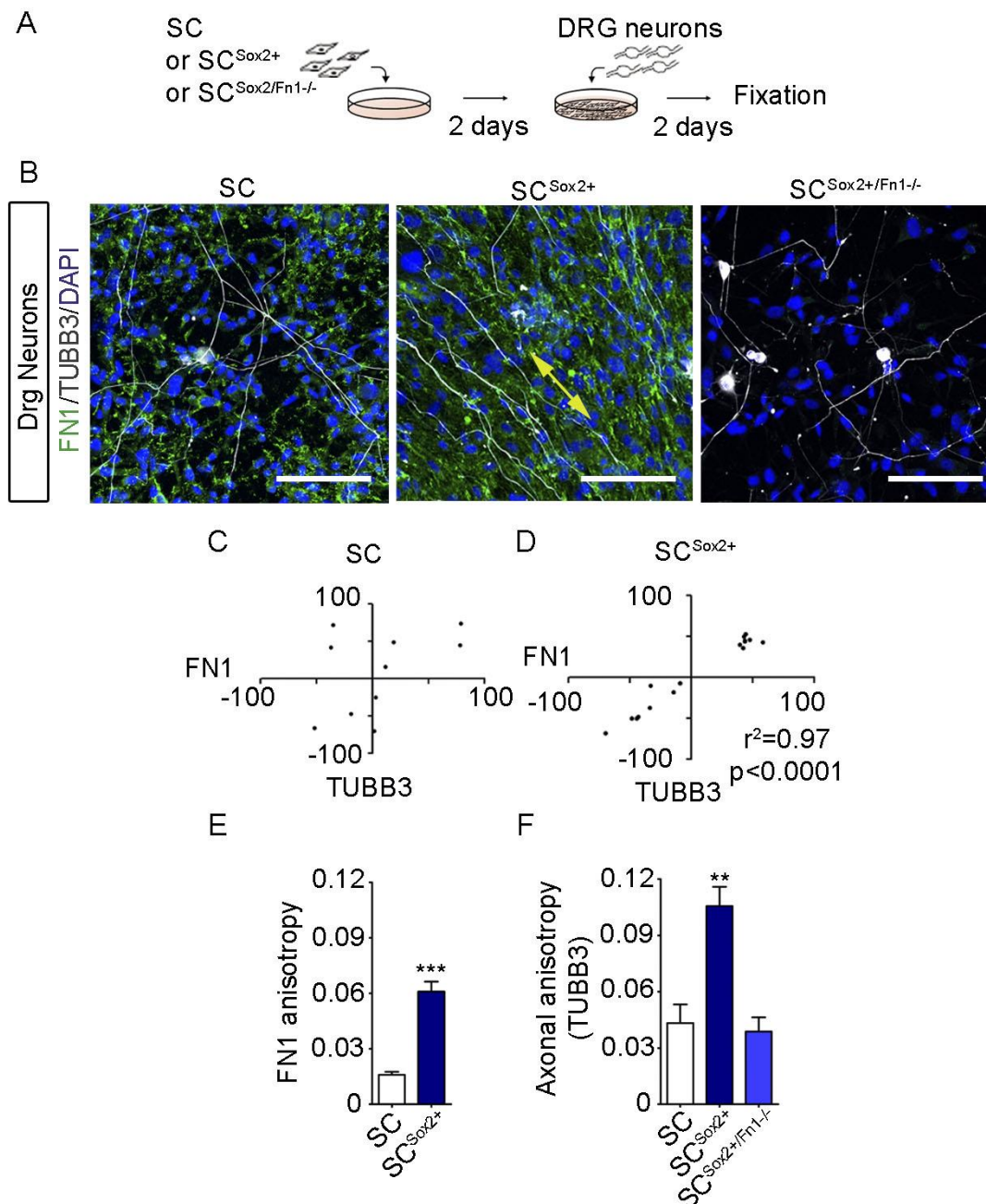


Figure 35. Axons of DRG neurons follow FN-dependent self-organized Schwann cells. A) Experimental design of co-culture between Schwann cells (SC, SC^{Sox2+} or SC^{Sox2+/Fn1-/-}) and primary DRG neurons derived from adult mice. B) Representative confocal images of FN1 (green) and TUBB3 (white) immunostainings of DRG neurons co-cultured with SC, SC^{Sox2+} or SC^{Sox2+/Fn1-/-}. Nuclei were counterstained with DAPI (blue). Double head arrow shows the alignment of axons with FN fibers in SC^{Sox2+}. Scale bar, 100 μ m. C) and D) Correlation of FN1 fiber angles of SC and SC^{Sox2+} with the axonal angles (TUBB3) (N=3). E) and F) Quantification of FN1 fibers and axonal anisotropy in DRG neurons co-cultured with: SC, SC^{Sox2+}, SC^{Sox2+/Fn1-/-} (N=3, n \geq 8 areas). Results are shown as the mean \pm s.e.m. FN1 anisotropy was analyzed using an

Unpaired t-test with Welch's correction *** $p < 0.0001$, Axonal anisotropy was analyzed using ANOVA ** $p < 0.005$.

The influence of FN on axon guidance could be a) directly, controlling the regrowing axons or b) indirectly, through the alignment of Schwann cells and then the glial cells guide the axons over direct contact with their surface. To confirm the specific role of FN, I used a detergent-based decellularization protocol for SC^{Sox2+} culture before plating the DRG neurons, in order to have only the matrix from the Sox2-positive Schwann cells and study the role of FN fibrils in axonal guidance (Figure 36A). FN fibers anisotropy did not change due to the process of decellularization (Figure 36B and 36C) but the remaining matrix was not sufficient to support directional axonal outgrowth (Figure 36B and 36D). Additionally, to test whether Schwann cells would be able to guide themselves using exogenous FN present in the extracellular environment to help axonal guidance, I seeded SC^{Sox2+/Fn1-/-} on decellularized SC^{Sox2+} cultures, where oriented FN matrix remains, as just described (Figure 36A). The immunostaining of FN and TUBB3 showed that DRG axons grew randomly in this condition as shown in Figure 36B, which was confirmed by axonal anisotropy analysis shown in Figure 36D. Analysis of FN fibers angles, from the remaining SC^{Sox2+} matrix, and axonal direction showed a complete loss of correlation between them (Figure 36E) and also in the presence of SC^{Sox2+/Fn1-/-} (Figure 36F). These results indicated that direct contact between Schwann cells and axons is necessary and that FN depleted Schwann cells are unable to use the surrounding FN matrix in order to get oriented to help axonal migration. Thus, axonal guidance occurs through direct contact with Schwann cells oriented by their own secreted FN matrix.

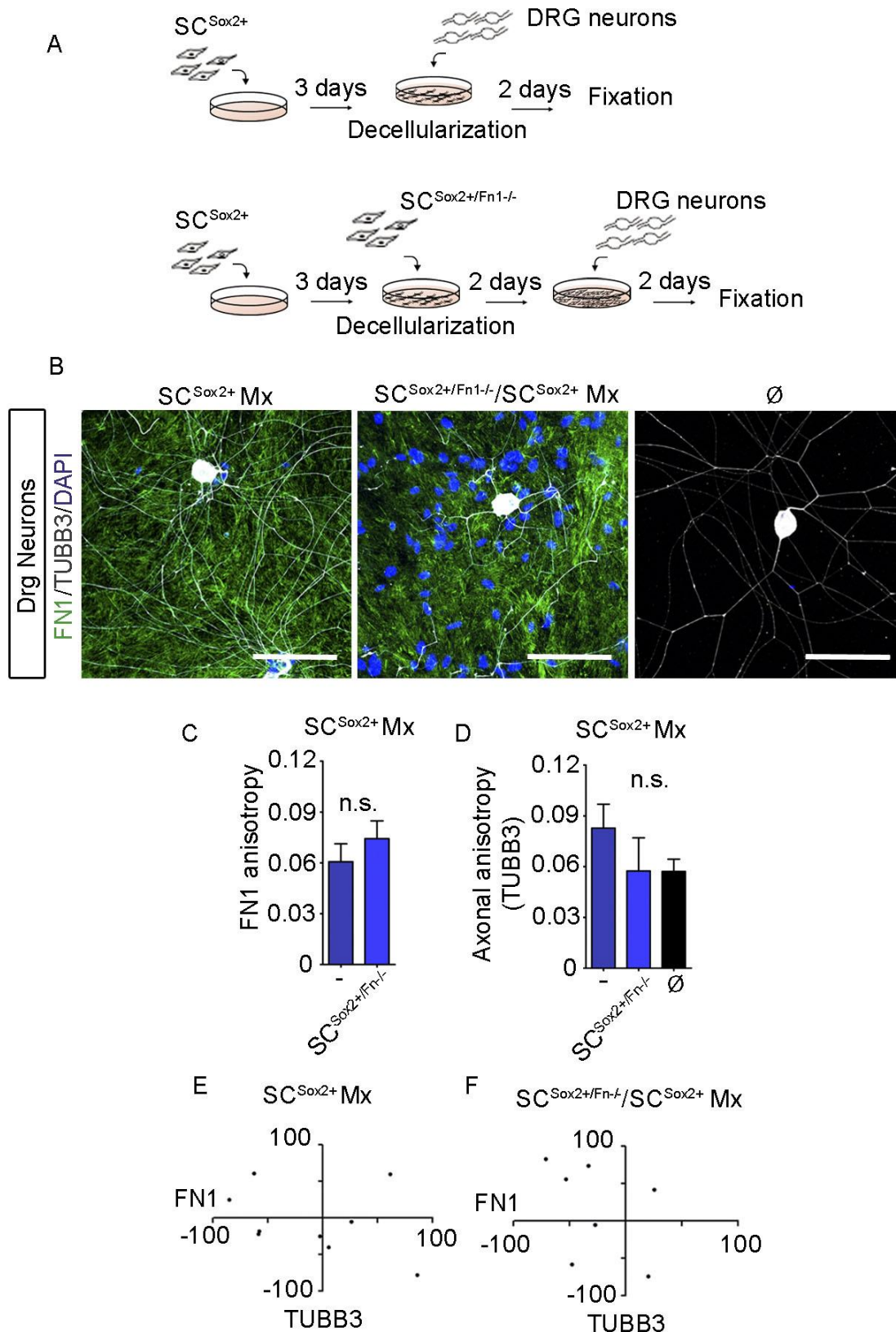


Figure 36. Direct contact with organized Schwann cells is necessary for axonal orientation. A) Experimental design of the matrix (Mx) generation from SC^{Sox2+} and co-culture between SC^{Sox2+/Fn1-/-} and primary DRG neurons. B) Representative confocal images of FN1 (green) and TUBB3 (white)

immunostainings of DRG neurons co-cultured on the SC^{Sox2+} Mx and with the SC^{Sox2/Fn1^{-/-}}. Ø corresponds to primary DRG neurons cultured alone. Nuclei were counterstained with DAPI (blue). Scale bar, 100 µm. C) Quantification of FN1 fibers anisotropy of DRG neurons cultured on the SC^{Sox2+}Mx (-) and with the SC^{Sox2/Fn1^{-/-}} (N=3, n≥7 areas). D) Axonal anisotropy of DRG neurons cultured on the SC^{Sox2+} Mx (-), with SC^{Sox2/Fn1^{-/-}} or alone (Ø) (N=3, n≥7 areas). Results are shown as the mean ± s.e.m. FN1 anisotropy was analyzed using an Unpaired t-test with Welch's correction, p=0.1906 (n.s.), Axonal anisotropy was analyzed using ANOVA, p=0.2447 (n.s.). E) Correlation of FN1 fiber angles of the SC^{Sox2+} Mx with the orientation of DRG neuron axons (TUBB3) (N=3). F) Correlation of FN1 fiber angles of SC^{Sox2+} Mx with the orientation of axons (TUBB3) in the co-culture condition SC^{Sox2+/Fn1^{-/-}} and DRG neurons (N=3).

3.4.2. Human iPSC-derived motoneurons are oriented by self-organized Schwann cells

Very little is known about collective migration of Schwann cells and axonal growth in humans after nerve injuries. In order to explore Schwann cell to axon interaction in such system, I used motoneurons differentiated from human pluripotent stem cells (hMN) and co-cultured them with the different Schwann cell lines. hMN were produced in the Helmholtz Zentrum München hiPSCs core facility.

3.4.2.1. *Characterization of human iPSC-derived motoneurons*

I first confirmed the identity of the hMN by immunostaining and semiquantitative RT-PCRs (Figure 37A, 37B and 37C). hMN production efficiency reported for the protocol used is about 70% (Sances et al., 2016). As it is shown in Figure 37A and 37B, the expression of the specific motoneuron markers ISL1 (ISL LIM Homeobox1, an early postmitotic motoneuron marker) and CHAT (Choline Acetyltransferase, a mature motoneuron marker) were detected in the cells after 21 days of culture under differentiation conditions (Figure 37A and 37B). mRNA of general neuronal markers were also detected in culture, specifically *MAP2*, *NFH* and *PAX6* (Figure 37B). Additionally, mRNA of *LHX3*, *GATA2* and *GATA3* were also detected suggesting the presence of interneurons in the cellular population.

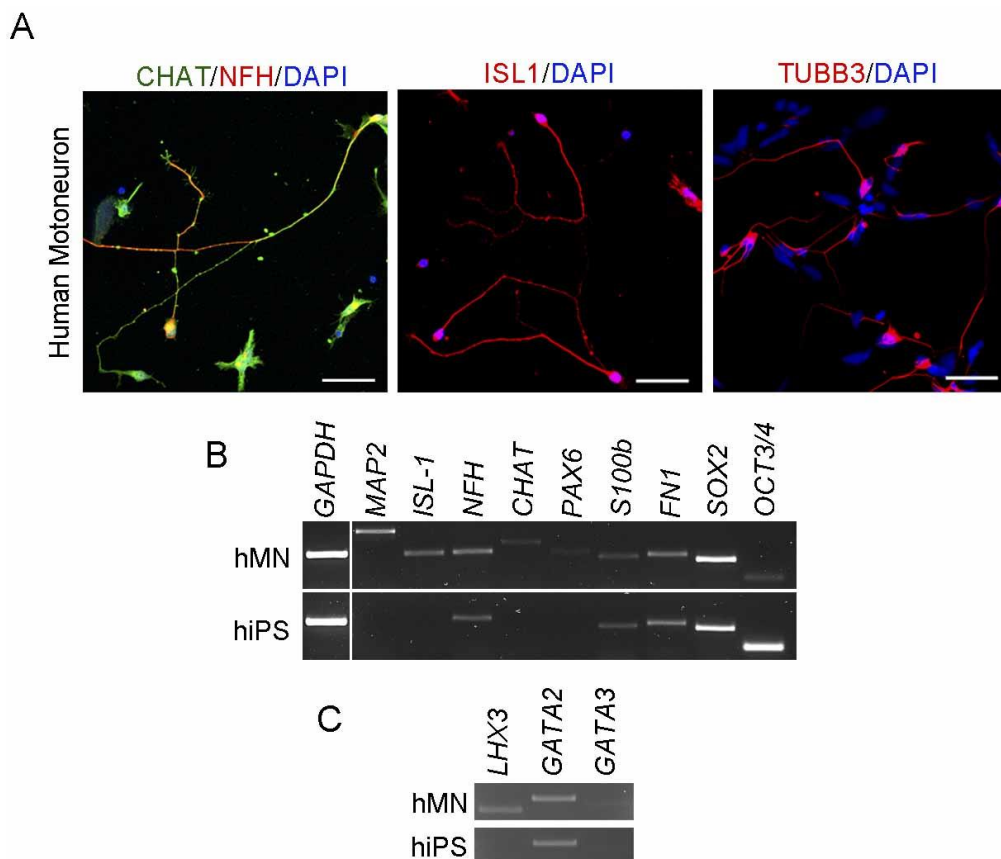


Figure 37. Characterization of the hMN. A) Immunostaining characterization of the hMN, showing CHAT and NFH double positive cells, ISL1 and TUBB3 positive neurons. Nuclei were counterstained with DAPI (blue). Scale bar, 50 μm . B) and C) Gene expression analysis of markers of: motoneurons, stem cell (B) and interneurons (C) at the end of differentiation (day 21) from cDNA extracted from hMN and human inducible pluripotent stem cells (hiPS). *Gapdh* was used as a reference gene.

3.4.2.2. Axon of human motoneurons regrow following Schwann cells direction

Once the identity of the hMN was confirmed, I used a similar approach to the one described in section 3.4.1 to analyze the capacity of the hMN to follow self-organized Schwann cells. I plated the hMN on the three Schwann cell cultures SC, SC^{Sox2+} and SC^{Sox2+/Fn1-/-} and analyzed the correlation between FN fibers and axon angles together with their anisotropy (Figure 38A). I observed that neurons follow only SC^{Sox2+} orientation (Figure 38B) and the angles of the

axons significantly correlated with FN fibers in this condition (Figure 38D). In contrast, co-culture of hMN with SC or SC^{Sox2+/Fn1-/-} did not show alignments between Axons and FN fibers (Figure 38B, 38C and 38D). FN anisotropy was again significantly higher in SC^{Sox2+} in agreement with the results presented in section 3.4.1 and axonal anisotropy was significantly increased when hMN were in culture with SC^{Sox2+} (Figure 38E and 38F). These data suggested that the crosstalk between Sox2-dependent ECM and axonal growth is a conserved mechanism across mammals.

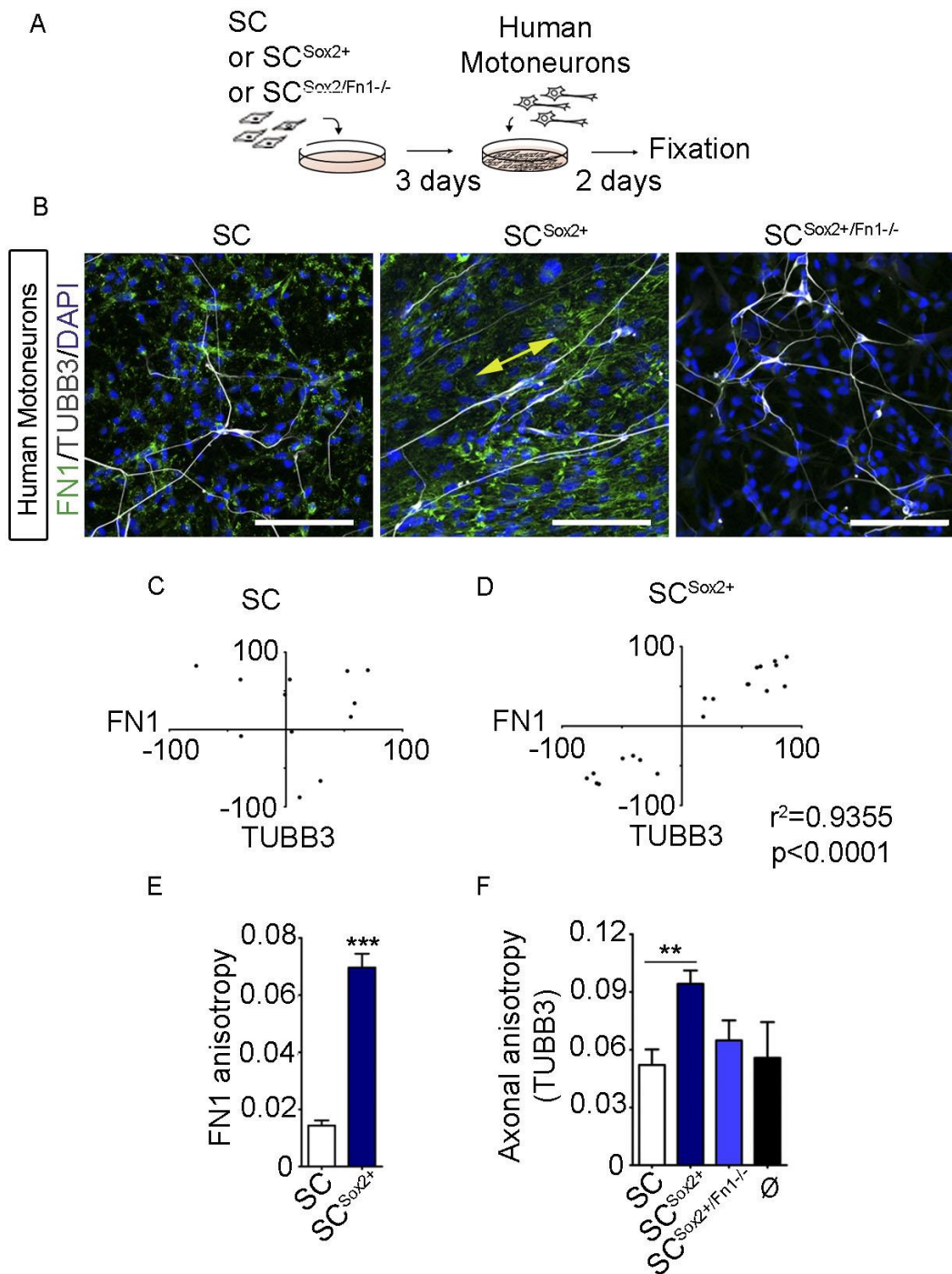


Figure 38. Human motoneurons follow Schwann cells organization. A) Experimental design of Schwann cells (SC, SC^{Sox2+} or SC^{Sox2+/Fn1-/-}) and hMN co-cultures. B) Representative confocal images of FN1 (green) and TUBB3 (white) immunostaining in hMN cultured with SC, SC^{Sox2+} or SC^{Sox2+/Fn1-/-}. Nuclei were counterstained with DAPI (blue). Double-head arrow shows the alignment of axons with FN1 fibers in SC^{Sox2+}. Scale bar, 100 μ m. C) and D) Correlation of FN1 fiber angles of SC and SC^{Sox2+} with the angles of hMN axons (TUBB3) (N=3). E) and F) Quantification of FN1 fibers (N=3, n \geq 18 areas) and axonal

anisotropy (N=3, n≥9 areas) in hMN co-cultured with: SC, SC^{Sox2+}, SC^{Sox2/Fn1-/-}. ∅ corresponds to hMN culture alone. Results are shown as the mean ± s.e.m. FN1 anisotropy was analyzed using an Unpaired t-test with Welch's correction, ***p<0.0001, Axonal anisotropy was analyzed using ANOVA **p<0.005.

3.4.3. FN is necessary for the growth of human motoneurons

In order to study if FN matrix has an additional effect on neuronal growth, I compared the capacity of mouse DRG neurons and hMN to grow in the FN matrix produced by the SC^{Sox2+} in a Laminin-coated dish with a condition where the culture dish only has Laminin. Interestingly, I found that DRG neurons were able to extend their axons in both conditions (Figure 39). However, hMN only grew in the presence of FN (Figure 39). These results showed that in these *in vitro* conditions, FN is required for the growth of hMN.

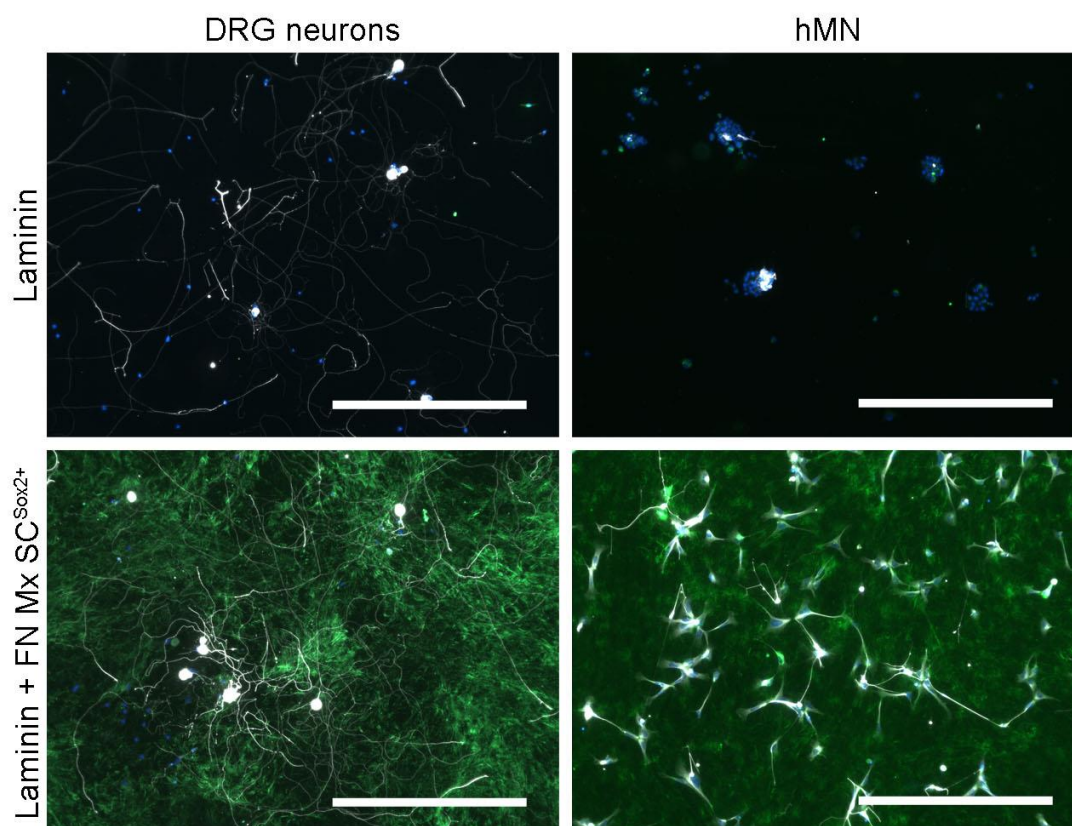


Figure 39. FN substrate promotes hMN growth. Representative confocal images of FN1 (green) and TUBB3 (white) immunostaining in hMN cultured in Laminin-coated substrate (upper panel) or Laminin + SC^{Sox2+} Matrix (Mx)

(bottom panel). Nuclei were counterstained with DAPI (blue). Scale bar, 400 μm .

3.4.4. SC-dependent axonal growth is not affected by the FN produced by embryonic fibroblasts

The results presented in the previous section showed that FN-depleted Schwann cells are disorganized and unable to guide themselves with surrounding FN matrix in order to aggregate, migrate directionally and guide axonal regrowth. Since Schwann cells are in direct contact with fibroblasts in the regenerating PNS and considering that fibroblasts express high levels of FN, one question that remained to be addressed was whether fibroblast-secreted FN influences Schwann cell aggregation, migration and finally axonal guidance. For this, a wild-type embryonic fibroblast cell line (FB) and a FN KO line (FB^{Fn1^{-/-}}; both cell lines were a gift from Prof. Reinhard Fässler, Max Planck Institute of Biochemistry) were used for co-culture studies with Schwann cells and DRG neurons.

First, I evaluated the expression of FN and the anisotropy of the cells. As expected, the wild-type FB expressed high levels of FN, which was lost in the KO cell line (Figure 40A). The orientation of FN fibrils and Actin fibers were significantly correlated. Actin fibers of FB presented a higher anisotropy compared to FB^{Fn1^{-/-}} (Figure 40B and 40C), suggesting that FN controls fibroblasts orientation. These observations confirmed a general role of FN in cellular orientation.

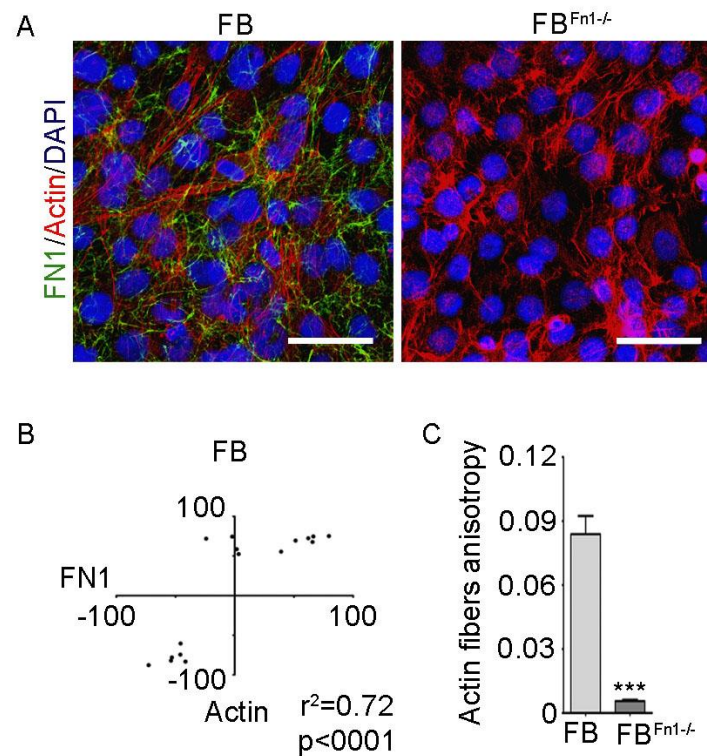


Figure 40. Cellular anisotropy of the wild type and the FN KO fibroblasts cell line. A) Representative confocal images of FN1 (green) and Actin fibers (red) immunostainings of FB and FB^{Fn1-/-}. Nuclei were counterstained with DAPI (blue). Scale bar, 100 μ m. B) Correlation of FN1 fiber angles with the orientation of actin fibers of FB (N=3). C) Quantification of actin fibers anisotropy of FB and FB^{Fn1-/-} (N=3, n \geq 18 areas). Graph shows the mean value \pm s.e.m. Mann Whitney test, ***p<0.0001.

To study axonal guidance, the following co-cultures conditions were evaluated (Figure 41A):

- i. FB and DRG neurons
- ii. FB, SC and DRG neurons
- iii. FB, SC^{Sox2+} and DRG neurons
- iv. FB, SC^{Sox2+/Fn1-/-} and DRG neurons
- v. FB^{Fn1-/-} and DRG neurons
- vi. FB^{Fn1-/-}, SC and DRG neurons
- vii. FB^{Fn1-/-}, SC^{Sox2+} and DRG neurons
- viii. FB^{Fn1-/-}, SC^{Sox2+/Fn1-/-} and DRG neurons

Independently of fibroblasts, DRG neurons were only able to orient when they were co-cultured on SC^{Sox2+} (Figure 41B). Evaluation of the FN fibers and axonal anisotropy, in the different co-culture conditions with FB, showed a significant increase of anisotropy only in the presence of SC^{Sox2+} (Figure 41C and 41D). Analysis of co-culture with FB^{Fn1-/-} showed a similar trend, the anisotropy of FN fibers and axons was significantly increased in the presence of SC^{Sox2+} (Figure 41E and 41F).

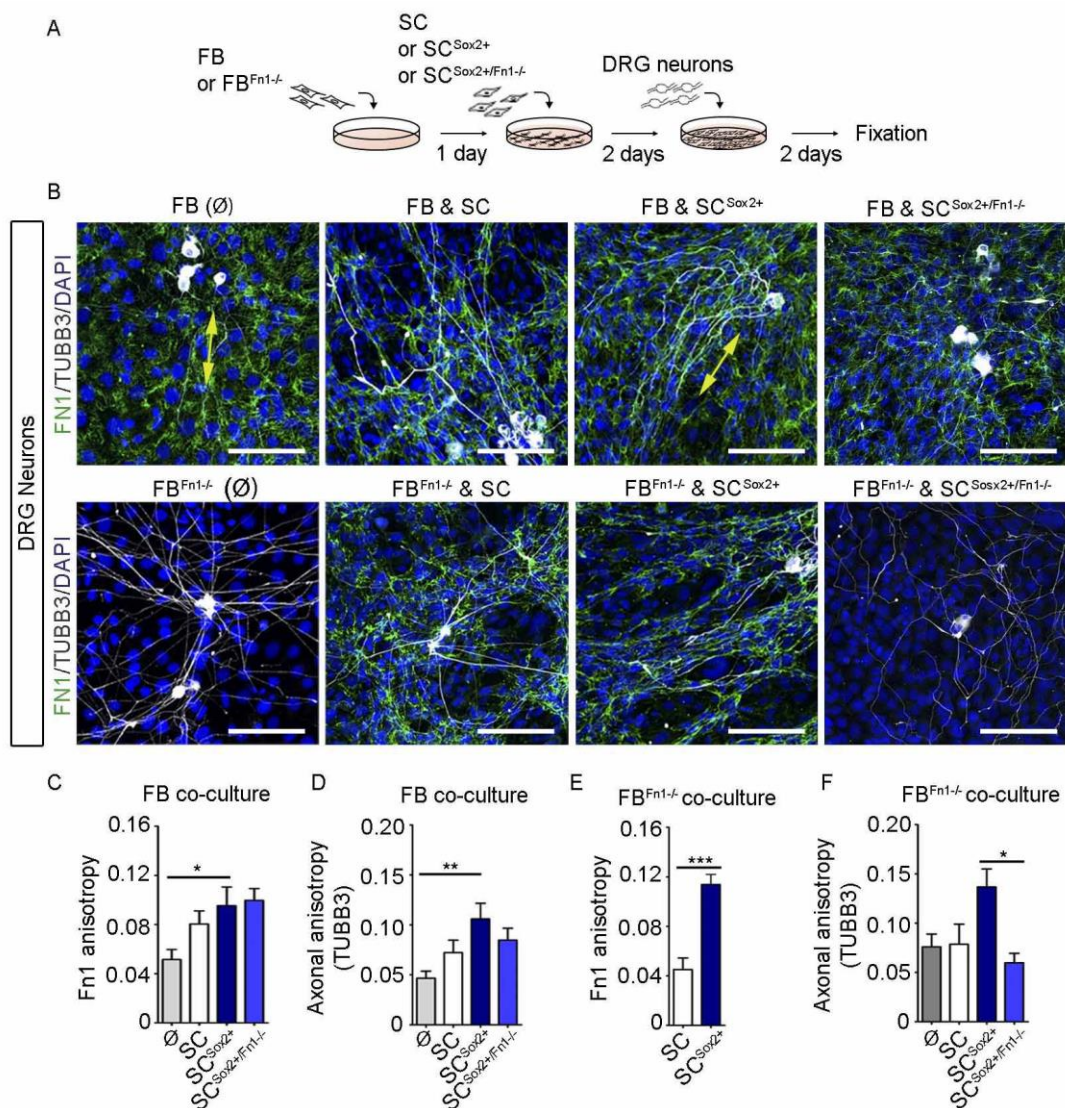


Figure 41. FN expressed by fibroblasts is not involved in Schwann cell organization and DRG neurons orientation. A) Experimental design of co-cultures between Fibroblasts (FB and FB^{Fn1-/-}), Schwann cells (SC, SC^{Sox2+} or SC^{Sox2+/Fn1-/-}) and primary DRG neurons from adult mice. B) Representative confocal images of FN1 (green) and TUBB3 (white) immunostainings of DRG

neurons co-cultured with FB plus SC, SC^{Sox2+} or SC^{Sox2/Fn1-/-} [top panels] and with FB^{Fn1-/-} plus SC, SC^{Sox2+} or SC^{Sox2/Fn1-/-} [bottom panels]. Nuclei were counterstained with DAPI (blue). Scale bar, 100 μ m. C) Quantification of FN1 anisotropy of the DRG neurons and FB co-culture conditions: alone (\emptyset), with SC, with SC^{Sox2+} or with SC^{Sox2/Fn1-/-} (N=3, n \geq 7 areas), ANOVA *p<0.05. D) Axonal anisotropy (TUBB3) of the DRG neurons in the co-culture conditions with: FB (\emptyset), FB plus SC, SC^{Sox2+} or SC^{Sox2/Fn1-/-} (N=3, n \geq 7 areas), ANOVA **p<0.005. E) Quantification of FN1 anisotropy of the DRG neurons and FB^{Fn1-/-} co-culture conditions: with SC or with SC^{Sox2+} (N=3, n \geq 6 areas), ***p=0.0007. F) Axonal anisotropy (TUBB3) of the DRG neurons in the co-culture conditions with: FB^{Fn1-/-} (\emptyset), FB^{Fn1-/-} plus SC, SC^{Sox2+} or SC^{Sox2/Fn1-/-} (N=3, n \geq 6 areas), ANOVA p<0.05. Graphs show the mean value \pm s.e.m.

Interestingly, SC in the presence of FB increased their fibrillogenesis but with a lower anisotropy in comparison to SC^{Sox2+}. SC fibrillogenesis was not enough to significantly influence axonal orientation (Figure 41B and 41F). Analysis of *Fn1* and *Sox2* mRNA levels, by semiquantitative RT-PCR in the aforementioned co-culture conditions (without DRG Neurons), did not show any increase in *Sox2* or *Fn1* mRNA levels when compared to single culture conditions (Figure 42). In summary, axons were only oriented in the conditions where SC^{Sox2+} were present, conditions (iii) and (vii), and FN coming from fibroblasts was not required for axonal orientation whereas FN from Sox2-expressing Schwann cells was necessary. These results confirmed that axonal guidance is conducted by FN-dependent oriented Schwann cells but not fibroblasts.

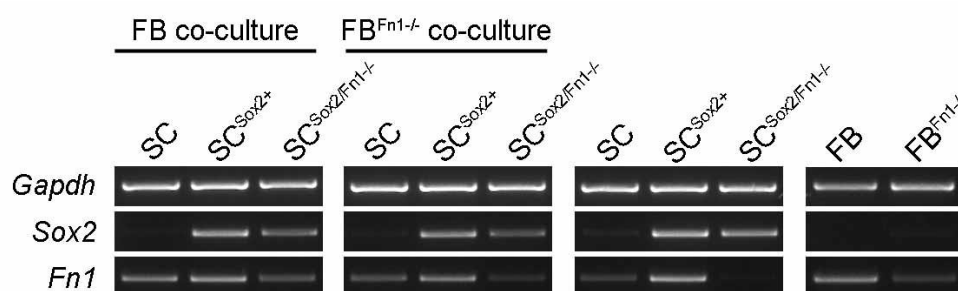


Figure 42. Mouse embryonic fibroblasts do not influence Sox2 and FN expression in Schwann cells. *Sox2* and *Fn1* mRNA expression analysis of Schwann cells (SC, SC^{Sox2+} or SC^{Sox2/Fn1-/-}) and fibroblasts (FB or FB^{Fn1-/-}) co-cultures. *Gapdh* was used as a reference gene.

3.5. *In vivo* expression of Sox2 and FN during regeneration of the peripheral nervous system

3.5.1. Sciatic nerve injury in adult rats

Sciatic nerve injury in adult rats is one of the most used models to study regeneration of the PNS. Among the two types of nerve injuries, neurotmesis has been less studied, although it implicates more cellular and architectural changes that can finally compromised the complete recovery. Sox2 expression has been reported after axonotmesis and neurotmesis in Schwann cells, inducing the expression of downstream genes involved in regeneration of peripheral nerves (Le et al., 2005). Considering that after neurotmesis basal lamina is disturbed and the expression of ECM proteins is necessary for the reconstruction of the nerves, we decided to analyze Sox2 and FN expression after a full transection of the sciatic nerve. The surgical procedure was done in collaboration with Drs. Charlotte Kleeberger and Ulf Dornseifer, experts in rat and human sciatic nerve microsurgery from the Klinikum Bogenhausen.

3.5.1.1. *Sciatic nerve surgery model*

To confirm our data *in vivo*, I evaluated Sox2 and FN expression after sciatic nerve axotomy in adult rats. We performed a complete transection of the sciatic nerve with a subsequent direct nerve coaptation (nerve reattachment) according to the standard clinical treatment (Figure 43A and 43B), in this case a small bridge is formed between the two cut ends of the nerve. The contralateral site of the animal was used as a control where a similar surgical procedure was performed to expose the nerve without transection (Figure 43A and 43B). Sciatic nerves were collected after 4, 7 and 10 days post-surgery (Figure 43C).

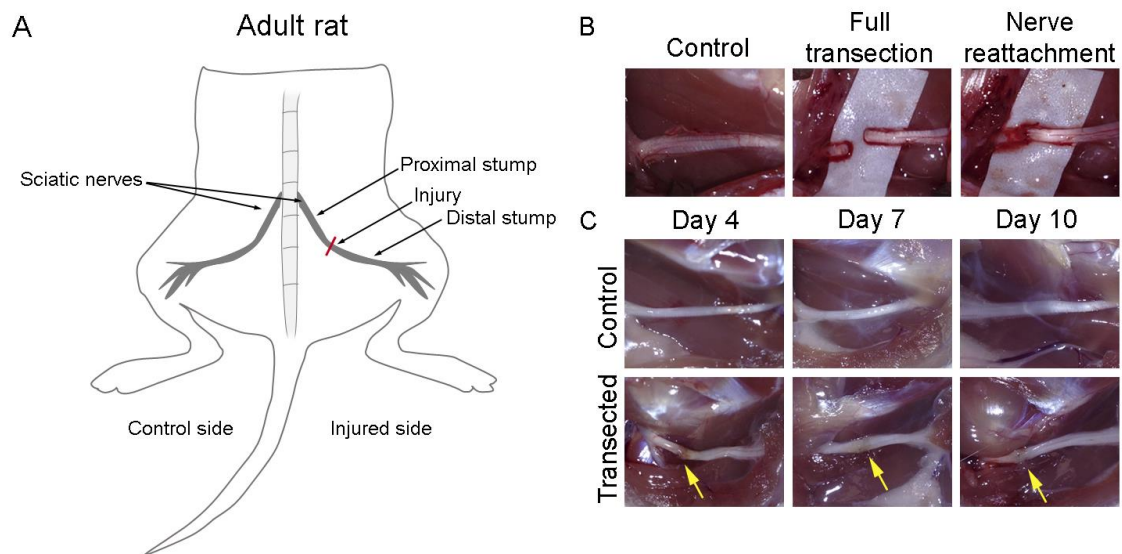


Figure 43. Sciatic nerve transection in adult rats. A) Schematic representation of the sciatic nerve injury model. B) Photographs of rat sciatic nerves before and after full transection and with the posterior reattachment. C) Photographs of the rat sciatic nerves at the time points evaluated after surgery.

First, I evaluated the expression of GFAP and TUBB3 by immunostaining to confirm that after surgery, the sciatic nerve followed a process of degeneration/regeneration during the different times points. As shown in Figure 44, at day 4, axons labeled with TUBB3 are degenerated in the distal stump and over time it was observed the regrowing process (Figure 44). As expected, GFAP was up-regulated in glial cells over time, first in the distal stump and later in the proximal stump as well in the cut area during nerve regeneration. Additionally, qPCR results showed that mRNA levels of *S100 β* were down-regulated in the regenerative nerves (Figure 45). These results confirmed that after surgical procedure nerves follow the expected degeneration/regeneration process and made the system suitable for the study of Sox2 and FN expression.

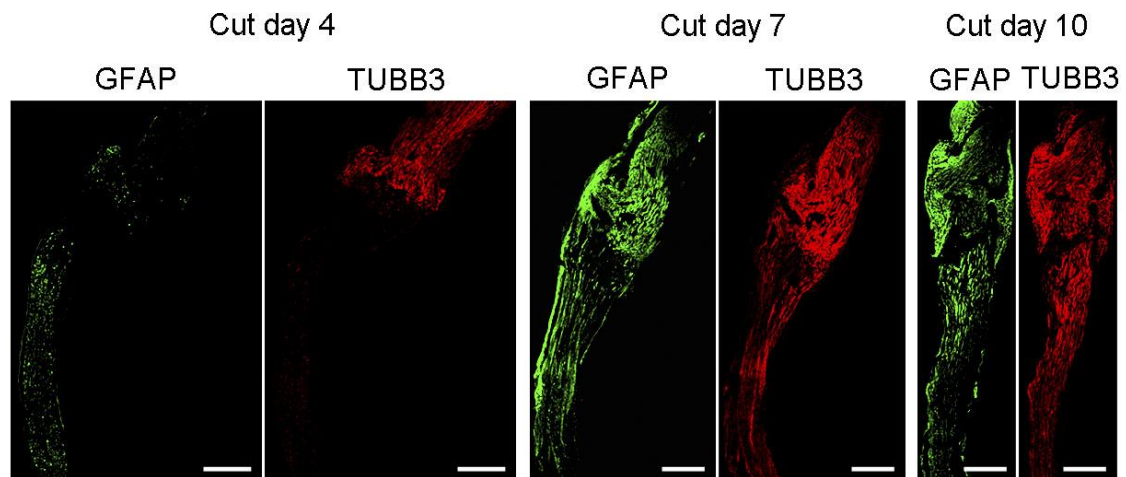


Figure 44. Degeneration-regeneration process of sciatic nerve after axotomy. Representative confocal images of GFAP (green) and TUBB3 (red) immunostainings of sciatic nerve after complete transection at day 4, 7 and 10 post surgery. Nuclei were counterstained with DAPI (blue). Scale bar, 2000 μm

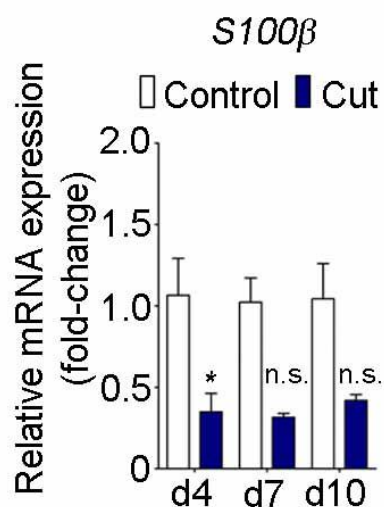


Figure 45. mRNA expression levels of *S100b* in sciatic nerves after axotomy. qPCR Graph shows RT-qPCR measurements of *S100β* from control and transected nerves at day 4, 7 and 10 post surgery. *Ankrd27* and *Rictor* were used as reference genes. (N=3). Graphs show the mean value \pm s.e.m. Mann Whitney test, d4 * $p=0.0286$, d7 $p=0.1$ (n.s.), d10 $p=0.1$ (n.s.).

3.5.1.2. *Sox2* and FN fibrillogenesis are up-regulated after sciatic nerve transection

Once the surgical procedure was validated, I proceeded with the confirmation of Sox2 expression by immunostaining in the sciatic nerves. Using double immunostaining of GFAP (to mark glial cells) together with Sox2, I found that at day 4, double-positive glial cells were located in the distal stump. At day 7, Sox2-positive Schwann cells were found in the cut area and the distal stump

(Figure 46). Finally, at day 10, Sox2-positive cells were found in the cut region, distal and proximal stumps (Figure 46). qPCR analysis showed that Sox2 mRNA levels increased over time, with a pick at day 10 (Figure 47). Then, I evaluated by immunostaining FN expression in the injured nerves together with Sox2 expression. FN matrix was modified during regeneration, there was an increase in fibrillogenesis at day 7 and 10 when Sox2 was also up-regulated (Figure 48).

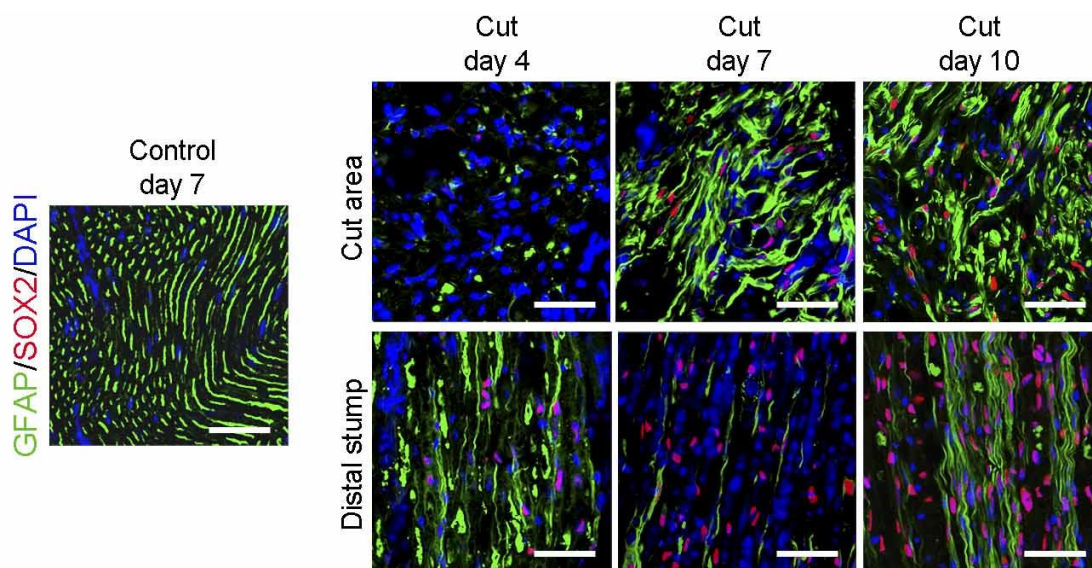


Figure 46. Sox2 expression by Schwann cells in sciatic nerves after axotomy. Representative confocal images of GFAP (green) and SOX2 (red) immunostainings of sciatic nerve in control condition (day 7) and after complete transection at day 4, 7 and 10 post surgery. Nuclei were counterstained with DAPI (blue). Scale bar, 50 μ m.

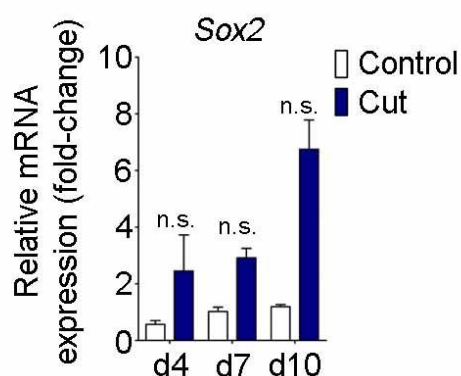


Figure 47. mRNA levels of Sox2 in sciatic nerves after axon injury. Graph shows real-time qPCR measurements of Sox2 from control and transected nerves at day 4, 7 and 10 post surgery. *Ankrd27* and *Rictor* were used as reference genes. (N=3). Graphs show the mean value \pm s.e.m. Mann Whitney test, d4 $p=0.2$ (n.s.), d7 $p=0.1$ (n.s.), d10 $p=0.1$ (n.s.).

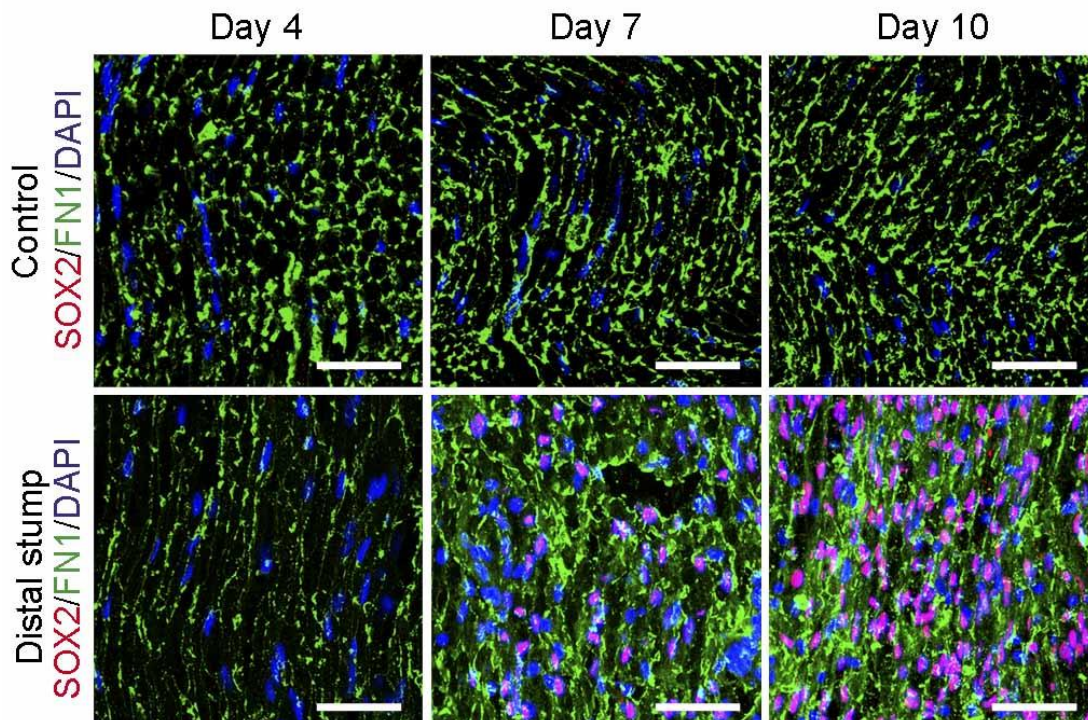


Figure 48. Sox2 and FN expression in sciatic nerves post injury. Representative confocal images of FN1 (green) and SOX2 (red) immunostainings of rat sciatic nerves in control conditions or after complete transection, at day 4, 7 and 10 post surgery. Nuclei were counterstained with DAPI (blue). Scale bar, 50 μ m.

3.5.1.3. *FN containing the spliced domain EIIIA is co-expressed in Sox2-positive Schwann cells after nerve injury*

FN containing the EIIIA spliced domain (*Fn1EIIIA*) is up-regulated after nerve damage and is suggested to be expressed in repair Schwann cells (Mathews & Ffrench-Constant, 1995; Voegelzang et al., 1999). To study the expression of this spliced domain during nerve regeneration, I designed specific primers and *in situ* probes to study this spliced domain and to evaluate mRNA levels by qPCR and *in situ* hybridization (ISH) in regenerative nerves. By ISH, the spliced domain was detected at day 4 in the cut area, mainly around the surgery site consistent with the immunostaining results (Figure 49). A high *Fn1EIIIA* expression was observed in cells of the cut area and in the distal stump at day 7. At day 10, a broad expression of *Fn1EIIIA* was detected in the proximal and distal stumps as well as in the cut area by ISH. However, real-time

qPCR results showed that the peak of mRNA expression of *Fn1EIIIA* was at day 7 after surgery (Figure 50).

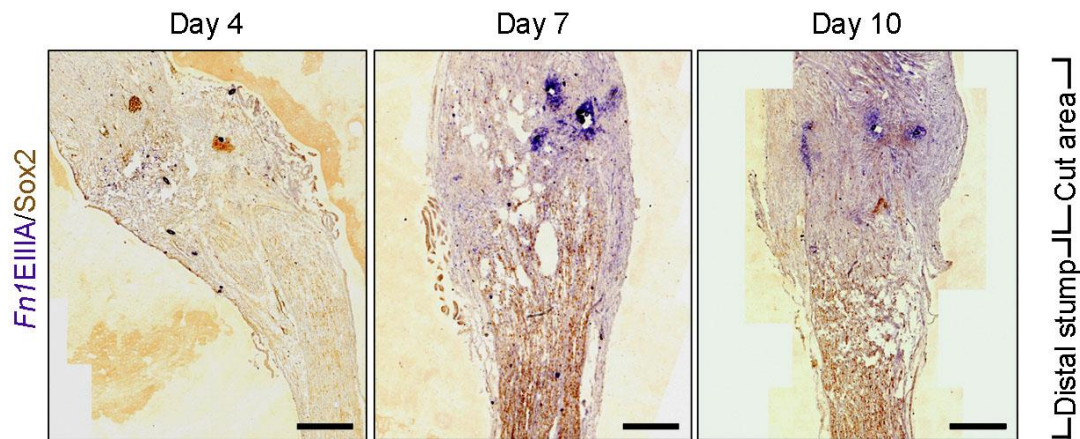


Figure 49. mRNA expression of *Fn1EIIIA* in sciatic nerves post injury. *In situ* hybridization using a probe against *Fn1EIIIA* (purple) and SOX2 DAB staining (brown) in control and transected nerves at day 4, 7 and 10 post surgery showing the cut area and the distal stump. Scale bar, 500 μ m.

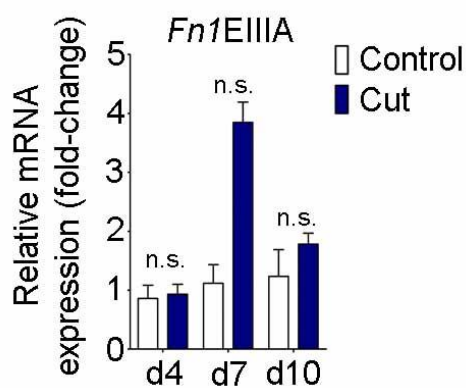


Figure 50. mRNA levels of *Fn1EIIIA* in sciatic nerves after axon injury. Graph shows real-time qPCR measurements of the *Fn1* containing the spliced domain EIIIA from control and transected nerves at day 4, 7 and 10 post surgery. *Ankrd27* and *Rictor* were used as reference genes. (N=3) Graphs show the mean value \pm s.e.m. Mann Whitney test, d4 $p=0.8571$ (n.s.), d7 $p=0.1$ (n.s.), d10 $p=0.4$ (n.s.).

Co-expression analysis of *Fn1EIIIA* mRNA and Sox2 protein expression by DAB staining, showed double-positive cells at day 7 and 10 (Figure 51). However, *Fn1EIIIA* expression was not exclusive of Schwann cells, fibroblast present in the distal area could also be responsible of *Fn1EIIIA* expression. These results supported the hypothesis that Schwann cells can produce their own *Fn1EIIIA in vivo* to incorporate it in their basal lamina, essential for regeneration.

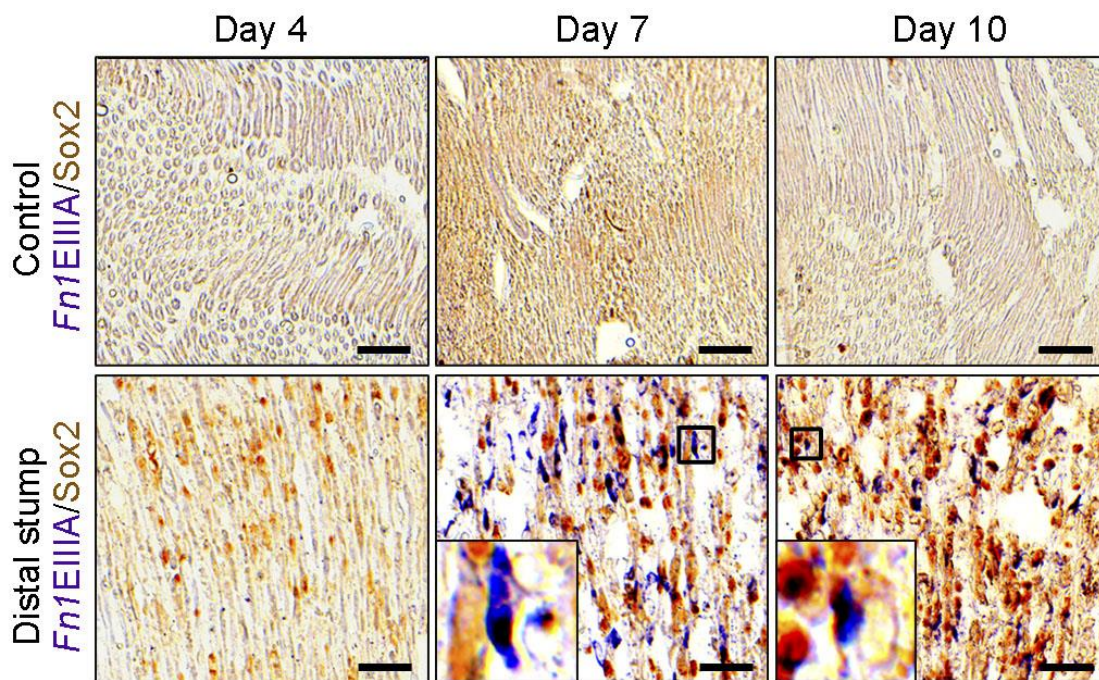


Figure 51. Co-expression of Sox2 and *Fn1EIIIA* in sciatic nerves after nerve injury. In situ hybridization using a probe against *Fn1EIIIA* (purple) and SOX2 DAB staining (brown) in control and transected nerves at day 4, 7 and 10 post surgery. Insets in the bottom panels show the co-expression of *Fn1EIIIA* with a SOX2-positive Schwann cell at day 7 and 10 post surgery. Scale bar, 50 μm .

3.5.2. Study of Sox2 expression in the posterior lateral line of zebrafish larvae

The lateral line is a sensory system of aquatic vertebrates, responsible of sensing the water flow leading to distinct behavioral responses in the fish. It is composed of mechanosensory organs (neuromasts) which are innervated by neurons located in the cranial ganglion (Ghysen & Dambly-Chaudiere, 2004). The lateral line is divided into anterior lateral line, which includes the neuromasts and neurons of the head, and the posterior lateral line (pLL) which includes the neuromasts and neurons of the body and tail (Ledent, 2002). In zebrafish, the pLL is composed of seven to eight neuromasts located along the horizontal myoseptum. The development of the pLL starts with the migration of the primordium from bilateral cephalic placodes to the tail and the deposition of cellular rosettes that mature to form the neuromasts (Pujol-Martí & López-Schier, 2013). During the development of the pLL, neurons accompany the

migratory primordium, meanwhile glial cells migrate behind the growth cones of the neurons forming a chain (Gilmour et al., 2002). This process is completed during the first three days post fertilization in the zebrafish larvae. Additionally, neurons of the pLL have the capacity to regenerate after complete transection. After an axotomy, Schwann cells, downregulate myelin related genes and guide the axons during the process of regeneration to reinnervate the original target (Xiao et al., 2015), similar to what it is observed in mammals.

One of the advantages of using zebrafish larvae as a model system is its transparency which allows the use of transgenic fluorescence lines together with microscopy techniques for the study of development and regeneration of the nervous system. In this regard, I used two transgenic zebrafish lines: the Tg[gSAGFF202A] in which Schwann cells are labeled with the green-fluorescent protein EGFP and the line Tg[SILL:mCherry] which expresses mCherry in afferent neurons (Xiao et al., 2015). These two lines were crossed in order to have a zebrafish larva where Schwann cells and axons of the pLL were labelled, which allowed me to study Sox2 expression in Schwann cells during development and regeneration.

3.5.2.1. *Development of the pLL of zebrafish*

In order to evaluate Sox2 expression in migratory glial cells during the development of the pLL, I looked at the transgenic larvae Tg[gSAGFF202A; SILL:mCherry] at 28 hours post fertilization. Fish were fixed and stained for Sox2. I detected Sox2 expression in the protoneuromast generated from the migratory primordium but not in migratory Schwann cells (Figure 52).

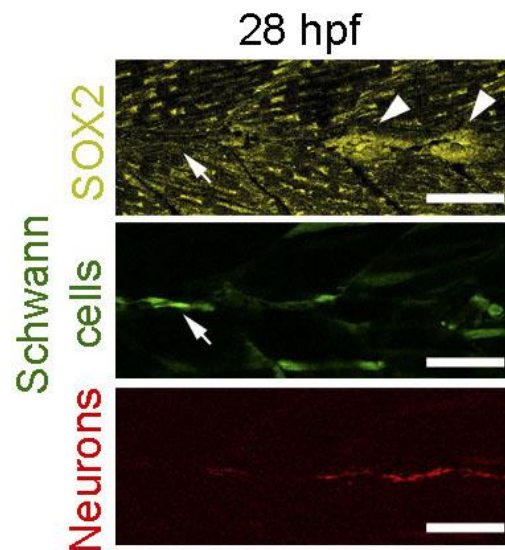


Figure 52. Schwann cells of the posterior lateral line do not express Sox2 during development. Confocal images of the developing posterior lateral line of the triple transgenic zebrafish line Tg[gSAGFF202A;UAS:EGFP;SILL:mCherry], 28 hours post fertilization. Immunofluorescence staining of SOX2 (yellow) show SOX2 positive cells in the protoneuromasts (arrow heads) and SOX2 negative migratory Schwann cells (arrows). Scale bar, 50 μ m.

3.5.2.2. *Regeneration of the pLL of zebrafish after axotomy*

I tested the implications of Sox2 during the regeneration of the pLL in zebrafish using a laser-mediated axon ablation of the posterior lateral line similar to the one described by Xiao et al (Xiao et al., 2015). I performed the axotomy at day 3-post fertilization and evaluated the process of regeneration 24 hours after injury. Despite the fact that I detected Sox2 positive cells in the neuromast by immunostaining, I did not find Sox2 expression in Schwann cells located in the injured area or in the distal part of the nerve (Figure 53). These results suggested that the Schwann cell behavior controlled by Sox2 during the regeneration of the mammalian PNS is not conserved within vertebrates.

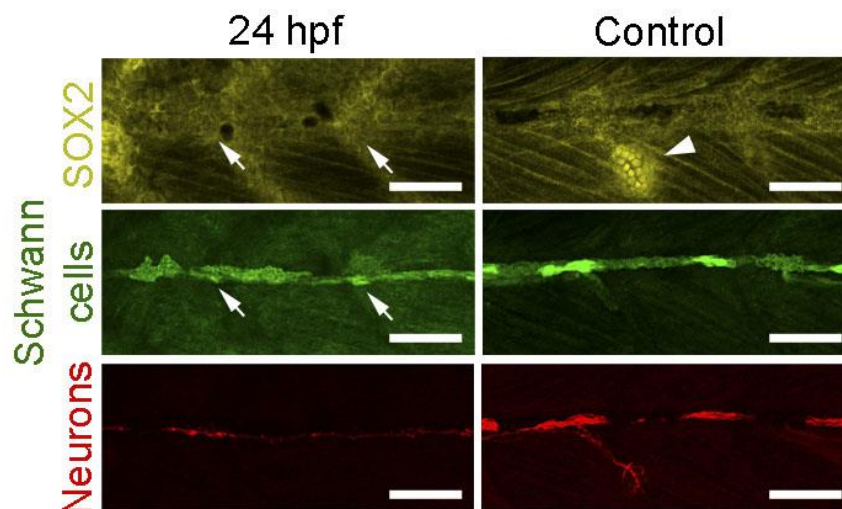


Figure 53. Schwann cells of the posterior lateral line do not express Sox2 after axons ablation. Confocal images of the posterior lateral line 24 hours after laser ablation using the transgenic line Tg[gSAGFF202A;UAS:EGFP; SILL:mCherry]. Immunostaining of SOX2 (yellow) shows SOX2-positive cells in a neuromast (arrow head) and negative SOX2-Schwann cell expression (arrow). Scale bar, 50 μ m.

4. Discussion

Cell organization is fundamental during development, tissue repair and tissue homeostasis. The interactions between cells and the ECM directly influence cell behavior. This communication is essential for the coordination of cell movement and the positioning of the cells inside the tissue. The ECM is rapidly remodeled by cells, which respond to the ECM modifications with changes in proliferation, migration, organization, adhesion and/or differentiation. One important behavioral change is cell to cell alignment. Cell alignment is observed in many tissues and organs. For example, myocytes are aligned in muscle tissue and their organization is necessary for muscle contraction (Pope et al., 2008). Endothelial cells are also aligned in the vasculature and this allows the blood vessels to have flexibility and resistance (Tzima et al., 2001). During regeneration of the PNS, Schwann cells form an aligned channel, the Band of Büngner, that allows axons to grow parallel to each other for them to find their target (Allodi et al., 2012). The exact mechanism that drives Schwann cell alignment during the process of regeneration remains unclear. Here I found that Sox2 directly binds to FN promoter to control its expression which induces the formation of focal adhesion structures and the activation of FN leading to its fibrillogenesis. FN fibrillogenesis facilitates the alignment and directional migration of Schwann cells. Organized migratory Schwann cells form cellular channels that finally support a guided axonal regrowth. These results identified Sox2 as a new regulator of Schwann cell-matrix adhesions for their proper migration necessary for an organized neuronal regeneration.

4.1. Sox2 controls Schwann cell behavior and modulates the expression of cell adhesion and ECM-related genes

Sox2 has been widely studied for its role in the maintenance of stem cell self-renewal during development, in adult stem cell niches and in cancer stem cells. However in the past years, evidences, particularly in the cancer field, demonstrated that Sox2 also controls cell adhesion and migration, inducing the

expression of FN or promoting epithelial to mesenchymal transition in tumor cells (Han et al., 2012; Lou et al., 2013). Here, I confirmed its role as an inducer of Schwann cell-cell adhesion and found a new function as a regulator of Schwann cell ECM, specifically regulating FN expression. Further studies about the role of Sox2 as a regulator of cell-matrix adhesion are necessary since the expression of this key transcription factor is crucial to maintain tissue homeostasis. As a cancer stem cell marker, Sox2 could also directly regulate the ECM remodeling of tumors which is another main element that influences tumor growth and metastasis. For example, Schwannomas and traumatic neuromas express Sox2 (Shivane et al., 2013). It would be interesting to study if Sox2 expression influences the ECM composition in these pathological conditions of the PNS and the impact of the ECM composition on the tumor formation and growth.

Our *in vitro* model also showed several ECM- and cell adhesion- related genes significantly regulated. Looking at the top up- and down-regulated genes in Sox2-positive Schwann cells and their relation with FN (based on the literature-derived network), we found that the highest up-regulated gene related with cell adhesion, *Cx3cl1*, was closely related to FN (see Figure 18). CX3CL1 is a chemokine member of the chemokine class CX3C that binds to the receptor CX3CR1 (Jones et al., 2010; Limatola & Ransohoff, 2014). In cancer, CX3CL1/CX3CR1 mediates cell adhesion and promotes metastasis via activation of $\text{itg}\beta 1$ and FAK (Marchesi et al., 2010). In the nervous system, CX3CL1 is expressed in neurons, endothelial cells, nerve fibers, and acts as a chemoattractant of specialized macrophages, particularly microglia, after nerve injury (Marchesi et al., 2010; Scholz & Woolf, 2007; Verge et al., 2004). Additionally to its role in the immune system, it was shown that CX3CL1 increases adhesion of CNS neurons to Laminin via activation of $\text{itg}\beta 1$ (Lauro et al., 2006). CX3CL1 is also modulated by other chemokines such as CXCL12 (also found up-regulated in Sox2-positive Schwann cells in the microarray data analysis) which induces CX3CL1 expression, its cleavage and promotes FN-dependent migration (Cook et al., 2010; Freret et al., 2011). This suggests that in repair Schwann cells, CX3CL1 expression could be one additional mechanism by which the glial cells recruit macrophages to the injured area to

favor the inflammatory response. But it could also promote Schwann cell adhesion and migration upon Sox2 expression. More studies, at the protein level, are needed to confirm these hypotheses. In addition, the direct regulation of CX3CL1 by Sox2 should be tested.

In the group of downregulated genes, various matrix metalloproteases (MMPs), enzymes responsible for ECM protein degradation, were found significantly decreased, such as Mmp13 and Mmp10, identified in the top ten of downregulated genes. Mmp13 (collagenase 3) cleaves all types of fibril collagens and Mmp10 target ECM proteins, among them FN (Platt et al., 2003). The role of these two metalloproteases in the PNS and during regeneration is not clear. Mmp10 and Mmp13 were reported to be expressed at low levels after sciatic nerve injury, with a possible implication in the degradation of collagen in the distal segment of the nerve (Hughes et al., 2002; Platt et al., 2003). In other systems, it was shown that Mmp10 null mice have problems to recover after liver injury due to increased fibrogenesis (Garcia-Irigoyen et al., 2014). This is particularly interesting since it demonstrates that MMPs downregulation facilitates matrix assembly which is in line with our *in vitro* results. The downregulation of MMPs during nerve repair could cooperate to restore the damaged basal lamina of Schwann cells after neurotmesis avoiding ECM degradation.

Additionally, Mmp3, although not grouped in the top ten genes, was also found significantly downregulated in Sox2-positive Schwann cell clones. This matrix metalloprotease constitutively expressed in Schwann cells *in vivo*, is downregulated during nerve regeneration (Hughes et al., 2002). Mmp3 expression inhibits Schwann cell proliferation through FN cleavage, resulting in a 29kDa fragment with anti-proliferative effects (Hughes et al., 2002). Furthermore during regeneration of the optic nerve, Mmp3 is highly up-regulated which could represent another factor decreasing CNS regeneration (Hughes et al., 2002). Although we did not observe a significant change in Schwann cell proliferation after Sox2 overexpression, probably due the fact that we were working with a highly proliferative Schwann cell line, it is known that Sox2 and FN promote Schwann cell proliferation. The downregulation of Mmp3 upon Sox2 expression could be an additional mechanism whereby proliferation

in Schwann cells is maintained. From our *in vitro* model, FN expression is highly increased and the presence of Mmp3 could lead to high levels of the FN antiproliferative fragment impairing mitosis. Additional experiments are needed to confirm this hypothesis.

Taken together, Sox2 overexpression seems to fine-tune the ECM microenvironment of Schwann cells *in vitro* to promote neural repair. Sox2 not only induces a significant increase of FN expression but also influences additional ECM-related genes, such as *Cx3cl1*, *Mmp3*, *Mmp10* and *Mmp13*, potentially modulating Schwann cell phenotype in an efficient manner.

4.2. Sox2 as a novel direct regulator of FN in cultured Schwann cells

Our results showed that FN expression is increased in Schwann cells after Sox2 overexpression and directly controlled by Sox2. In other systems, Sox proteins have been demonstrated to regulate FN expression, which is the case of Sox7 and Sox17 (SoxF family) in the extraembryonic endoderm (Shirai et al., 2005). Shirai et al. showed that FN is up-regulated during the differentiation of mouse embryonic stem cells to extraembryonic endoderm and its expression is regulated by Sox7 and Sox17. These Sox proteins are restricted to the extraembryonic endoderm and they act as enhancers of *Fn1* gene expression (Shirai et al., 2005). Interestingly, the DNA binding sequence of Sox2 and Sox3 (members of the SoxB family) is very similar to Sox7 and Sox17, suggesting a possible general regulatory mechanism of FN by these Sox proteins. Specifically, Sox2 has been shown to modulate ECM components to induce migration and adhesion. In a study using a human ovarian cancer cell line, the authors reported that Sox2 promotes cancer cell migration, invasion and colony formation through the up-regulation of FN (Lou et al., 2013). In this study, the authors evaluated a wide region (4 kb) upstream of the FN TSS and found that FN expression was dependent of Sox2 levels. Additionally, the authors suggested possible binding sites located at -1950 and -3750 bp of the TSS. Nevertheless, neither the binding nor the functionality of these binding sites were tested in their *in vitro* model system (Lou et al., 2013). Here we identified specific Sox2 binding sites in the proximal region of the FN rat promoter that were confirmed by ChIP. Moreover, we found that the closest

binding site located at -200 bp upstream of the rat FN TSS was conserved in human and I validated its functionality by reporter assays.

These results demonstrated that Sox2 directly controls FN to induce its expression which leads to the activation of fibril formation responsible for Schwann cell aggregation and oriented collective migration in our *in vitro* model. Future experiments should focus on testing the same regulatory mechanism that we found in our *in vitro* model system but using primary Schwann cells, where we already reported Sox2 expression together with fibronectin fibrillogenesis. Furthermore, considering that Sox2 and FN are both expressed in many tissues during development and that they are linked to increased metastasis, it is possible that the control of FN by Sox2 is a general mechanism in tissue remodeling. A wide analysis of the identified binding sites in other models, particularly in Sox2-dependent tumor cells, would be of great interest in the cancer field, especially for the study of metastasis.

4.3. Sox2 regulates cell-matrix adhesion dynamics in Schwann cells

Sox2 overexpression increased cell adhesion and fibrillogenesis in Schwann cells in our *in vitro* model. Our results showed that both focal adhesion and fibrillar adhesion structures are present in Schwann cells upon Sox2 transduction. The first steps in the signaling cascade of cell-matrix adhesion and FN fibrillogenesis include the activation of integrins which increases their affinity to FN (Moser et al., 2009). Integrins, have been implicated in Schwann cell adhesion, as part of the cell-matrix dynamics, and important for Schwann cell migration (Eva & Fawcett, 2014; Feltri et al., 2002; Milner et al., 1997; Previtali et al., 2001).

4.3.1. Integrin expression in SC^{Sox2+}

mRNA levels analysis of the integrin subunits confirmed the expression of $\alpha 5$, αv and $\beta 1$ independently of Sox2 transduction in our *in vitro* model. I did not detect $\beta 3$ expression but I found an up-regulation of the integrin subunit $\beta 8$ in SC^{Sox2+}. A previous study showed (by immunostaining) that the heterodimer $\alpha 5\beta 1$ is expressed in Schwann cells during development and regeneration of

chick peripheral nerves, potentially modulating FN signaling (Lefcort et al., 1992). Another study about the different integrin subunits present in migratory primary rat Schwann cells *in vitro*, showed that $\beta 1$ and αv are also expressed in Schwann cells, but immunoprecipitation assays suggested that $\beta 1$ is not associated with αv in these cells (Milner et al., 1997). The authors found that $\beta 1$ is associated with $\alpha 1$, $\alpha 2$ and $\alpha 6$ and that $\beta 1$ is involved in laminin-dependent Schwann cell migration, probably through $\alpha 6\beta 1$. On the other hand, the same study showed that αv is associated with $\beta 3$ and $\beta 8$ in Schwann cells. Based on the protein expression levels, the authors showed that $\alpha v\beta 8$ resulted as the most abundant heterodimer compared to $\alpha v\beta 3$ (Milner et al., 1997). Furthermore, they also found that FN-dependent Schwann cell migration was reliant on the subunit αv but not on $\beta 1$ or $\beta 3$. However, coating with both substrates showed that $\beta 1$ was the most relevant subunit for glial cell migration (Milner et al., 1997). A more recent study also suggested that $\beta 1$ integrin is not important for primary Schwann cell migration along blood vessels in a 3D *in vitro* model. The author speculate that this subunit is not important during the first steps of regeneration, when Schwann cells invade the bridge between the cut ends of the nerve (Cattin et al., 2015).

These evidences are interesting since they suggest that, in our *in vitro* model, αv probably associated to $\beta 8$ is an important receptor in the signaling cascade of FN to induce migration in Schwann cells. Further studies are necessary to confirm the hypothesis of $\alpha v\beta 8$ as a relevant receptor for FN in migratory Schwann cells *in vivo* and the specific role of the receptor $\alpha 5\beta 1$ in repair Schwann cells. In this regard, another 2D model using fibroblasts to study the early steps in the adhesion dynamic, showed that αv -class integrins first bind to FN inducing the clustering and subsequent binding of the integrin $\alpha 5\beta 1$ to FN, which strengthens the adhesion to the matrix (Bharadwaj et al., 2017). It would be interesting to study if the same crosstalk between FN and these integrins is happening in Schwann cells to better understand the migratory mechanism used by these cells. Additionally, in the *in vitro* model developed in this thesis, it is also necessary to evaluate by immunostaining the activation state of $\alpha 5\beta 1$. This study will confirm if $\alpha 5\beta 1$ changes to a high-affinity state to

promote the formation of fibrillar adhesion upon Sox2 expression and subsequently FN up-regulation.

4.3.2. Focal and fibrillar adhesion structures are present in Sox2-positive Schwann cells

In SC^{Sox2+}, Paxillin and its phosphorylation were observed in long structures in the cell periphery, in agreement with previous studies where Paxillin and pPaxillin stainings showed a similar localization forming focal adhesions (Zaidel-Bar et al., 2007). Paxillin is normally found in the protein complex that forms focal adhesions and acts as an adaptor molecule that recruits other proteins important for cell adhesion, such as FAK. In turn, FAK has the ability to phosphorylate Paxillin (Geiger et al., 2001; Schaller, 2001). Fibrillar adhesions arise from focal adhesions and are associated with the formation of FN fibrillogenesis (Geiger et al., 2001). Focal and fibrillar adhesions are highly dynamic and can be observed in the same migratory cells, as it was shown in fibroblasts in culture (Zamir et al., 2000). Similar to these results, in SC^{Sox2+}, we observed Paxillin and FAK in focal adhesion structures but at the same time, cells were assembling FN in their matrix. In fact, it was reported that localization of FAK in focal adhesion structures is necessary as a first step to fibrillogenesis. Studies have shown that in developing mouse embryos, FN fibril assembly depends on FAK autophosphorylation as an initial step of FAK activation and on its roles as adaptor protein linking focal contacts with the cytoskeleton (Ilić et al., 2004). FAK is normally recruited in the focal adhesion structures to mediate FN-integrin signaling. It facilitates the translocation of FN-integrin complexes of the focal adhesion structure along the actin bundles, which generates ECM contacts and initiation of FN fibrillogenesis (Pankov et al., 2000). Absence of FAK impairs the formation of actin stress fibers necessary for the formation of fibrillary adhesion (Ilić et al., 2004). Our results are consistent with the reported mechanism since we observed an increase in FAK in SC^{Sox2+} together with fibrillogenesis. Additionally, it is still important to evaluate in our *in vitro* model the expression and localization of the protein Tensin. Fibrillar adhesions are characterized by the presence of Tensin (Geiger et al., 2001; Zaidel-Bar et al., 2007). Although we deduced the formation of fibrillar adhesion

in Schwann cells by the existence of FN fibrillogenesis, the presence of Tensin will confirm the formation of this type of adhesion structure.

In Schwann cells, FAK and Paxillin are important for Schwann cell adhesion to the basal lamina and migration. It was shown that Schwann cells increase their expression of FN, integrin $\alpha 5\beta 1$ and FAK, upon Neuregulin1 stimulation in culture, suggesting the formation of focal adhesion structures (Wakatsuki et al., 2014). Before myelination, $\beta 1$ integrin-FAK-Paxillin form a complex important for Schwann cell adhesion to the basal lamina prior to myelination (L.-M. Chen et al., 2000). It is possible that during regeneration in Schwann cells, the same complex is formed ($\beta 1$ integrin-FAK-Paxillin) influencing the adhesion of Schwann cells to their basal lamina for the formation of the Bands of Büngner. Additionally, Paxillin has also been implicated in Schwann cell migration, particularly during development (Miyamoto et al., 2012). Paxillin can be phosphorylated by JNK at Ser-178; this interaction and phosphorylation is necessary for Schwann cell migration along DRG neurons during development (Miyamoto et al., 2012). It would be interesting to investigate the phosphorylation of Paxillin by JNK as well as the formation of the complex $\beta 1$ integrin-FAK-Paxillin during regeneration and their implications for Schwann cell migration and the formation of the Band of Büngner.

4.3.3. FN expression could modulate N-Cadherin-dependent Schwann cell-cell adhesion.

One mechanism responsible for Schwann cell-cell adhesion is Sox2-dependent relocalization of N-Cadherin from the cytoplasm to the plasma membrane (Parrinello et al., 2010). In our system, we confirmed that, upon Sox2 expression, N-Cadherin is localized in the membrane of Schwann cells, specifically in cell-cell junctions, independently of FN expression. However, FN-dependent Schwann cell organization increased the formation of N-cadherin positive cell-cell junctions during their collective movement. Interestingly, in other cell types such as myofibroblasts, it was shown that FN fibril assembly modulates N-cadherin-N-cadherin adhesion complexes (Lefort et al., 2011). The authors proposed a model where N-cadherin recruits integrin $\alpha 5\beta 1$ and tensin, both component of fibrillar adhesion structures. Once FN starts to form the

matrix assembly, N-cadherin/integrin/tensin complex is disrupted allowing the formation of fibrillary adhesion structures which release N-Cadherin into new cell extensions (Lefort et al., 2011). According to the proposed model by Lefort et al., it is possible that FN also has a role in N-Cadherin-dependent Schwann cell-cell adhesion. FN expression could promote a more transient cell-cell adhesion between glial cells that helps to maintain a loose arrangement during their collective migration to form the Band of Büngner. In this regard, it was shown that collective migration of Schwann cells during development was prevented in low calcium medium (Cadherins are calcium-dependent adhesion molecules) due to repulsion between glial cells (Letourneau et al., 1991; Parrinello et al., 2010). Similar effects were shown in other models such as migratory cerebellar granule cells. These cells collectively migrate forming a chain which is disrupted in the absence of N-cadherin (Rieger et al., 2009). These evidences support our hypothesis that in Schwann cells, N-cadherin is necessary for the maintenance of cell-cell adhesion during collective migration, and FN fibrillogenesis induces loose adhesions between cells, disrupting N-Cadherin adherent junctions, which facilitate their dynamic movement during directed migration.

4.4. FN controls Schwann cell alignment and directional migration

We found that Schwann cells align along their self-produced FN matrix which controls their directed migration. Previous studies have already shown that in 2D models, fibroblasts, macrophages and Schwann cells elongate and align along anisotropic FN fibers and have a directional migration (Ahmed & Brown, 1999; Wojciak-Stothard et al., 1997). However, the expression of FN by Schwann cells in vivo was still controversial considering that cells can take FN from endogenous sources and incorporate it to their ECM (Baron-Van Evercooren et al., 1982; Cornbrooks et al., 1983; Lefcort et al., 1992). FN influences cytoskeletal organization, cell adhesion and migration, specifically, it stimulates the polymerization of F-actin bundles (stress fibers) aligned with the matrix (Wojciak-Stothard et al., 1997). These stress fibers, specifically ventral fibers, are connected to focal adhesion and align parallel to the direction of movement (Burrige & Guilly, 2016; Wojciak-Stothard et al., 1997).

Additionally, FN forms fibrillary trails, which provide adequate tension for the directed movement of cells (Doyle & Yamada, 2016). In our *in vitro* model, the staining of F-actin fibers confirmed their alignment with the FN matrix, demonstrating that FN influences Schwann cell cytoskeletal, cell-matrix adhesion and induces a persistent migration. On the other hand, in SC^{Sox2+/Fn1-/-}, directionality was impaired but we observed an increase in the traveled distance. Considering that focal and fibrillary adhesions are strong types of adhesion to the substrate, the increased speed in migration observed in SC^{Sox2+/Fn1-/-} could be explained by the fact that the adhesion to the substrate was reduced in FN KO cells. In summary, in the established *in vitro* model, the up-regulation of FN, controlled by Sox2, promotes the formation of focal adhesions which connect to ventral stress fibers, mature to fibrillar adhesion and induce directional migration of Schwann cells. Additional experiments adding FN to the culture medium of SC and SC^{Sox2+/Fn1-/-} cells to recover the Sox2-dependent phenotype will reinforce our finding, confirming the importance of FN expression induced by Sox2.

4.5. Cell to cell contact between axons and Schwann cells is necessary for proper axon guidance

4.5.1. Self-organized Schwann cells control axon guidance

Different types of ECM proteins have been used as substrates in order to design better materials to improve regeneration (Berrocal et al., 2013; Y. Gu et al., 2014). FN is important for Schwann cell proliferation, migration and influences axonal growth of peripheral neurons (Bailey et al., 1993; Mottaghitlab et al., 2013; Rogers et al., 1983; Whitworth et al., 1995). Here I found that axon guidance only occurs when Schwann cells are present, since FN matrix from decellularized SC^{Sox2+} was not sufficient to guide axons. These results are in agreement with several studies that showed that the presence of Schwann cells in tissue graft or in predesigned conduits improve functional nerve regeneration (Berrocal et al., 2013; Bunge et al., 1989; Dornseifer et al., 2011; Whitworth et al., 1995). Axon growth and guidance is a complex process orchestrated by ECM proteins but also by other proteins expressed and secreted by Schwann cells (Fawcett & Keynes, 1990). For example, Schwann

cells during regeneration express the cell surface adhesion molecules L1CAM, Ng-CAM and NCAM (Daniloff et al., 1986). Blocking these adhesion molecules affect neurite growth on Schwann cells *in vitro*, explaining the higher efficiency observed in tissue graft containing Schwann cells (Bixby et al., 1988). Thus, FN promotes axonal growth but direct contact between axons and Schwann cell surface is necessary for proper neuronal regeneration.

For this reason, new approaches are being developed where more complex structures inside the conduit are designed. For example, tubular structures with not only aligned ECM proteins but also containing neurotrophic support (for example adding NGF and Neuregulin-1 both present in regenerative nerve) have proven to induce the formation of band of Büngner and improve regeneration (Ribeiro-Resende et al., 2009). Interestingly a similar trend is observed in the CNS. Some neurons of the CNS (from embryonic rat cortex and olfactory bulb) cultured in peripheral grafts containing only Schwann cell basal lamina can re-grow, but the efficiency of the grafting is increased when they are cultured together with Schwann cells (Bunge et al., 1989). In this regard, it is important to mention that one difference in the structure of the CNS compared to the PNS, is that neurons are not organized in basal lamina tubes like peripheral nerves (Vracko, 1974). This demonstrates the importance of both basal lamina (rich in ECM proteins) and Schwann cells for the process of nerve regeneration and the potential application for CNS regeneration.

Taken together our results suggest that FN secreted by Schwann cells is mainly important for their own organization. FN expression *in vivo* could be relevant for rebuilding the basal lamina disturbed after neurotmesis and necessary for the maintenance of peripheral nerve architecture and regeneration. Nevertheless, additional direct effects of FN in regenerating axons cannot be discarded, such as increasing axonal growth.

4.5.2. Self-organized Schwann cells guide the axons of mouse sensory neurons and human motor neurons

Regeneration of peripheral neurons depends on the presence of Schwann cells and the existence of a permissive microenvironment that

promotes axon regrowth (Fawcett & Keynes, 1990). Sensory and motor neurons have distinct requirements for their growth and maintenance (Brenner et al., 2006). In fact, Schwann cells from motor neurons differ in the expression of growth factors compared to Schwann cells associated with sensory neurons. For example during regeneration, BDNF is mainly expressed by sensory Schwann cells and GDNF is highly expressed in motor Schwann cells (Höke et al., 2006). Therefore, regeneration of each type of neuron depends on specific cues in the microenvironment. This is one reason why tissue grafts from sensory nerves have a poor functional recovery when used for treatment of motor neuron lesions (Brenner et al., 2006).

Our results showed that mouse sensory neurons and human motoneurons aligned along FN-dependent self-organized Schwann cells independently of their origin (mouse or human) and fate (sensory or motoneuron). This result confirms the importance of Schwann cell presence in the system and suggests that the FN-dependent Schwann cell organization to guide the axons is a general mechanism during nerve repair. However, FN could also play a role inducing axon growth. We observed that in control conditions, where neurons were grown in the absence of Schwann cells but in Laminin-coated culture dishes, sensory neurons grew long axons. On the contrary, motor neurons did not grow in laminin-coated dishes in the absence of FN. In agreement with our results, Gonzales-Perez et al. showed that FN promotes the growth of motoneurons in contrast to Laminin that induces the growth of sensory neurons (Gonzalez-Perez et al., 2016). This difference could be related to a differential expression of integrins in both types of neurons (Gonzalez-Perez et al., 2016). Additionally, it was shown that neurites from human fetal sensory ganglia grow only when they are cultured on laminin-coated dishes but not on FN-coated ones (Evercooren et al., 1982). These data suggest that besides the expression of specific trophic factors by the Schwann cells associated with the two types of neurons, the ECM composition differentially influences the capacity of motor and sensory neurons to regrow. However, our results also show that the process of axonal guidance is a general mechanism that depends on the direct contact with self-organized Schwann cells independently of the type of neurons.

4.5.3. FN fibrillogenesis from fibroblasts is not necessary for axonal guidance

Fibroblasts are present in the nerve tissue and they produce a high amount of FN *in vivo* and *in vitro*. During PNS regeneration, fibroblasts accumulate at the injury site where they do not intermingle with Schwann cells but instead repulse them to trigger their sorting and clustering through the upregulation of Sox2 (Parrinello et al., 2010). The results from this study suggest that fibroblasts do not have a direct impact on axon guidance. As FN can be incorporated from exogenous sources, we wanted to study if FN from fibroblasts can be used by Schwann cells to facilitate their alignment and induce the effect on axon guidance. Even though we observed an increase in FN fibrillogenesis in SC upon fibroblasts contact, we did not observe a significant change in axon guidance. In our *in vitro* model, we used embryonic fibroblasts. These cells have a different origin compared to fibroblasts from peripheral nerve tissues (see below). Nevertheless, both type of fibroblasts produces high amount of FN, therefore we assumed that our data related to the role of FN in our *in vitro* system is relevant.

Fibroblasts from peripheral nerves, also known as endoneurial fibroblast-like cells (EFLCs), are originated from neural crest cells (Richard et al., 2012), whereas common fibroblasts have a mesenchymal origin. Consequently, the gene expression pattern can differ between them. EFLCs, unlike skin fibroblasts, express Neural/Glial Antigen 2 (NG2) (Morgenstern et al., 2003; Richard et al., 2014) and this can differentially modulate the responses of surrounded cells. NG2 has an inhibitory effect on axon growth. It was proposed that its expression by endoneurial fibroblasts-like cells during regeneration increases the mobility of non-neuronal cells and at the same time repulses the axons, which keeps the axons in contact with Schwann cells and not with the fibroblasts (Morgenstern et al., 2003). These evidences suggest that EFLCs do not directly affect axon guidance. In our model, despite the origin of the fibroblasts, we also did not observe changes in axon guidance in the presence of fibroblasts. More studies using co-cultures between EFLCs, Schwann cells and neurons will help to understand the role of the FN produced by EFLCs and by Schwann cells in axonal regeneration.

4.6. Schwann cell migration: comparison of 2D and 3D *in vitro* models

Migration of cells is determined by intrinsic and extrinsic factors. Physical properties of the cell microenvironment is one parameter that defines the type of migration (Charras & Sahai, 2014). Among the physical properties are the rigidity of the substrate, the grade of confinement, the adherent properties and the topology of the surface (Charras & Sahai, 2014). Thus, the same cell can have various types of migration depending on the properties of the extracellular microenvironment (Doyle & Yamada, 2016; R. J. Petrie & Yamada, 2012).

In vitro models have been widely used to study the molecular dynamics of cell-matrix adhesion and migration (Doyle & Yamada, 2016). One of the advantages of *in vitro* compared to *in vivo* systems is the possibility to control molecular and mechanical parameters that modulate cell behavior. Besides, *in vitro* models allow to test several factors in shorter times. Schwann cell migration has been extensively studied using diverse *in vitro* systems, using 2D and 3D models. Interestingly, in 2D models using various ECM substrates, it has been shown that Schwann cell migration is integrin-dependent (Barros et al., 2011; Lefcort et al., 1992; Wakatsuki et al., 2014). However, in a recent study using a 3D microenvironment made of fibrin or Matrigel, it was proposed that Schwann cell migration do not depend on integrins, specifically integrin $\beta 1$ (Cattin et al., 2015). The author observed that Schwann cells do not form focal adhesion, as it is shown in 2D models. Schwann cells, when co-cultured with endothelial cells in 3D fibrin gel or Matrigel, use endothelial cells as scaffold and have an amoeboid type of migration (Cattin et al., 2015). Considering that cells can switch the mode of migration depending on the matrix structure and composition (R. J. Petrie & Yamada, 2012), it cannot be discarded that Schwann cells also have diverse types of migration depending on the extracellular environment conditions. It would be interesting to test a 3D matrix with and without FN and evaluate Schwann cell migration before and after Sox2 expression since in the aforementioned study about Schwann cell migration in 3D matrices, Sox2 expression was not considered or reported. In summary, our *in vitro* 2D system allowed us to stablish a model where we identified differentially expressed ECM-related genes such FN, which resulted as a key

component in Schwann cell behavior dependent on Sox2. The future experiments should be focus on translating these findings to *in vivo* conditions to better characterize ECM dynamics during PNS regeneration.

4.7. Role of Sox2 in Schwann cells during regeneration in vertebrates

4.7.1. Sox2-dependent FN fibrillogenesis could regulate the formation of the Band of Büngner in mammals

Previous studies on PNS regeneration after neurotmesis, have shown that Schwann cells enter the bridge between the nerve stumps using blood vessels as a migratory scaffold and that fibroblasts in the injury area induce Sox2 expression in Schwann cells which promotes cell-cell adhesion via N-Cadherin adherent junctions (Arthur-Farraj et al., 2012; Cattin et al., 2015). These processes are important for the formation of the Band of Büngner to help axonal growth. We demonstrated *in vitro* that Sox2-dependent Schwann cell organization via FN fibrillogenesis governs axon guidance. This process happens indirectly through the coordinated alignment of the Schwann cells. Based on our *in vitro* results, we hypothesized that Sox2 up-regulation could regulate repair Schwann cell collective migration in a FN-dependent manner and guide the axons through the Band of Büngner *in vivo*. Future *in vivo* experiments in mice models, using FN conditional KO in Schwann cells during the regeneration, will also confirm the importance of FN expression by the Schwann cells during nerve repair.

Another reported regulator of the Band of Büngner formation is C-Jun. According to Arthur-Farraj et al., c-Jun is important for the maintenance of the bipolar phenotype of repair Schwann cells necessary for the formation of the Band of Büngner (Arthur-Farraj et al., 2012). It is possible that Sox2 and c-Jun have a synergistic role to first modify Schwann cells morphology and behavior, then guide neurons and finally promote neuronal survival. More studies are needed to understand their possible interactions. Until now, it was only showed that Sox2 is not downstream of c-Jun, since Sox2 expression is not affected in c-Jun null mice (Arthur-Farraj et al., 2012). Further *in vivo* studies with conditional Sox2 KO in Schwann cells would be necessary to investigate the

importance of Sox2 in FN fibrillogenesis, basal lamina formation, collective migration of Schwann cells and its possible interaction with C-Jun.

4.7.2. Sox2 could induce FN expression in repair Schwann cells also *in vivo*

In agreement with previous studies, we observed that FN fibrillogenesis is highly activated upon rat nerve injury in the gap between the two cut ends of the nerve and in the distal stump (Lefcort et al., 1992; Wakatsuki et al., 2014). Additionally, we showed that Schwann cells can produce their own FN to incorporate it in their ECM. The fact that we observed in repair Schwann cells that Sox2 expression was upregulated at day 4 and it was followed by FN expression suggested that *in vivo* Sox2 could also directly regulate FN expression. To confirm this hypothesis, a Sox2 conditional KO is needed to evaluate if FN expression is impaired in Sox2 null Schwann cells during PNS regeneration.

4.7.3. The FN containing EIIIA spliced domain could be important for Schwann cell matrix assembly *in vivo*

We confirmed *in vivo* the expression of the FN containing the spliced domain EIIIA and its up-regulation upon nerve injury in the PNS. We also confirmed *in vitro* the upregulation of this isoform together with EIIB after Sox2 overexpression. The specific role of the FN domain EIIIA and EIIB in the PNS is still not well understood. We hypothesized that inclusion of the EIIIA domain in FN could play a major role in Sox2-dependent Schwann cells organization and migration for proper axonal growth, through the modulation of matrix assembly. This domain has been suggested to affect matrix levels (Purva Singh et al., 2010) and to decrease cell adhesion and spreading when expressed alone in fibroblasts, leading to their rapid migration (Hashimoto-Uoshima et al., 1997). In the PNS, EIIIA and EIIB are expressed upon injury in the endoneurial tubes and in Schwann cells in culture (Mathews & French-Constant, 1995), suggesting a possible role in the assembly and/or maintenance of the matrix important for the directed migration of Schwann cells. Additionally, FN isoforms containing the EIIIA and EIIB domains are important for angiogenesis during embryonic development and wound healing (R. Hynes, 2007). Since Schwann

cells and new generated blood vessels are in close contact in the injured area of regenerative nerves, it would be of great interest to investigate the specific role of the FNEIIIA and FNEIIIB domains in the dynamic between Schwann cells migration, axonal guidance and blood vessels formation in this context. More studies about the expression of all the distinct FN isoforms are also needed to have an accurate characterization of the FN matrix in the basal lamina of Schwann cells important for regeneration and PNS homeostasis.

In addition, it remains to be elucidated which integrin receptor is mediating FNEIIIA signaling in Schwann cells *in vivo*. The $\alpha 4\beta 1$ and $\alpha 9\beta 1$ integrins have been described as receptors of this spliced domain (Liao et al., 2002). The $\alpha 4\beta 1$ receptor is expressed in leukocytes, important for their adhesion and in fibroblasts to induce their differentiation to myofibroblasts (White & Muro, 2011). The $\alpha 9\beta 1$ integrin is expressed in lymphatic endothelial cells and its interaction with the EIIIA spliced domain promotes matrix assembly, important for the formation of lymphatic valve leaflets *in vivo* (Bazigou et al., 2009). In wounded skin, $\alpha 9\beta 1$ -EIIIA interaction in keratinocytes is important for re-epithelization processes such as cellular migration, differentiation or proliferation (P. Singh et al., 2004). These data suggest that $\alpha 9\beta 1$ could be a possible receptor in Schwann cells for FNEIIIA, already reported to be expressed in Schwann cells (Clegg et al., 2003). Characterization of the integrin expression in proregenerative Schwann cells *in vivo* including the αv and $\beta 1$ subunits (important for Schwann cell migration according to *in vitro* studies) would contribute to the understanding of FN matrix dynamic during nerve regeneration.

4.7.4. Sox2 is not involved in the zebrafish posterior lateral line regeneration

To study the relevance of Sox2 in the PNS of non-mammalian vertebrates, I evaluated Sox2 expression in Schwann cells during the development and regeneration of the pLL in zebrafish larvae. Contrary to what occurs in mammals, we found that migratory zebrafish Schwann cells do not express Sox2 during development or after peripheral nerve injury. These results suggest that the Sox2-dependent mechanism observed in mammal Schwann

cells is not conserved within vertebrates. Sox2 expression has been investigated in the pLL and its expression has been confirmed in the protoneuromast and in supporting cells of the neuromast, important for the regeneration of the hair cells of the mechanosensory organ (Hernandez et al., 2006; Pinto-Teixeira et al., 2015). Our results are consistent with these since we detected Sox2 expression in the protoneuromast during development and in the sustentacular cells (supporting cells) of the neuromast. However, it was not reported if Sox2 has a role in Schwann cells during the regeneration of the pLL. Here I demonstrated that Sox2 is not present in Schwann cells during regeneration. Nevertheless, it cannot be discarded that other Sox protein could be involved in the process of nerve regeneration in zebrafish. The SoxB1 family in zebrafish is composed of 6 genes, Sox1a/b, Sox2, Sox3 and Sox19a/b (Y. Okuda et al., 2006) and specifically Sox2, Sox3 and Sox19a/b are functionally redundant during early steps of development (Yuichi Okuda et al., 2010). Studies have also shown that Sox1a/b, Sox3 and Sox19a/b are expressed during development of the CNS in zebrafish (Yuichi Okuda et al., 2010; Y. Okuda et al., 2006). Moreover, Sox3 expression during the first 26 hours of zebrafish development was shown to be important for the generation of the pLL placodes (Nikaido et al., 2007). Further analysis of SoxB1 proteins during the regeneration of the pLL in zebrafish are needed to investigate if they are necessary for axon regeneration in non-mammalian vertebrates.

4.8. Concluding remarks and future perspectives

Cell movement is a complex process driven by diverse intrinsic and extrinsic factors related to the cell microenvironment. A deeper understanding of the mechanisms that control cell behavior will facilitate the improvement of therapies for tissue repair. The results obtained in this doctoral thesis provided new insights into PNS glial cell migration, where we found that the key transcription factor Sox2 targets FN to promote the organization and oriented migration of the Schwann cell line RSC96 for proper axonal growth, describing a novel role of Sox2 in cell-matrix dynamics. These results could contribute to our understanding on the dynamic cross-talk between Schwann cells and ECM during tissue repair, with potential applications in regenerative therapies.

Nowadays, nerve graft is the best option after severe neurotmesis, with 50% of successful recovery but with significant side effects (W. Daly et al., 2012). In order to have an alternative treatment, it is necessary to design more complex conduits that modulate in space and time the processes taking place in a regenerative nerve. For example, conduits coated with different ECM molecules have been tested but functional recovery is still poor (W. Daly et al., 2012). Here I presented evidence that FN matrix alone is not enough for proper axonal growth *in vitro*. In this regard, we need a better characterization of additional ECM components produced by Schwann cells and other cell types *in vivo* as well as additional signaling molecules involved in the formation of the Band of Büngner and relevant for directional axonal growth. Furthermore, in the developed *in vitro* system, I also identified additional ECM-related genes significantly regulated in Sox2-positive Schwann cells with potential roles in the repair Schwann cell phenotype. Further investigation on these additional candidates will improve our knowledge on Schwann cell biology during PNS regeneration.

5. Materials and Methods

5.1. Materials

All reagents and equipment used in this work were purchased from: American type culture collection, ATCC, Virginia, USA; Thermo Fisher Scientific, Massachusetts, USA; Clontech takara, California, USA; Bioline, Singapore; Qiagen, Venlo, Netherlands; GE Healthcare, Little Chalfont, United Kingdom; Vector Labs, California, USA; Illumina, California, USA; InvivoGen, California, USA; New England Biolabs, NEB, Massachusetts, USA; ROCHE, Basel, Switzerland; Carl Zeiss, Inc, Jena, Germany; Vilver Lourmat, Eberhardzell, Germany; Diagenode, Seraing, Belgium; BD Biosciences, California, USA; Eppendorf, Hamburg, Germany; Bio-rad, California, USA; PeqLab, VWR, Erlangen, Germany; Hettich Lab technology, Edersberg, Germany; Bio-rad, California, USA; Berthold Technologies, Bad Wildbad, Germany; Life technologies, Invitrogen and Gibco (Thermo Fisher); Sigma-Aldrich, Missouri, USA; Miltenyi Biotech, Bergisch Gladbach, Germany; ENZO, New York, USA; Stemcell Technologies, Vancouver, Canada; R&D, Vienna, Austria. Genomatix, Munich, Germany; Laborversand, Würzburg, Germany; Cell Biolabs, Inc. California, USA, Mirus Bio, Wisconsin, USA. Abcam, Cambridge, United Kingdom; Merck Millipore, Massachusetts, USA.

5.1.1. Animal strain

Animal model	Source	Identifier
Wild type mice, CD-1	Charles Rivers	Strain code: 022
Zebrafish: Tg[gSAGFF202A;UAS:EGFP]	Xiao et al, 2015	
Zebrafish: Tg[SILL:mCherry]	Xiao et al, 2015	
Zebrafish larvae: Tg[gSAGFF202A;UAS:EGFP;SILL:mCherry]	This work	
Wild type adult female rats:		Strain code:

Sprague-Dawley	Charles River	400
----------------	---------------	-----

5.1.2. Cell lines

Cell line	Source	Identifier
Rat Schwann cells: RSC96 (SC)	ATCC	CRL-2765
Rat Schwann cells overexpressing Sox2: RSC96_Sox2+ (SC ^{Sox+})	This work	
Rat Schwann cells overexpressin Sox2, Fn1 knockout: RSC96_Sox2_Fn1KO (SC ^{Sox2+/Fn1-/-})	This work	
Rat Schwannoma: RT4-D6P2T	ATCC	CRL-2768
Mouse Fibroblast Flox/Flox: FB	Prof. Reinhard Fässler	
Mouse Fibroblast Fn1 knockout: FB ^{Fn1-/-}	Prof. Reinhard Fässler	
Human HEK retroviral packaging cells: GP2-293	Dr. Salvador Aznar Benitah	
Mouse fibroblast: NIH/3T3	Prof. Magdalena Götz	ATCC CRL-1658
Human skin fibroblast for iPSC reprograming: BJ	ATCC	CRL-2522
Fibroblast-derived iPS cells	Dr. Micha Drukker	

5.1.3. Bacteria strain

Bacteria strain	Source	Cat#
Escherichia coli DH5 alpha	Thermo Fisher	18265017

5.1.4. Reagents

Reagent	Company	Cat. #
Laminin	Sigma	L2020-1mg
DPBS	Life technologies	14190094
Fibronectin from human plasma	Sigma	F0895-1mg
Poly-L-Ornithine	Sigma	P3655-10mg
High-Glucose Dulbecco's modified Eagle's medium, DMEM	Life technologies	10938-025
Fetal bovine serum (FBS)	Life technologies	10270106
L-Glutamine	Life technologies	25030-024
Penicillin plus 50 mg/ml Streptomycin	Life technologies	15140-122
DMEM/F12 medium	Life technologies	11320074
N-2 supplement A	Life technologies	17504-044
Insulin	Life technologies	12585014
Non-essential amino acid	Sigma	M7145-100ml
2-mercaptoethanol	Life technologies	21985-023
Neurobasal medium	Life technologies	21103049
B27 supplement with Vitamin A	Life technologies	17504-044
Knock-out DMEM medium	Gibco	10829-018
Knock-out serum replacement	Gibco	10828-028
Recombinant mouse beta Nerve growth factor, mNGF	R&D	1156-NG-100
mTeSR1 medium	Stemcell Technologies	05850
LDN193189	ENZO	BV-1995-5
SB431542	Miltenyi; StemMACS	130-106-275
Human BDNF	Miltenyi Biotech	130-096-286
Human GDNF	Miltenyi Biotech	130-098-449
Db cAMP	Sigma	D0260

MATERIALS AND METHODS

Human IGF-1	Miltenyi Biotech	130-093-886
Human SHH C24II	Miltenyi Biotech	130-095-727
Retinoic acid	Sigma	R2625
DMEM-D-Valine	PAA/GE Healthcare	Med-250
Bovine pituitary extract	Sigma	P1476
Forskolin	Sigma	F6886
Amphotericin B	Sigma	A2942
Collagenase I	Sigma	C0130
Triton X-100	Sigma	T8787
cOmplete, EDTA-Free inhibitor cocktail	Protease Roche	11 873 580 001
40% Acrylamide/Bis Solution	Bio-Rad	161-0144
Tissue-Tek O.C.T compound	Laborversnad	--
Aquatex mounting medium	Merk Millipore	108562
Paraformaldehyde, PFA	VWR	43368.9M
Polybrene	Sigma	107689-10G

5.1.5. Consumables

Product description	Company	Cat. #
StemPri EZPassage™, disposable Stem cell passaging tool	Thermo Fisher	23181-010
10 mm cover glasses	VWR	6310149
Peel-A-Way embedding molds	Sigma	E6032
PVDF WB membrane	Roche	3010040001
0.65 ml Bioruptor Pico Microtubes	Diagenode	C30010011
Opaque 96-well/plate	BD Falcon	353219

5.1.6. Commercial Kits

Kit	Company	Cat. #
Xfect reagent	Clontech takara	631318
Pierce BCA Protein Assay	Thermo Fisher Scientific	23227
TransIT-S2 Dynamic Delivery System	Mirus,	MIR 6003
MAGnify Chromatin Immunoprecipitation System	Thermo Fisher Scientific	492024
Gelatin Sepharose 4B	VWR	17-0956-01
SuperScript III First-Strand Synthesis SuperMix	Thermo Fisher Scientific	18080400
PureLink HiPure Plasmid Maxiprep	Thermo Fisher Scientific	K210017
Isolate II RNA Mini		Bio-52072
Taq PCR Core	Qiagen	201223
QIAprep spin Miniprep	Qiagen	27104
QIAquick gel extraction	Qiagen	28704
QIAquick PCR purification	Qiagen	28104
Amersham ECL prime western blotting detection reagent	GE Healthcare	RPN2236
Illustra microspin G-50 columns	GE Healthcare	27-5330-01
DAB peroxidase substrate	Vector Labs	VEC-SK-4100
VECTASTAIN ABC kit	Vector Labs	VEC-PK-6101
SurePrint G3 Rat Gene Expression 8x60K Microarray (amamid ID: 028279)	Agilent	G4853B
Quanti-Luc	InvivoGen	rep-qlc1
Q5 Site-Directed Mutagenesis	NEB	E0554
DIG RNA labelling (SP6/T7)	ROCHE	11175025910
Power Syber Green Master Mix	Thermo Fisher Scientific	4367659

TOPO TA cloning kit	Invitrogen, Life technology	451641
---------------------	--------------------------------	--------

5.1.7. Cell culture media and solutions

Laminin coating solution:

- 5 µg/ul Laminin
- 50 ml DPBS

FN coating solution:

- 500 µg/µl FN from human plasma
- 50 ml DPBS

Poly-L-Ornithine coating solution:

- 15 µg/µl Poly-L-Ornithine
- 50 ml DPBS

Collagen I and IV coating

- 10 µg/cm²
- 50 ml DPBS

Maintenance DMEM medium:

- 500 ml High-Glucose Dulbecco's modified Eagle's medium, DMEM
- 10% (v/v) Fetal bovine serum
- 4 mM L-Glutamine
- 50 U/ml Penicillin plus 50 mg/ml Streptomycin

N-2 medium:

- 500 ml DMEM/F12 medium
- 1% (v/v) N-2 supplement A
- 5 µg /ml Insulin
- 1 mM L-Glutamine
- 100 µM Non-essential amino acid
- 100 µM 2-mercaptoethanol

- 50 U/ml Penicillin plus 50 mg/ml Streptomycin

B-27 medium:

- 500 ml Neurobasal medium
- 1% (v/v) B27 supplement with Vitamin A
- 1 mM L-Glutamine
- 50 U/ml Penicillin plus 50 mg/ml Streptomycin

KSR medium:

- 500 ml Knock-out DMEM medium
- 10% (v/v) Knock-out serum replacement
- 4 mM L-Glutamine
- 50 U/ml Penicillin plus 50 mg/ml Streptomycin

DrqN medium:

- 500 ml Neurobasal medium
- 1% (v/v) N-2 supplement A
- 1% (v/v) B27 supplement with Vitamin A
- 100 U/ml Penicillin plus 100 mg/ml Streptomycin
- 4 mM L-Glutamine
- 50 ng/ml Recombinant mouse beta Nerve growth factor, mNGF

mTeSR1 medium:

- 500 ml mTeSR1

Neural induction medium:

- 100 ml Mixture of N-2 Medium plus B-27 Medium (ratio 1:1)
- 100 nM LDN193189
- 10 μ M SB431542

Human Motor Neurons, maintenance medium:

- 100 ml Mixture of N-2 Medium plus B-27 Medium (ratio 1:1)
- 20 ng/ml Human BDNF
- 20 ng/ml Human GDNF
- 0.1 μ M Db cAMP

- 100 ng/ml Human IGF-1
- 100 ng/ml Human SHH C24II
- 100 nM Retinoic acid

Human motor neurons, co-culture medium:

- 100 ml Mixture of N-2 Medium plus B-27 Medium (ratio 1:1)
- 20 ng/ml Human BDNF
- 20 ng/ml Human GDNF
- 100 ng/ml Human IGF-1

Primary rat Schwann cells medium:

- 500 ml DMEM-D-Valine or standard DMEM
- 20 µg/ml Bovine pituitary extract
- 2 mM L-Glutamine
- 10 %(v/v) Fetal bovine serum
- 1 %(v/v) N-2 supplement A
- 5 µM Forskolin
- 0.25 µg/ml Amphotericin B
- 100 U/ml Penicillin plus 100 mg/ml Streptomycin

Collagenase solution:

- 50 ml High-Glucose Dulbecco's modified Eagle's medium, DMEM
- 0.05% (wt/v) Collagenase I

Decellularization solution:

- 10 ml DPBS
- 0.5% (v/v) Triton X-100
- 20 mM Ammonium hydroxide

5.1.8. Immunohistochemistry solutions

Permeabilization solution:

- 0.3% Triton X-100
- 10% Goat or Donkey serum
- Phosphate buffer saline, PBS

Antibody solution:

- 10% Goat or Donkey serum
- PBS

In situ solutions:

Prehybridization buffer (for 50 ml):

- 25 ml deionised formamide
- 12.5 ml 20X SSC (DEPC treated)
- 1.25 ml tRNA (10mg/ml)
- 5 ml 50X Denhardt's solution
- 2.5 ml Herring sperm (10mg/ml)
- 6.25 ml DEPC treated H₂O

Buffer 1:

- 0.1 M Tris-HCl pH:7.5
- 0.15 M NaCl
- H₂O Milliq up to desire volume

20X SSC, pH:7.0:

- 3 M NaCl
- 300 mM Trisodium citrated
- H₂O Milliq up to desire volume

Blocking solution for *in situ*:

- 10% Donkey serum in Buffer 1

NTMT 2X:

- 25 ml 4M NaCl
- 100 ml 1M Tris-HCl pH:9.5
- 100 ml 0.5M MgCl₂
- 10 ml 10% Tween-20
- 265 ml H₂O Milliq

50% formamide, 5X SSC:

- 100 ml Formamide
- 50 ml 20X SSC
- 50 ml H₂O Milliq

10% PVA:

- 20 g PVA power
- 200 ml H₂O Milliq
- Heat at 180 on a hot plate while stirring until it is completely dissolved

Acetylation solution:

- 5.32 ml Triethanolamine
- 0.64 ml HCl
- 1 ml Acetic acid anhydride
- 400 ml H₂O DEPC treated

5.1.9. Immunocytochemistry solutions

Fixative solution, 4% PFA:

- 4% (v/v) Paraformaldehyde, PFA 16%
- PBS

Permeabilization solution:

- 0.3% Triton X-100
- 0.5% Bovine serum albumin, BSA
- Phosphate buffer saline, PBS

Antibody solution:

- 1% BSA
- PBS

Mowiol:

- 2.4 g Mowiol 4-88
- 6 g Glycerol
- 6 ml H₂O

- 12 ml Tris-Cl 0.2M, pH:8.5
- Heat to 50°C for 10 min and clarify by centrifugation at 5000g for 15 min

30% sucrose solution:

- 30 g Sucrose
- Up to 100 ml H₂O

Heat-Induced antigen retrieval buffer:

- 10mM Sodium citrate
- Distilled H₂O up to desire volume.
- pH: 6.0, adjusted before adding the Tween-20
- 0.05% (v/v) Tween-20

5.1.10. Molecular solutions

TAE-buffer (10x):

- 180 mM Tris-Base, pH:8.3
- 180 mM Acetic acid
- 5 mM EDTA

Agarose gels:

- 1% or 2% (v/v) agarose
- 1X TAE buffer

LB medium

- 10 g/l Bacto-Trypton
- 5 g/l Bactor-yeast extract
- 10 g/l NaCl
- pH: 7, Autoclave (120°C, 20 minutes)

LB agar

- 10 g/l Bacto-Trypton
- 5 g/l Bactor-yeast extract
- 10 g/l NaCl
- 15 g/l Bacto-agar

- pH: 7, Autoclave (120°C, 20 minutes)

5.1.11. Protein isolation solutions

RIPA buffer (radioimmunoprecipitation assay buffer):

- 150 mM NaCl
- 1.0% NP-40
- 0.5% sodium deoxycholate
- 0.1% SDS (sodium dodecyl sulphate)
- 50 mM Tris-HCl, pH 8.0
- 1% (wt/v) cOmplete, EDTA-Free Protease inhibitor
- 5 mM EDTA, pH:8
- H₂O up to desire volume

Running buffer (Tris-Glycine/SDS):

- 25 mM Tris base
- 190 mM glycine
- 0.1% SDS
- H₂O up to desire volume

Transfer buffer:

- 25 mM Tris base
- 192 mM Glycine
- 20% Methanol
- H₂O up to desire volume

Laemmli 4x buffer/loading buffer:

- 8% SDS
- 1 M DTT, Dithiothreitol
- 40% Glycerol
- 1% Bromophenol blue
- 200 mM Tris ph:6.8
- H₂O up to desire volume

TBS:

- 50 mM Tris base
- 150mM NaCl

TBS-T:

- TBS
- 0.1% Tween-20

Blocking Solution:

- 5% of Milk or BSA (in case of phosphorylated antibodies) in TBS-T buffer

Stripping solution:

- 20 ml SDS 10%
- 12.5 ml Tris HCl pH 6.8 0.5M
- 67.5 ml ultra pure water
- Add 0.8 ml β -mercaptoethanol under the fumehood.

Acrylamide stacking gel 4% (8 ml):

- 4.2 ml H₂O
- 1.6 ml 40% Acrylamide/Bis Solution
- 2 ml Tris 1.5 M, pH:8.8
- 80 μ l SDS 10%
- 80 μ l APS (ammonium persulfate) 10%
- 8 μ l TEMED (N,N,N',N'-Tetramethylethylenediamine)

Acrylamide resolving gel 8% (5ml):

- 3.1 ml H₂O
- 0.5 ml 40% Acrylamide/Bis Solution
- 1.25 ml Tris 0.5 M, pH:6.8
- 50 μ l SDS 10%
- 50 μ l APS 10%
- 5 μ l TEMED

5.1.12. Plasmid list

Plasmid	Company	Cat. #
pMXs-Sox2	Gift from Shinya Yamanaka, Addgene	13367
pMXs	Cell Biolabs	RTV-010
pCMV-VSV-G	Addgene	8454
pSpCas9(BB)-2A-GFP	Gift from Feng Zhang, Addgene	48138
pDRIVE5Lucia-hFibronectin	InvivoGen	pdrive5lc-hfn
pDRIVE5Lucia control	This work	
pDRIVE5Lucia-hFibronectin Sox2 binding site mutation	This work	
pGEM-2 Rat Fibronectin EIIIA	Gift from Richard Hynes, Addgene	14059
pCS2+	Laboratory of Dr. Hernán López-Schier	
pCS2+Fn1EIIIA	This work	

5.1.13. Antibody list

Antibody	Company	Cat#	Dilution IHC/ICC	Dilution WB	Dilution CHIP
Donkey anti-Rabbit IgH (H+L) Alexa Fluor 488	Thermo Fisher	A-21206	500		
Donkey anti-Mouse IgH (H+L) Alexa Fluor 555	Thermo Fisher	A-31570	500		
Donkey anti-Goat IgH (H+L) Alexa Fluor 555	Thermo Fisher	A-21432	500		
Goat anti-Rabbit IgH (H+L) Alexa Fluor 633	Thermo Fisher	A-21070	500		
Goat anti-Mouse IgH (H+L) Alexa Fluor 633	Thermo Fisher	A-21052	500		
Alexa Fluor 568 Phalloidin	Thermo Fisher	A-12380	200		

MATERIALS AND METHODS

Alexa Fluor 488 Phalloidin	Thermo Fisher	A-12379	200		
Anti-Choline Acetyltransferase (CHAT)	Abcam	ab18736	1:200		
Anti-Focal adhesion kinase (FAK)	Cell signaling	3285	1:50	1:500	
Anti-phospho (pFAK)	Invitrogen	44-6246	1:50	1:4.000	
Anti-Fibronectin	DAKO	AO215	1:1.000	1:4.000	
Anti-GAPDH HRP	Sigma	G9295		1:50.000	
Anti-GFAP	DAKO	ZO334	1:200		
Anti-Histone3 (H3)	Cell signaling	9715			1:15
Anti-phosphoHistone 3	Millipore	06-570	1:200		
Anti-Rabbit HRP	Jackson Labs	11-035-003		1:5.000	
Anti-Mouse HRP	Sigma	A5278		1:10.000	
Anti-IgG (From MAGnify KIT)	Invitrogen	Module 3, 49-2024			1:100
Anti-Islet 1	Abcam	ab20670	1:200		
Anti-Neurofilament heavy polypeptide (NFH)	Abcam	ab4680	1:400		
Anti-Paxillin	Cell Signaling	12065	1:50	1:40.000	
Anti-phospho Paxillin	Cell Signaling	2541	1:50		
Anti-Sox2 (For immunocytochemistry)	Cell Signaling	4900S	1:100	1:3.000	
Anti-Sox2 (For ChIP)	Cell Signaling	2748			1:25
Anti-Sox2 (For zebrafish immunostaining)	Abcam	ab97959	1:100		
Anti-Sox2 (For immunohistochemistry)	Santa Cruz	sc-17320	1:100		
Anti-TUBB	Sigma	G9295		1:4.000	
Anti-TUBB3	Biolegend	MMS-435P	1:500		
Anti-Goat biotinylated	Vector	BA-5000			

DAPI	Thermo Fisher	D-1306	1:100
PI	Abcam	Ab14083	1:1000

5.1.14. Primer list for semiquantitative RT-PCR**Rat primer**

Gene	Forward Primer	Reverse Primer	Cycles
<i>Adamts9</i>	caaccagaccaagcaacc	gaccaagcactctgaccac	35
<i>Antxr1</i>	gaacagtcaaggatacaggacag	cagcaagtaagtatcttctacagc	35
<i>Cdh6</i>	cggaaacaggtatcatcaagac	tctccacatcagcatcac	35
<i>c-Jun</i>	gtgaccgactgttctatgac	gtgatgtgccattgtg	35
<i>Clmp</i>	catccaagcccaagtgtgag	gcgcttctcggatttcattagg	35
<i>Clu</i>	gctccaagaactgtccactc	gtatgtatgatgccagacgcc	35
<i>Cx3cl1</i>	gcgcttttcatctgtgtactc	tctcgtctccaggatgatgg	35
<i>Emb</i>	tacatgagtaatggaactgcac	attctttcccatcatctgggtc	35
<i>Fbln1</i>	atgtcagaagaatgtgccca	cactcatcaatatcttcgcagg	35
<i>Fgfr1</i>	gatgtaatccagcgtactcgt	ggcaacaccacaaacttctg	35
<i>Fn1</i>	caagaccatacctgccgaat	ccgtgtaagggtcaaagcat	28
<i>Gapdh</i>	aatgcatcctfcaccaccaac	ggaggccatgtaggccatgag	28
<i>Gfap</i>	ccaagtttgacagacctcaca	tccttaatgacctcgccatc	28
<i>Hpse</i>	cctcgttctgtccatcac	accgcaaatatcattgtgtc	35
<i>Itga1</i>	gttcaacgtagcctcaccg	ctcctcactgtcactgtgtg	35
<i>Itga5</i>	cagaaggaggagatttggg	agggcatttcaggactgtg	35
<i>Itgav</i>	aggtgacgggactcaacaac	agccgagctttagaggaca	35
<i>Itgb1</i>	cgcatatctggaaacttggga	ctgaagaaagggaattgtaggc	35
<i>Itgb3</i>	ggtgaaagaactgacggatactg	ggtgatattggtgaagggtgga	35
<i>Itgb5</i>	tagacagcattgtcaaagacga	gtccactgagccattgtagg	35
<i>Itgb6</i>	gagatacagcatcctcaacg	cattcaccacagtcacagtc	35
<i>Itgb8</i>	tctcaatccaactgcatccag	gccatccaatatgactctcacag	35

<i>Krox20</i>	cagtaccctggtgccagctg	tgtggatctctctggcacgg	35
<i>Krox24</i>	ccacaacaacagggagacct	tcttgcgttcatcactcctg	35
<i>Lama5</i>	agcagttcagtgctaccctg	cccaatgttctcgtcaatgc	35
<i>Lmo1</i>	tggtttggaccaagaggac	cagatgttgggcggtactga	35
<i>Mmp3</i>	cttgaaggtctgggaggag	gctacacattggttaaggtctcag	35
<i>Mmp10</i>	tctgctcagcatatcctctg	gtctccatgttctccaactg	35
<i>Mmp13</i>	gacctctacagttgatagactcc	agtcaccatgttctttagttcc	35
<i>Mybpc2</i>	tgtcaaagagcctccagtc	tgcccgttaccttctcatcag	35
<i>N-cad</i>	gtgtgaaagtttgccaat	aagtcatagtctctgtct	30
<i>Nestin</i>	aaccacaggagtgggaactg	gcctctttggtcctttcc	35
<i>p75NTR</i>	gagggcacatactcagacgaa	gtctatatgttcaggctggta	30
<i>Plat</i>	gtgatatagataccagagcaacct	ttccaacatagcagtcctcag	35
<i>Podxl</i>	tacttactacatccaaaccgacag	tccttcagcagttcaaacac	35
<i>Ptn</i>	gaatgtgacctcaataccgcc	catcttctcctgtttcttgct	35
<i>Ptprq</i>	acgccaaccatacttctgct	cagcctctggaacagactcc	35
<i>S100b</i>	atagcacctccgttgacag	gtcctatggggacaatggtg	35
<i>Serpine2</i>	tgatgcgatacaatgtgaacgg	tttgtagaccagagcgg	35
<i>Sox2</i>	agaacccaagatgcacaac	atgtaggctcgcgagctggt	30
<i>Sox10</i>	atcagccctcaggaccctat	agggttattctggggatgc	35
<i>Tgm2</i>	gctcaaattccatcaacaattcc	atgctgttctcagagtaggg	35
<i>Tnc</i>	gtctccacagccaaagaacc	aatatcccttcatcagcagtcca	35
<i>Tnfaip6</i>	aacccgaacgcaaaggag	gtgctgatgatgtcttctgg	35

Mouse primers

Gene	Forward Primer	Reverse Primer	Cycles
<i>Gpc1</i>	tggggacctgtatacgcaga	acaccgccaatgacactctc	35
<i>Gpc4</i>	ctgctttccatcgggtctcattctg	aggctctggctgcaacaaatgcg	35

c

Human Primers

Gene	Forward Primer	Reverse Primer	Cycles
<i>GAPDH</i>	ccccttcattgacctcaactaca	ttgctgatgatcttgaggctgt	28
<i>MAP2</i>	gcagttctcaaaggctagac	ttgatcgtggaactccatct	35
<i>ISL-1</i>	gccaatatttcccacttagcc	tcccgtaacaacctgatataatctc	35
<i>NFH</i>	cctaccaggaagccattcag	cctcttctcagtcacttctcag	35
<i>CHAT</i>	actcaacgaatagtaaagaacct	ctagtggagaggacaaaccg	35
<i>PAX6</i>	ccggcagaagattgtagagc	ctagccagggtgcgaagaac	35
<i>S100β</i>	acaaggaagaggatgtctgag	ctcatgttcaaagaactcgtgg	35
<i>FN1</i>	gtcttaacaaatctcctgcct	ccgtaagtgatcctgtaatatctc	35
<i>SOX2</i>	gccgagtggaaacttttgc	gttcatgtgcgcgtaactgt	35
<i>OCT3/4</i>	agtttgtgccagggttttg	acttcaccttccctccaacc	35
<i>LHX3</i>	cccaggacttcgtgtacca	ggaaccaaacctgcaccac	35
<i>GATA2</i>	tagctactatgggcacccag	gcctgttaacattgtgcagc	35
<i>GATA3</i>	gcttcacaatattaacagacc	gcttcatgatactgctcct	35

Cycling conditions:

Step	Temperature	Time
Initial Denaturation	94°C	3 minutes
3-steps cycling		
Denaturation	94°C	1 minute
Annealing	60°C	1 minute
Extension	72°C	1 minute
Final extension	72°C	10 minutes
Hold	10°C	---

5.1.15. Primer list for evaluation of Sox2 binding in the rat *Fn1* promoter by semi-quantitative PCR

	Forward Primer	Reverse Primer	Cycles
P0	aggaaagagacgaggggga	ccccaagagcagaggcttat	50
P1	ccccaacttcatcagccagt	gcttagaccccggtttctcc	50
P2	atccctaccccaatcctcc	cacctgggctccttttctt	50
P3	tggagagagcacttcccaga	ttcgccaaaagttccgctg	50
P4	ttacagccgtttccatccc	gccccgaacaaaagagatgc	50
P5	ccccacctcaggacttttcc	cctctgctcttcccggttt	50
P6	cgagagcaagcctgaacgta	ggtccataatcgggagccag	50

Cycling conditions:

Step	Temperature	Time
Initial Denaturation	94°C	3 minutes
3-steps cycling, 50 cycles		
Denaturation	94°C	1 minute
Annealing	60°C	1 minute
Extension	72°C	1 minute
Final extension	72°C	10 minutes
Hold	10°C	---

5.1.16. Primer list for real time RT-PCR

Gene	Forward Primer	Reverse Primer
<i>Ankrd27</i>	cccaggatccgagaggtgctgc	cagagccatattggacttcaggggg
<i>Rictor</i>	gaggtggagaggacacaagccc	ggccacagaactcggaacaagg
<i>Sox2</i>	aaaccaccaatcccatcca	aagcgctaactgtaccac
<i>Fn1</i>	agacaaccatctctggacg	ggaactggaactgtaagg
<i>Fn1EIIIA</i>	gcagtgaccaacattgacc	ccctgtacctggaaactgc
<i>Gfap</i>	gctccaagatgaaaccaacc	tcacccgctcctgtctg

S100b acttctctggaggaaatcaaagag gacgaaggccataaaactcctg

5.1.17. Primer list for site-directed mutagenesis

Generation of the of the pDRIVE5Lucia control (empty) vector:

Forward primer: ctcaagcttATGGAAATCAAGGTGCTGTTTGC

Reverse primer: ctctctgagCTAGTGGGCCCTGCAGGA

Cycling conditions:

Step	Temperature	Time
Initial Denaturation	98°C	30 seconds
25 cycles	98°C	10 seconds
	67°C	30 seconds
	72°C	80 seconds
	72°C	2 minutes
Final extension	72°C	2 minutes
Hold	10°C	---

Generation of the pDRIVE5Lucia-hFibronectin Sox2 binding site mutation:

Forward primer: cccgGCTGCGAACCCACAGTCC

Reverse primer: ggggGAGATGCTGATGGCCCCGC

Cycling conditions:

Step	Temperature	Time
Initial Denaturation	98°C	30 seconds
25 cycles	98°C	10 seconds
	70°C	30 seconds
	72°C	110 seconds
	72°C	2 minutes
Final extension	72°C	2 minutes
Hold	10°C	---

5.1.18. sgRNA sequences for generation of fibronectin-knockout Schwann cell line by CRISPR/Cas9

Top: CACCGAATGGAGGATAGGCTTCTCG

Bottom: AAACCGAGAAGCCTATCCTCCATTc

Primer for amplification of the CRISPR/Cas9 targeted sequence:

Fwd: 5´-TCATTTAACTGTTTCTCCACCT-3´

5.1.19. Instruments

Invitrogen EVOS FL Auto Cell Imaging System (Thermo Fisher Scientific, Massachusetts, USA). Confocal LSM 510 Laser Scanning Microscope (Carl Zeiss, Inc, Jena, Germany). FUSION-SL4 advanced Imaging system (Vilver Lourmat, Eberhardzell, Germany). Bioruptor Pico sonication device (Cat# B01060001, Diagenode, Seraing, Belgium). BD FACSAria III (BD Biosciences, California, USA). Mastercycler nexus PCR (Eppendorf, Hamburg, Germany). QuantStudio 12K Flex Real-Time PCR (qPCR) (Thermo Fisher Scientific, Massachusetts, USA). Mini Trans-Blot Cell and Mini-Protean tetra electrophoresis system (Bio-rad, California, USA). Midi Horizontal gel system PerfectBlue (PeqLab, VWR, Erlangen, Germany). Rotina 420R Bench-Top centrifuge (Hettich Lab technology, Edersberg, Germany). PowerPac HC High-Current Power Supply (Bio-rad, California, USA). Ultracentrifuge rotor TLA-55 (Beckman coulter, Brea, California USA). Sorvall RC-5B Superspeed centrifuge (Thermo Fisher Scientific, Massachusetts, USA). Stereo Lumar.V12 (Carl Zeiss, Inc, Jena, Germany). Microcentrifuge 5418R (Eppendorf, Hamburg, Germany). Centro LB 960 luminometer (Berthold Technologies, Bad Wildbad, Germany). Inverted spinning-disc confocal microscope (Visitron, Puchheim, Germany), Incubator, hood. Cryostat (Leica Microsystems, Wetzlar, Germany). GraphPad Software, San Diego California USA. Columbus® software version 2.5.0 provided by Perkin Elmer, USA. Tube rotator RM-2M (Neolab, Cat#7-0045).

5.1.20. Software and databases

Plasmid	Company	Cat. #
FIJI software package	Schindelin et al, 2012	fiji.sc
MTrack ImageJ plug-in	Meijering et al, 2012	imagej.net/ MTrackJ
LSM software	Carl Zeiss, Inc	
ImageJ software package	Schneider et al, 2012	imagej.nih.gov/ij/

FibrilToll ImageJ plug-in	Boudaoud et al, 2014	
Columbus® software version 2.5.0	Perkin Elmer	
Pannoramic Viewer version 1.15.2	3DHISTECH, Budapest, Hungary	
FusionCapt Advance software	Vilver Lourmat	
Feature Extraction software 10.7	Agilent	
"limma" R / Bioconductor package	Ritche et al, 2015	bioconductor.org
gplots package of R statistical software	Gregory et al, 2016	www.r-project.org
Pathway Studio program, version 11	Elsevier	www.elsevier.com/ solutions/ pathway-studio- biological-research
BioMart	Ensembl	www.ensembl.org/ biomart/martview
GePS, Pathway System of Genomatix, Release 2.6	Genomatix	www.genomatix.de
MatInspector program	Genomatix, Cartharius et al, 2015	www.genomatix.de
DiAlign TF program, Genomatix software suite GEMS Launcher	Genomatix	www.genomatix.de
database EIDorado	Genomatix	www.genomatix.de
NEBaseChanger online tool	NEB, BioLabs	nebasechanger. neb.com
online CRISP Design Tool	Heigwer et al, 2014	www.e-crisp.org
GraphPad Prism version 5.00	GraphPad Software	www.graphpad.com

5.2. Methods

5.2.1. Cell culture

The Rat Schwann cell line RSC96, the rat Schwannoma cell line RT4D6P2T and the packaging cell line GP2-293 were purchased from American Type Culture Collection. The mouse fibroblast cell lines Fibroblast Fn1flox/flox (FB) and Fibroblast Fn1KO (FB^{Fn1^{-/-}}) were a gift from Prof. Reinhard Fässler. They were generated by immortalization of mouse embryonic fibroblasts with the adenovirus TLarge SV-40 or with the same virus expressing "CRE-deleter".

The rats Schwann cells and the mouse fibroblasts were cultured on laminin-coated dishes (5µg/ml) with the maintenance DMEM medium (defined in section 6.1.7) in 5% CO₂ and at 37°C. Cells were passaged every 3 days and maintained in culture until passage 15. For FN expression studies, 23.000 cells/cm² were seeded in Laminin-coated (5µg/ml) plates and cultured with KSR medium (defined in section 6.1.7) which is FN free. GP2-293 packaging cells were cultured in non-coated dishes with the maintenance DMEM medium in 5% CO₂ and at 37°C.

5.2.2. Retroviral transduction

GP2-293 packaging cell were co-transfected with pMXs-Sox2 and pCMV-VSV-G vectors using the Xfect reagent in accordance with the manufacturer's instructions. A pMXs-empty plasmid was used as a negative control for Sox2 expression. Briefly, one 10 cm dish of confluent GP2-293 packaging cells was co-transfected with 20 µg of the pMXs-Sox2 or the empty vector and 20 µg of the pCMV-VSV-G vector. Virus-containing supernatant was collected 48h after transfection and concentrated in 300 µl PBS. RSC96 cells were seeded at a density of 2,600 cells/cm². 48h after seeding, cells were infected with the viral particles (Ratio 1:5 of virus suspension to the maintenance DMEM medium) in the presence of 10 µg/ml polybrene for 24h. RSC96_Sox2+ clones were selected using a single-cell derived culture in a 96-well plate and kept in culture as previously described.

5.2.3. Surgical Procedure of rat sciatic nerves

Animal studies were approved by the local animal care committee. The current German regulations for animal welfare and the institutional research guidelines for care and use of laboratory animals were followed. All surgical procedures were performed under general anaesthesia (2 mg/kg midazolam, 150 µg/kg medetomidine, and 5 µg/kg fentanyl) and aseptic conditions. In female Sprague-Dawley rats (280–310 g), the sciatic nerve was bilaterally exposed and then transected on one site 5 mm proximal to its branching. Following transection, the nerve was subsequently coaptated with 11/0 sutures. The non-transected contralateral site served as control. Following nerve repair or nerve exposure, the biceps femoris muscle was carefully sutured back into place, the skin incision was closed and the anaesthesia reversed (0.75 mg/kg atipamezole, 200 µg/kg flumazenil, and 150 µg/kg naloxone). For postoperative analgesia, the rats received metamizol (100 mg/kg) directly after waking up, and meloxicam (0,8 mg/kg) every 24 h as well as metamizol every 6 hours for 3 days. At day 4, 7 and 10 following surgery, three of the rats were anesthetized as described above, and the sciatic nerve was bilaterally harvested. Whole trunk samples containing the microsurgically reconstructed section and the area at the same level of the control site were fixed overnight in 4% PFA at 4°C. After fixation, the nerves were kept in 30% sucrose solution for 24 hours at 4°C. They were finally embedded in OCT medium and frozen at -80°C. Longitudinal cryosections of 12 µm were used for immunostainings and *in situ* hybridization. After nerve harvest, the rats were euthanized by intraperitoneal lethal injection of sodium pentobarbital (320 mg per animal).

5.2.4. Live-cell imaging

SC and SC^{Sox2+} were seeded at a density of 23.000 cells/cm², in maintenance DMEM medium or KSR medium in case of FN studies. Time-lapse imaging of Schwann cells were recorded every 25 min for 85 hours at 37°C in 5% CO₂ with the EVOS FL Cell Imaging System with a 10X objective. All images were processed with FIJI software package and analysed using the MTrack ImageJ plug-in. For quantification, 10 cells/condition were tracked during the last 42

hours and the distance and persistence were evaluated. Persistence was calculated as the displacement divided by the total distance travelled by the cell (Ryan J Petrie et al., 2009).

5.2.5. Immunocytochemistry

10 mm cover glasses were placed into 48-well plate and coated with laminin (5 μ g/ml). Cells were seeded at a density of 23,000 cells/cm² in the previously coated cover glasses. After 72 hours of culture, cells were fixed with 4% PFA for 20 min at room temperature. After washing with PBS (3x5 minutes), samples were incubated with the permeabilization solution (defined in section 6.1.9) for 30 minutes. After washing with PBS (3x5 minutes), the samples were incubated with the primary antibodies (in the antibody solution, section 6.1.9) overnight at 4°C. After washing with PBS (3x5 minutes), secondary antibodies and DAPI were incubated in the antibody solution for 1 hour at room temperature and washed with PBS (3x5 minutes). Finally, samples were mounted in microscope slides using Mowiol as a mounting medium. The list of antibodies and concentrations are summarized in section 6.1.13. Images were acquired using a confocal microscope and LSM software. Fluorescent imaging and phase-contrast imaging were acquired with the EVOS FL Cell Imaging System. Images were processed with ImageJ software package. Analysis of anisotropy and fibers orientation was done using the FibrilToll ImageJ plug-in.

Images of the phosphoPaxillin and Paxillin stainings were analyzed using the Columbus® software version 2.5.0 provided by Perkin Elmer, USA. For quantification, the image region was defined by applying the building block 'Find Image Region' to the GFP channel. The next building block 'Select Population' removed border objects. Morphological parameters were calculated using the command 'Calculate Morphology Properties'.

5.2.6. Immunohistochemistry

Nerves were harvested from the rats at the time points of interest (day 0, day 4, day 7 and day 10 post surgery) and fixed overnight in 4% PFA at 4°C. After fixation, nerves were kept in 30% sucrose solution for 24 hours at 4°C to

cryoprotect the tissue. Samples were mounted with Tissue-Tek O.C.T compound in Peel-A-Way embedding molds and frozen at -80°C . Longitudinal sections of $10\ \mu\text{m}$ thickness were done with a cryostat and kept at -80°C until analysis. For immunostainings, sections were thawed for 30 minutes. After washing the samples with PBS (3x5 minutes), sections were incubated in Heat-Induced antigen retrieval buffer (defined in section 6.1.8) for 8 minutes at 200W in the microwave. Samples were cooled down for 30 minutes at room temperature and then washed with PBS (3x10 minutes). Permeabilization was performed for 45 minutes at room temperature with the permeabilization solution (defined in section 6.1.9). Primary and secondary antibodies were incubated under the same conditions explained in section 6.2.5. as well as the image acquisition and processing.

5.2.7. *In situ* hybridization

Probes generation

The rat *Fn1* containing the spliced domain EIIIA (*Fn1*EIIIA) specific region was cloned from the plasmid pGEM-2 into the pCS2+ plasmid (for probe generation) using the restriction enzyme EcoRI. The orientation of the fragment was confirmed by sequencing. $10\ \mu\text{g}$ of the pCS2+ *Fn1*EIIIA plasmid was linearized using XbaI and HindIII-HF restriction enzymes for the synthesis of the sense and antisense probes respectively ($10\ \mu\text{g}$ plasmid, $3\ \mu\text{l}$ enzyme, $10\ \mu\text{l}$ 10X Cutsmart buffer). Labelled probes were generated using the DIG RNA labelling kit following the manufacture's protocol using $1\ \mu\text{g}$ of the digested plasmid. After confirmation of the transcription reaction by agarose gel electrophoresis (1% agarose gel), the probes were purified using the Illustra microspin G-50 columns following the commercial protocol. Probes were re-suspended 1:200 in hybridization buffer (defined in section 6.1.8) and kept at -80°C .

In situ protocol

Sections from the rat sciatic nerves were used for *in situ* hybridization. Samples were thawed at room temperature for 30 minutes. Slides were washed in PBS

(DEPC treated) for 3 x 5 minutes and incubated for 10 minutes in the acetylation solution (defined in section 6.1.8). Samples were washed 3 x 5 minutes with PBS (DEPC treated). Sections were incubated for 2 hours at room temperature with the hybridization buffer. Probes (sense and antisense) were diluted 1:200 in hybridization buffer and denatured for 10 min at 95°C and then incubated for 5 minutes on ice. Slides were incubated with diluted probes overnight at 70°C in a humidified chamber (filter paper soaked with 5X SSC defined in section 6.1.8, 50% formamide). Slides were washed with 5X SSC at room temperature for 5 minutes and then 2 x 30 minutes washes in 0.2X SSC at 70°C and one finale wash for 5 minutes in 0.2X SSC at room temperature. Sections were incubated for 5 minutes with Buffer 1 (defined in section 6.1.8) at room temperature and then 2 hours with the blocking solution (defined in section 6.1.8) for *in situ* hybridization at room temperature. Anti-digoxigenin antibody was dilutes 1:2500 in the blocking solutions. Sections were incubated with the diluted antibody at 4°C overnight. Samples were washed 3 x 5 minutes with Buffer 1 at room temperature and then 2 x 10 minutes with 1X NTMT (defined in section 6.1.8). Sections were incubated with the staining solution (defined in section 6.1.8) at 37°C until the signal was visible. Slides were washed 3 x 10 minutes in PBS to stop the reaction and then they were used for DAB staining.

5.2.8. DAB staining

After the *in situ* hybridization, sections were used for DAB staining. The tissue was permeabilized with 0.3% Triton X-100 in the (blocking solution defined in section 6.1.9) for 45 min. Then it was incubated with the primary antibody in the blocking solution overnight at 4°C in a humidified chamber. Sections were washed 3 x 5 minutes with PBS and incubated with the biotinylated antibody diluted in the blocking solution (1:230) for 1 hour. Sections were washed 3 x 5 minutes with PBS and then incubated with the ABC solution (prepared 30 minutes in advance according to the manufacture's protocol). After 3 x 5 minutes PBS washes the sections were incubated with the DAB solution using the Vector kit. The reaction was stopped when reached the desired intensity with 3 x 10 minutes PBS washes. Sections were washed with milliQ water and

mounted using the aquatex mounting medium. Images were collected with the Mirax Desk scanner v1.9 and processed with the software Pannoramic Viewer version 1.15.2.

5.2.9. Immunoblotting

Cells were collected after 3 day of culture and lysed in RIPA buffer (defined in section 6.1.11). Samples were centrifuged for 45 min at 16,000 rcf at 4°C. Protein concentration was measured with the BCA protein kit. Protein were separated in 8% sodium dodecyl sulphate–polyacrylamide gel using the Mini-Proteam tetra electrophoresis system and blotted onto a PVDF membrane, previously incubated in 100% methanol. Transfer was performed with the wet system Mini Trans-Blot cell, for 14 hours, at 90 mA and at 4°C. After TBS-T wash (defined in section 6.1.11), membrane was blocked with the blocking solution (defined in section 6.1.11) for 1 hour and incubated with the primary antibodies overnight in blocking solution. Secondary antibodies were incubated for 1 hour at 4°C in blocking solution and developed using the Amersham ECL prime western blotting detection reagent. Details about the antibodies are summarized in section 6.1.13. Blots were scanned using the imaging system FUSION-SL4 advanced. Images were analyzed with the FusionCapt Advance software. For reprobing, membranes were incubated with the stripping solution (defined in section 6.1.11) for 30 minutes at 50°C and washed with water (5x10 minutes), TBS-T (3x10 minutes), blocked for 1 hour with the blocking solution and tested again with the antibody of interest.

5.2.10. RNA isolation and reverse transcription

Total RNA purification was done using the RNeasy mini kit and the reverse transcription was performed using the SuperScript III First-Strand Synthesis SuperMix according to the following procedure:

- 1 µg of total RNA, (For the nerves samples from the *in vivo* study a total of 20 ng of RNA was used)
- 1 µl of 50 ng/µl of random hexamers
- 1 µl of Annealing buffer

- Up to 8 μ l RNase/Dnase-free water

Incubation for 5 minutes at 65°C

Addition of:

- 10 μ l of 2x First-Strand Reaction Mix
- 2 μ l of SuperScriptIII/RNaseOUT Enzyme mix

Vortex and incubation as followed: 10 minutes at 25°C, followed by 50 minutes at 50°C and finally 5 minutes at 85°C. Samples were stored at -20°C.

5.2.11. Semiquantitative-PCR and real time PCR

Semiquantitative PCR was done using the Taq PCR core kit and the list of primers and cycle conditions are summarized in section 6.1.12. Samples were pre-diluted 1:2 with DNase-Free water.

Semiquantitative RT-PCR reaction mix was prepared according to the following recipe:

- 0.6 ml DNA sample
- 2.5 ml of 10X buffer
- 0.6 ml Primers 25 mM (forward and reverse)
- 0.2 ml Taq Polymerase
- DNase-Free water up to 25 ml final volume.

Real time PCR (qPCR) was performed using the Power Sybergreen master mix using the QuantStudio 12K Flex Real-Time PCR thermocycler

qPCR reaction mix was prepared according to the following recipe:

- 5 μ l master mix syber green
- 2 μ l cDNA (total cDNA=1.8 ng)
- 2 μ l of Primer mix (forward and reverse primers in a final concentration of 300 nM)
- 1 μ l of H₂O

5.2.12. Transformation

Chemically competent cells, *E.coli* DH5 alpha, were transformed according to the manufacture instructions. Briefly, 50 μ l of cells were thawed on ice for 20 minutes and mixed with 5 μ l of DNA of interest. After a 30 minutes incubation on ice, cells were heat shocked for 20 seconds at 42°C in a thermoblock. Cells were incubated for 2 minutes on ice and then re-suspended in 950 μ l of SOC medium and incubated for 1 hour at 37°C. Transformed cells were plated on pre-warmed LB agar selective plates (defined in section 6.1.10) with the respective antibiotic and cultured overnight at 37°C.

5.2.13. Cloning procedure

Fragments were amplified with specific primers by PCR adding the restriction enzymes sites of interest or subcloned from other constructs. Insert and backbone were digested for one hour at 37°C according to the manufacture protocol (NEB) and purified using the QIAquick gel extraction or Gel or QIAquick PCR purification kits. After purification, fragments and backbones were ligated overnight at 16°C in a ratio of 1:3 (vector:insert) using the T4-DNA ligase (NEB). A digested vector without insert was used as a negative control of the ligation reaction. Positive colonies were first screened by PCR using the same conditions explained in section 6.1.14 with 35 cycles. Selected colonies were grown in 5 ml of LB medium (defined in section 6.1.10) with the respective antibiotic overnight and purified as it is mentioned below.

5.2.14. Plasmids purification

Plasmids were purified from *E.coli* cultures in LB medium supplemented with the corresponding antibiotic. After 24 hours of culture at 37°C in constant shaking, cells were centrifuged for 10 min, at 4000 rpm at 4°C. Purification was done using the MaxiKit HiPure or the Mini Prep kit in case of purification for sequencing following the manufacture's protocol.

5.2.15. Microarray analysis

Slides were measured on an Agilent DNA Microarray Scanner (G2539A) using one color scan setting for “Agilent SurePrint G3 Rat Gene Expression 8x60K Microarray” (amadis ID: 028279). The intensity data of each individual hybridization were extracted and the quality was assessed with the Feature Extraction software 10.7 (Agilent).

Data processing

Measured raw intensities of 62976 probes were corrected for background noise using the normexp method. Quantile normalization was applied to assure comparability across samples. The intensities of the probes were log₂ transformed before statistical evaluation. P-values were computed by using a moderated t-test with help of the "limma" R / Bioconductor package (bioconductor.org) to determine significant differences between groups of three replicates for each clone and the control. P-values were adjusted by multiple testing using the method according to Benjamini & Hochberg (Benjamini & Hochberg, 1995) to derive the expected percentage of false positives (i.e. the false discovery rate (FDR)).

Heat map

The expression profile of normalized log₂ transformed raw data from the Agilent microarrays was represented by a heat map. In order to display only significantly expressed probes across samples, a one-way ANOVA was applied to three groups, i.e. two different clones and the control including three replicates each, in a pre-filtering step. Probe signals for hierarchical clustering were considered if the false discovery rate (FDR) according to a Benjamini and Hochberg is less than 0.002. In addition, only probes were taken into account if the log₂ intensity ratio of the means across three replicates of a clone and the control were greater or equal 1 or less or equal -1. For the generation of the heat map we used the heatmap.2 function within the gplots package of R statistical software (www.r-project.org). Agglomerative hierarchical clustering by the hclust function (method = “complete”) was applied to group experimental conditions (columns) as well as probe intensities of genes (rows) for the heat map. Rows were scaled and represented as z-score. A dendrogram was shown

for columns as well as rows. To assign subtrees of the row dendrogram, representing similar gene expression profiles as a result of the hierarchical clustering procedure to biological functions, the tree was cut so that six clusters remained. All genes of each cluster were then investigated separately for enrichment in the Gene Ontology (GO) category “biological process” using the Pathway Studio program version 11 (Elsevier). The top significantly up- and downregulated genes in both clones, which are assigned to one of the GO terms “extracellular space”, “proteinaceous extracellular matrix”, “extracellular region” or “extracellular matrix” were highlighted next to the heatmap.

Venn Diagram

A Venn diagram was constructed between probes of the two clones from the microarray with the following adjustments: Significance cut-offs were set at FDR adjusted p-values < 0.002 to consider the expected percentage of false positives. Only probes with a fold change (FC) greater than 2 and lower than -2 were selected. The number of different genes in each dataset was determined by summarizing the Agilent probe identifiers to their corresponding gene symbols.

Pathway analysis

Significantly differentially expressed genes from the overlap of both clones were ranked according to their FC and assigned to the GO categories extra cellular matrix and cell adhesion. From the top ranked list genes were selected for experimental validation. Further, the probes from the overlap of the Venn diagram were explored for enrichment in GO categories biological process and cellular component by the Pathway Studio software (version 9) using Fisher’s exact test. For the obtained p-values of the GO categories a FDR correction was applied by using the R function p-adjust with method = “fdr”. Overlapping Agilent probe identifiers of the two clones were mapped to Entrez Gene IDs using BioMart (www.ensembl.org/biomart/martview) by setting the version ‘Ensembl Genes 75’ as well as ‘Rattus norvegicus genes (Rnor:5.0)’ and imported into GePS (Pathway System of Genomatix, Release 2.6). Using GePS, a literature-derived network based on sentence level co-citations was generated.

5.2.16. In silico promoter analysis

The MatInspector (Genomatix) program (Cartharius et al., 2005) was used to identify potential Sox2 binding sites of the V\$SORY family within the promoter sequence of *Fn1*. For the detection of V\$SOX2.01 and V\$SOX3.01 binding sites within the *FN1* promoter sequences, the optimized matrix similarity was used.

Rat *Fn1*

The promoter sequence of rat *Fn1* was derived from the retrieval database EIDorado (Genomatix), version 12-2013 (NCBI build 5). Genomatix / Entrez Gene identifier: GXP_241420 / 25661. Position weight matrices were applied according to Matrix Family Library Version 9.1.

Human *FN1*

The promoter sequence of human *FN1* was derived from the retrieval database EIDorado (Genomatix), version 02-2016 (GRCh38). Genomatix / Entrez Gene identifier: GXP_106290 / 2335. Position weight matrices were applied according to Matrix Family Library Version 9.4.

Evolutionary conserved Sox2 binding sites

Promoter sequences of *Fn1* from nine species were aligned with the DiAlign TF program in the Genomatix software suite GEMS Launcher to evaluate overall promoter similarity and to identify conserved Sox2 binding sites. The corresponding position weight matrix V\$SOX2.01 was applied for detection of potential binding sites according to the Matrix Family Library, version 9.3 (March 2015). The promoter sequences were defined as in EIDorado (version 02-2016). The Genomatix / Entrez Gene identifier were used for *FN1*: GXP_106290 / 2335 (human); GXP_1045519 / 613269 (rhesus monkey); GXP_5899143 / 459926 (chimp); GXP_223655 / 14268 (mouse); GXP_241420 / 25661 (rat); GXP_1651307 / 100034189 (horse); GXP_3882392 / 280794 (cow); GXP_3541955 / 397620 (pig); GXP_951696 / 100014118 (opossum). Binding sites were considered as conserved when the promoter sequences could be aligned in the region of the Sox2 binding site using the DiAlign TF program and optimized matrix similarity.

5.2.17. Chromatin immunoprecipitation

Cells were collected after 3 days in culture and crosslinked with 1% PFA for 10 minutes. Chromatin immunoprecipitation was done using the MAGnify Chromatin Immunoprecipitation System following the manufacturer's protocol, using 200,000 cells/immunoprecipitation. The Bioruptor Pico was used for shearing the chromatin. 100 μ l of each sample was added to special Bioruptor Pico Microtubes and sonicated with the following conditions: 8 cycles of 30 seconds ON, 30 seconds OFF. Antibodies were coupled to the Dynabeads for 2 hours in a tube rotator RM-2M at 4°C; the amount of antibody for the chromatin immunoprecipitation step is described in section 6.1.11. Chromatin samples were bound to the beads overnight in the tube rotator at 4°C. After the purification of the DNA, the samples were evaluated by semi-quantitative PCR. Primers were designed according to the rat promoter sequence obtained from the promoter sequence retrieval database EIDorado 12-2013 (Genomatix) in the region of predicted SOX2.01 (V\$SORY) BSs. Primers and PCR conditions are summarized in section 6.1.15.

5.2.18. Lucia luciferase reporter assay

The expression of the Lucia Luciferase synthetic gene was used as a reporter assay to test the activity of Sox2 in the human *FN1* promoter. This gene encodes for a secreted coelenterazine-utilizing luciferase that can be measured in the cell culture medium. The plasmid used was the commercial plasmid pDRIVE5Lucia-hFibronectin. Sox2 binding site was identified by *in silico* analysis in the human *FN1* promoter and was mutated in the pDRIVE5Lucia-hFibronectin plasmid using the Q5 Site-Directed Mutagenesis kit following the kit protocol. Primers were designed for a substitution of 8 nucleotides including the core sequence within the binding site using the NEBaseChanger online tool (nebasechanger.neb.com). An empty vector with the human *FN1* promoter was generated by direct mutagenesis using the same kit. Primers were design for a substitution of the entire human promoter with 3 restriction enzyme sequences (5' XhoI SacI HindIII). Primers are described in section 6.1.17. Cells were seeded in a 48-well laminin-coated plate (5 μ g/ml) at a density of 23.000

cells/cm² with KSR medium. Cells were transiently transfected after 48 hours, with the Xfect according to the manufacturer's conditions, using 0.5 µg of DNA. The NIH/3T3 cell line was used as a control of *FN1* expression. These cells were cultured in the same conditions as described for Schwann cells but the transfection was performed with the TransIT-S2 Dynamic Delivery System following the manufacturer's protocol with a ratio of 1:3 (DNA to reagent). Lucia Luciferase expression was measured 72 hours post transfection with the Quantic-Luc reagent according to the manufacturer's protocol using the Quantic-Luc luminescence assay reagent with the Centro LB 960 luminometer. Measurement conditions: in an opaque 96-well plate, 20 µl of the cell medium mixed with 100 µl of the Quantic-Luc reagent; 4 seconds of incubation and 0.1 reading time.

5.2.19. Generation of *Fn1* knockout Schwann cell line

The CRISPR/Cas9 genome-editing system was used to generate a *Fn1* knockout (KO) in the SC^{Sox2+}. The sgRNA sequence was designed against an upstream region of the rat *Fn1* gene using the online CRISP Design Tool (<http://www.e-crisp.org>), details about the sequences are in section 6.1.16. The sgRNA was cloned into the pSpCas9(BB)-2A-GFP (PX458) vector. SC^{Sox2+} were transiently transfected using the Xfect transfection reagent according to the manufacturer's protocol. GFP-positive cells were sorted using a FACSAria III and cultured for one week. A single cell derived culture was performed to select KO clones which were confirmed by sequencing (GATC biotech, Konstanz, Germany). For subcloning of mutant alleles, PCR reactions were carried out using the Fusion High-Fidelity DNA Polymerase (BioLabs) in a total volume of 25 µl. PCR products were subcloned using the TOPO TA cloning kit following the manufacturer's protocol. Positive *E.coli* colonies were analyzed by sequencing.

5.2.20. FN depletion in normal serum

FN was depleted from the FBS according to the protocol from Pankov and Momchilova (Pankov & Momchilova, 2009) using gelatin sepharose due the high affinity of gelatin for FN. 5 ml of Gelatin Sepharose 4B were added to a 50

ml falcon tube and washed with 20 ml of DPBS in sterile conditions and centrifuged at 200 rcf for 1 minute to collect the Gelatin Spharose 4B beads. The supernatant was removed and the beads were washed two more times following the same procedure. After the washing steps, the DPBS was completely removed from the beads and 10 ml of FBS were added to deplete FN from the serum. The tube was shaken for 30 min in the tube rotator RM-2M at room temperature. After this incubation time, the tube was centrifuged and the supernatant containing the FN-depleted FBS (FNdFBS) was transferred to a new tube containing cleaned beads. A second depletion step was performed using the same procedure and finally, the FNdFBS was aliquoted and kept at -20° C.

5.2.21. Dorsal root ganglion neurons extraction and co-culture

All animal procedures were performed according to the German Federal guidelines and approved by the Helmholtz Zentrum München Institutional Animal Care Committee. Dissociated dorsal root ganglion neurons (DrgN) were extracted from adult male CD-1 mice according to the JOVE protocol from de Luca et al, (De Luca et al., 2015) and cultured in laminin-coated plates (5µg/ml) at a density of 100 cell/cm² in DrgN medium (defined in section 6.1.7), for 48 hours, in 5% CO₂ and at 37°C.

For co-culture, Schwann cells and fibroblasts were first seeded at a density of 23.000 cells/cm² in Laminin-coated plates (5µg/ml) and cultured with KSR medium. After 48 hours, DrgN were seeded on top of Schwann cells or Fibroblasts and cultured in DrgN medium for 48 hours. For the specific co-culture condition of DrgN/Schwann cells/Fibroblasts, Fibroblasts were first seeded at a density of 11.500 cells/cm² in KSR medium. After 24 hours, Schwann cells were added at the same density and after 48 hours DrgN (in DrgN medium) were seeded on top of the Schwann cells/Fibroblasts and fixed after 48 hours.

5.2.22. Preparation of the extracellular matrix layer.

The ECM layer was generated according to Prewitz et al., (Prewitz et al., 2013). Briefly, cells were cultured at 23.000 cells/cm² in laminin-coated dishes (5µg/ml). After 72 hours, the decellularization was performed using 0.5% Triton X-100 solution in PBS supplemented with 20 mM ammonium hydroxide for 5 min at room temperature. The ECM layer was washed 3 times with PBS and stored in sterile conditions for further experiments.

5.2.23. Human pluripotent stem cell derived-motor neurons

Fibroblast-derived human pluripotent stem (iPS) cells were obtained from Dr. Micha Drukker. Briefly skin fibroblasts from ATCC were reprogrammed according to Diecke et al, 2015 (Diecke et al., 2015). The protocol used for the human motor neuron differentiation (hMN) was a modification of the one published by Qu et al (Qu et al., 2014). Briefly, iPS cells were maintained on Geltrex-coated dishes in mTeSR1 medium, in 5% CO₂ at 37°C. For neural induction, cells were seeded in Geltrex-coated plates at a density of 7x10⁴cells/cm². Neural induction was started after 3 to 4 days when the cells reached 60-70% confluency using neural induction medium (defined in section 6.1.7). The medium was changed every day. At day 4 and 5, 100 nM retinoic acid was added to the induction medium. From day 6 to day 12, 100ng/ml of SHH and 100 nM of retinoic acid were added to the neural induction medium. At day 13, cells were re-seeded in polyornithine (15µg/ml), laminin (5µg/ml), FN (500µg/ml) and collagen IV (10µg/cm²)-coated dishes. For passaging, cells were collected with the StemPri EZPassage™ in a 15 ml falcon tube with 2 ml medium and seeded in a ratio of 1:2 (cells:medium). The medium was supplemented with 10 µM ROCK inhibitor during the first 24 hours after re-seeding. From day 13 till 20, the medium was changed from neural induction medium to maintenance medium (defined in section 6.1.7). The medium was changed every day. At day 21, rosettes were picked and dissociated for co-culture experiments.

5.2.24. Human pluripotent stem cell derived-motor neurons co-culture

Co-cultures of hMN and rat Schwann cells were performed under the same conditions previously described for the DrgN, using the hMN medium supplemented with ROCK inhibitor only during the first 24 hours.

5.2.25. Primary Rat Schwann cell culture

Primary rat Schwann cells were extracted from sciatic nerves of adult rats according to the protocol described by Kaewkhaw et al (Rossukon Kaewkhaw et al., 2012), this protocol is based on the use of DMEM medium containing D-Valine in order to restrict fibroblasts growth. To analyze the dynamic between primary Schwann cells and fibroblasts coming from sciatic nerves, cells were kept in normal DMEM medium for 20 days. Cells were seeded in laminin-coated dishes (5µg/ml) at a density of 46.000 cells/cm² and fixed after 5 days in culture for immunostaining procedures.

5.2.26. Zebrafish experiments

Zebrafish were maintained under standardized conditions and experiments were conducted in embryos of undetermined sex. We used the triple transgenic line Tg[gSAGFF202A;UAS:EGFP;SILL:mCherry]. The developing posterior lateral line was evaluated 28 hours post fertilization by immunostaining. Lateral axons ablation was performed according to Xiao et al (Xiao et al., 2015) using the iLasPulse laser system mounted on a Zeiss Axio Observer inverted microscope using the 63x water objective lens. Briefly, 72 hours post fertilization zebrafish larvae were anesthetized and mounted in a glass petri dish with methylcellulose, laser pulses were applied to the lateral axons using the disappearance of the red fluorescent signal as a confirmation of the axotomy. Immunostainings of Sox2 was done 24 hours post axotomy according to Pinto-Teixeira et al, (Pinto-Teixeira et al., 2015). Briefly, samples were fixed overnight in 4% PFA+0.2% Tween-20 in PBS. Permeabilization was carried out in acetone for 8 minutes at -20°C. Blocking was performed using 10% BSA plus 1%Tween-20 in PBS. Primary antibody was incubated 48 hours in PBS containing 0.2% Tween-20 and secondary antibody was incubated overnight in

PBS with 0.2% Tween-20. Samples were mounted in Vectashield mounting medium. Images were obtained using a confocal microscope. Antibody references are specified in the key resource table.

5.2.27. Statistical analysis

The statistical analysis was performed with GraphPad Prism version 5.00 for Windows (GraphPad Software, San Diego California USA, www.graphpad.com). Data were analyzed with a parametric Student's t-test (comparison of two experimental groups) or unpaired t-test with Welch's correction in case of unequal variance and unbalance sample size. A one-way ANOVA was used for comparison of three or more experimental groups with a post hoc Tukey's test. Analysis of Western blots and qPCR data were performed using a non-parametric Mann-Whitney test (comparison of two experimental groups). Correlations were done computing the Pearson correlation coefficients. Animal sample size calculation for *in vivo* sciatic nerve surgery was performed using a t-Test for Pearson Correlation. Experiments were repeated at least 3 times (N=number of independent experiments, n=number of data points) and data are presented as a mean \pm s.e.m, differences with $p < 0.05$ were considered significant.

6. References

- Ahmed, Z., & Brown, R. A. (1999). Adhesion, alignment, and migration of cultured Schwann cells on ultrathin fibronectin fibres. *Cytoskeleton*, *42*(4), 331-343.
- Allodi, I., Udina, E., & Navarro, X. (2012). Specificity of peripheral nerve regeneration: interactions at the axon level. *Prog Neurobiol*, *98*(1), 16-37. doi:10.1016/j.pneurobio.2012.05.005
- Arnold, K., Sarkar, A., Yram, M. A., Polo, J. M., Bronson, R., Sengupta, S., Seandel, M., Geijsen, N., & Hochedlinger, K. (2011). Sox2+ adult stem and progenitor cells are important for tissue regeneration and survival of mice. *Cell Stem Cell*, *9*(4), 317-329.
- Arthur-Farraj, P. J., Latouche, M., Wilton, D. K., Quintes, S., Chabrol, E., Banerjee, A., Woodhoo, A., Jenkins, B., Rahman, M., & Turmaine, M. (2012). c-Jun reprograms Schwann cells of injured nerves to generate a repair cell essential for regeneration. *Neuron*, *75*(4), 633-647.
- Avilion, A. A., Nicolis, S. K., Pevny, L. H., Perez, L., Vivian, N., & Lovell-Badge, R. (2003). Multipotent cell lineages in early mouse development depend on SOX2 function. *Genes Dev*, *17*(1), 126-140. doi:10.1101/gad.224503
- Badache, A., & De Vries, G. H. (1998). Neurofibrosarcoma-derived Schwann cells overexpress platelet-derived growth factor (PDGF) receptors and are induced to proliferate by PDGF BB. *Journal of cellular physiology*, *177*(2), 334-342.
- Bailey, S., Eichler, M., Villadiego, A., & Rich, K. (1993). The influence of fibronectin and laminin during Schwann cell migration and peripheral nerve regeneration through silicon chambers. *Journal of neurocytology*, *22*(3), 176-184.
- Barczyk, M., Carracedo, S., & Gullberg, D. (2010). Integrins. *Cell and tissue research*, *339*(1), 269-280.
- Baron-Van Evercooren, A., Kleinman, H. K., Seppä, H., Rentier, B., & Dubois-Dalcq, M. (1982). Fibronectin promotes rat Schwann cell growth and motility. *J Cell Biol*, *93*(1), 211-216.
- Barros, C. S., Franco, S. J., & Muller, U. (2011). Extracellular matrix: functions in the nervous system. *Cold Spring Harb Perspect Biol*, *3*(1), a005108. doi:10.1101/cshperspect.a005108
- Bazigou, E., Xie, S., Chen, C., Weston, A., Miura, N., Sorokin, L., Adams, R., Muro, A. F., Sheppard, D., & Makinen, T. (2009). Integrin-alpha9 is required for fibronectin matrix assembly during lymphatic valve morphogenesis. *Dev Cell*, *17*(2), 175-186. doi:10.1016/j.devcel.2009.06.017
- Bely, A. E. (2010). Evolutionary loss of animal regeneration: pattern and process. *Integrative and comparative biology*, *50*(4), 515-527.
- Benjamini, Y., & Hochberg, Y. (1995). Controlling the False Discovery Rate: A Practical and Powerful Approach to Multiple Testing. *Journal of the Royal Statistical Society. Series B (Methodological)*, *57*(1), 289-300. doi:10.2307/2346101
- Berrier, A. L., & Yamada, K. M. (2007). Cell-matrix adhesion. *J Cell Physiol*, *213*(3), 565-573. doi:10.1002/jcp.21237
- Berrocal, Y. A., Almeida, V. W., Gupta, R., & Levi, A. D. (2013). Transplantation of Schwann cells in a collagen tube for the repair of large, segmental peripheral nerve defects in rats: Laboratory investigation. *Journal of neurosurgery*, *119*(3), 720-732.
- Bharadwaj, M., Strohmeyer, N., Colo, G. P., Helenius, J., Beerenwinkel, N., Schiller, H. B., Fassler, R., & Muller, D. J. (2017). alphaV-class integrins exert dual roles on

- alpha5beta1 integrins to strengthen adhesion to fibronectin. *Nat Commun*, 8, 14348. doi:10.1038/ncomms14348
- Bhatheja, K., & Field, J. (2006). Schwann cells: origins and role in axonal maintenance and regeneration. *Int J Biochem Cell Biol*, 38(12), 1995-1999. doi:10.1016/j.biocel.2006.05.007
- Bixby, J. L., Lilien, J., & Reichardt, L. F. (1988). Identification of the major proteins that promote neuronal process outgrowth on Schwann cells in vitro. *J Cell Biol*, 107(1), 353-361.
- Bonnans, C., Chou, J., & Werb, Z. (2014). Remodelling the extracellular matrix in development and disease. *Nature Reviews Molecular Cell Biology*, 15(12), 786-801.
- Bremer, M., Frob, F., Kichko, T., Reeh, P., Tamm, E. R., Suter, U., & Wegner, M. (2011). Sox10 is required for Schwann-cell homeostasis and myelin maintenance in the adult peripheral nerve. *Glia*, 59(7), 1022-1032. doi:10.1002/glia.21173
- Brenner, M. J., Hess, J. R., Myckatyn, T. M., Hayashi, A., Hunter, D. A., & Mackinnon, S. E. (2006). Repair of motor nerve gaps with sensory nerve inhibits regeneration in rats. *The Laryngoscope*, 116(9), 1685-1692.
- Bunge, M. B., Bunge, R., Kleitman, N., & Dean, A. (1989). Role of peripheral nerve extracellular matrix in Schwann cell function and in neurite regeneration. *Developmental neuroscience*, 11(4-5), 348-360.
- BurrIDGE, K., & GuILLUY, C. (2016). Focal adhesions, stress fibers and mechanical tension. *Exp Cell Res*, 343(1), 14-20. doi:<http://dx.doi.org/10.1016/j.yexcr.2015.10.029>
- Cartharius, K., Frech, K., Grote, K., Klocke, B., Haltmeier, M., Klingenhoff, A., Frisch, M., Bayerlein, M., & Werner, T. (2005). MatInspector and beyond: promoter analysis based on transcription factor binding sites. *Bioinformatics*, 21(13), 2933-2942.
- Cattin, A.-L., Burden, J. J., Van Emmenis, L., Mackenzie, F. E., Hoving, J. J., Calavia, N. G., Guo, Y., McLaughlin, M., Rosenberg, L. H., & Quereda, V. (2015). Macrophage-induced blood vessels guide Schwann cell-mediated regeneration of peripheral nerves. *Cell*, 162(5), 1127-1139.
- Clegg, D. O., Wingerd, K. L., Hikita, S. T., & Tolhurst, E. C. (2003). Integrins in the development, function and dysfunction of the nervous system. *Front Biosci*, 8, d723-d750.
- Cook, A., Hippensteel, R., Shimizu, S., Nicolai, J., Fatatis, A., & Meucci, O. (2010). Interactions between Chemokines: REGULATION OF FRACTALKINE/CX3CL1 HOMEOSTASIS BY SDF/CXCL12 IN CORTICAL NEURONS. *Journal of Biological Chemistry*, 285(14), 10563-10571. doi:10.1074/jbc.M109.035477
- Cornbrooks, C., Carey, D., McDonald, J., Timpl, R., & Bunge, R. (1983). In vivo and in vitro observations on laminin production by Schwann cells. *Proceedings of the National Academy of Sciences*, 80(12), 3850-3854.
- Chambers, I., & Tomlinson, S. R. (2009). The transcriptional foundation of pluripotency. *Development*, 136(14), 2311-2322.
- Chang, H.-M., Shyu, M.-K., Tseng, G.-F., Liu, C.-H., Chang, H.-S., Lan, C.-T., Hsu, W.-M., & Liao, W.-C. (2013). Neuregulin facilitates nerve regeneration by speeding Schwann cell migration via ErbB2/3-dependent FAK pathway. *PLoS One*, 8(1), e53444.
- Charras, G., & Sahai, E. (2014). Physical influences of the extracellular environment on cell migration. *Nat Rev Mol Cell Biol*, 15(12), 813-824. doi:10.1038/nrm3897
- Chen, L.-M., Bailey, D., & Fernandez-Valle, C. (2000). Association of β 1 integrin with focal adhesion kinase and paxillin in differentiating Schwann cells. *The Journal of Neuroscience*, 20(10), 3776-3784.
- Chen, S., Rio, C., Ji, R. R., Dikkes, P., Coggeshall, R. E., Woolf, C. J., & Corfas, G. (2003). Disruption of ErbB receptor signaling in adult non-myelinating Schwann cells causes progressive sensory loss. *Nat Neurosci*, 6(11), 1186-1193. doi:10.1038/nn1139
- Daly, W., Yao, L., Zeugolis, D., Windebank, A., & Pandit, A. (2012). A biomaterials approach to peripheral nerve regeneration: bridging the peripheral nerve gap and enhancing functional recovery. *J R Soc Interface*, 9(67), 202-221. doi:10.1098/rsif.2011.0438

- Daly, W., Yao, L., Zeugolis, D., Windebank, A., & Pandit, A. (2012). A biomaterials approach to peripheral nerve regeneration: bridging the peripheral nerve gap and enhancing functional recovery. *Journal of the Royal Society Interface*, *9*(67), 202-221.
- Daniloff, J. K., Levi, G., Grumet, M., Rieger, F., & Edelman, G. M. (1986). Altered expression of neuronal cell adhesion molecules induced by nerve injury and repair. *J Cell Biol*, *103*(3), 929-945.
- De Luca, A. C., Faroni, A., & Reid, A. J. (2015). Dorsal root ganglia neurons and differentiated adipose-derived stem cells: an in vitro co-culture model to study peripheral nerve regeneration. *JoVE (Journal of Visualized Experiments)*(96), e52543-e52543.
- Diecke, S., Lu, J., Lee, J., Termglinchan, V., Kooreman, N. G., Burridge, P. W., Ebert, A. D., Churko, J. M., Sharma, A., & Kay, M. A. (2015). Novel codon-optimized mini-intronic plasmid for efficient, inexpensive, and xeno-free induction of pluripotency. *Sci Rep*, *5*.
- Dornseifer, U., Fichter, A. M., Leichtle, S., Wilson, A., Rupp, A., Rodenacker, K., Ninkovic, M., Biemer, E., Machens, H. G., & Matiasek, K. (2011). Peripheral nerve reconstruction with collagen tubes filled with denatured autologous muscle tissue in the rat model. *Microsurgery*, *31*(8), 632-641.
- Doyle, A. D., & Yamada, K. M. (2016). Mechanosensing via cell-matrix adhesions in 3D microenvironments. *Exp Cell Res*, *343*(1), 60-66.
- Eva, R., & Fawcett, J. (2014). Integrin signalling and traffic during axon growth and regeneration. *Current opinion in neurobiology*, *27*, 179-185.
- Evercooren, B. V., Kleinman, H. K., Ohno, S., Marangos, P., Schwartz, J. P., & Dubois-Dalcq, M. E. (1982). Nerve growth factor, laminin, and fibronectin promote neurite growth in human fetal sensory ganglia cultures. *J Neurosci Res*, *8*(2-3), 179-193.
- Fawcett, J., & Keynes, R. J. (1990). Peripheral nerve regeneration. *Annu Rev Neurosci*, *13*(1), 43-60.
- Feltri, M. L., Porta, D. G., Previtali, S. C., Nodari, A., Migliavacca, B., Cassetti, A., Littlewood-Evans, A., Reichardt, L. F., Messing, A., Quattrini, A., Mueller, U., & Wrabetz, L. (2002). Conditional disruption of $\beta 1$ integrin in Schwann cells impedes interactions with axons. *J Cell Biol*, *156*(1), 199-210. doi:10.1083/jcb.200109021
- Ferri, A. L., Cavallaro, M., Braidà, D., Di Cristofano, A., Canta, A., Vezzani, A., Ottolenghi, S., Pandolfi, P. P., Sala, M., DeBiasi, S., & Nicolis, S. K. (2004). Sox2 deficiency causes neurodegeneration and impaired neurogenesis in the adult mouse brain. *Development*, *131*(15), 3805-3819. doi:10.1242/dev.01204
- Freret, M., Gouel, F., Buquet, C., Legrand, E., Vannier, J.-P., Vasse, M., & Dubus, I. (2011). Rac-1 GTPase controls the capacity of human leukaemic lymphoblasts to migrate on fibronectin in response to SDF-1 α (CXCL12). *Leukemia research*, *35*(7), 971-973.
- Garcia-Irigoyen, O., Carotti, S., Latasa, M. U., Uriarte, I., Fernández-Barrena, M. G., Elizalde, M., Urtasun, R., Vespasiani-Gentilucci, U., Morini, S., Banales, J. M., Parks, W. C., Rodriguez, J. A., Orbe, J., Prieto, J., Páramo, J. A., Berasain, C., & Ávila, M. A. (2014). Matrix metalloproteinase-10 expression is induced during hepatic injury and plays a fundamental role in liver tissue repair. *Liver International*, *34*(7), e257-e270. doi:10.1111/liv.12337
- Gaudet, A. D., Popovich, P. G., & Ramer, M. S. (2011). Wallerian degeneration: gaining perspective on inflammatory events after peripheral nerve injury. *Journal of neuroinflammation*, *8*(1), 1.
- Geiger, B., Bershadsky, A., Pankov, R., & Yamada, K. M. (2001). Transmembrane crosstalk between the extracellular matrix and the cytoskeleton. *Nature Reviews Molecular Cell Biology*, *2*(11), 793-805.
- Ghysen, A., & Dambly-Chaudière, C. (2004). Development of the zebrafish lateral line. *Curr Opin Neurobiol*, *14*, 67 - 73.
- Gilmour, D. T., Maischein, H.-M., & Nüsslein-Volhard, C. (2002). Migration and function of a glial subtype in the vertebrate peripheral nervous system. *Neuron*, *34*(4), 577-588.

- Gonzalez-Perez, F., Udina, E., & Navarro, X. (2013). Extracellular matrix components in peripheral nerve regeneration. *Int Rev Neurobiol*, *108*, 257-275.
- Gonzalez-Perez, F., Alé, A., Santos, D., Barwig, C., Freier, T., Navarro, X., & Udina, E. (2016). Substratum preferences of motor and sensory neurons in postnatal and adult rats. *European Journal of Neuroscience*, *43*(3), 431-442.
- Graham, V., Khudyakov, J., Ellis, P., & Pevny, L. (2003). SOX2 functions to maintain neural progenitor identity. *Neuron*, *39*(5), 749-765.
- Gu, X., Ding, F., & Williams, D. F. (2014). Neural tissue engineering options for peripheral nerve regeneration. *Biomaterials*, *35*(24), 6143-6156.
doi:10.1016/j.biomaterials.2014.04.064
- Gu, Y., Zhu, J., Xue, C., Li, Z., Ding, F., Yang, Y., & Gu, X. (2014). Chitosan/silk fibroin-based, Schwann cell-derived extracellular matrix-modified scaffolds for bridging rat sciatic nerve gaps. *Biomaterials*, *35*(7), 2253-2263.
- Han, X., Fang, X., Lou, X., Hua, D., Ding, W., Foltz, G., Hood, L., Yuan, Y., & Lin, B. (2012). Silencing SOX2 induced mesenchymal-epithelial transition and its expression predicts liver and lymph node metastasis of CRC patients. *PLoS One*, *7*(8), e41335.
doi:10.1371/journal.pone.0041335
- Hashimoto-Uoshima, M., Yan, Y. Z., Schneider, G., & Aukhil, I. (1997). The alternatively spliced domains EIIIB and EIIB of human fibronectin affect cell adhesion and spreading. *J Cell Sci*, *110*(18), 2271-2280.
- Heermann, S., Schmucker, J., Hinz, U., Rickmann, M., Unterbarnscheidt, T., Schwab, M. H., & Kriegelstein, K. (2011). Neuregulin 1 type III/ErbB signaling is crucial for Schwann cell colonization of sympathetic axons. *PLoS One*, *6*(12), e28692.
doi:10.1371/journal.pone.0028692
- Heermann, S., & Schwab, M. H. (2013). Molecular control of Schwann cell migration along peripheral axons: keep moving! *Cell adhesion & migration*, *7*(1), 18-22.
- Hernandez, P., Moreno, V., Olivari, F., & Allende, M. (2006). Sub-lethal concentrations of waterborne copper are toxic to lateral line neuromasts in zebrafish (*Danio rerio*). *Hear Res*, *213*, 1 - 10.
- Hockfield, S., & McKay, R. (1985). Identification of major cell classes in the developing mammalian nervous system. *The Journal of Neuroscience*, *5*(12), 3310-3328.
- Höke, A., Redett, R., Hameed, H., Jari, R., Zhou, C., Li, Z., Griffin, J., & Brushart, T. (2006). Schwann cells express motor and sensory phenotypes that regulate axon regeneration. *Journal of Neuroscience*, *26*(38), 9646-9655.
- Hughes, P. M., Wells, G. M. A., Perry, V. H., Brown, M. C., & Miller, K. M. (2002). Comparison of matrix metalloproteinase expression during Wallerian degeneration in the central and peripheral nervous systems. *Neuroscience*, *113*(2), 273-287.
doi:[http://dx.doi.org/10.1016/S0306-4522\(02\)00183-5](http://dx.doi.org/10.1016/S0306-4522(02)00183-5)
- Hynes, R. (2007). Cell-matrix adhesion in vascular development. *Journal of Thrombosis and Haemostasis*, *5*(s1), 32-40.
- Hynes, R. O. (2002). Integrins: bidirectional, allosteric signaling machines. *Cell*, *110*(6), 673-687.
- Hynes, R. O., & Yamada, K. M. (1982). Fibronectins: multifunctional modular glycoproteins. *J Cell Biol*, *95*(2), 369-377.
- Ilić, D., Kovačič, B., Johkura, K., Schlaepfer, D. D., Tomašević, N., Han, Q., Kim, J.-B., Howerton, K., Baumbusch, C., & Ogiwara, N. (2004). FAK promotes organization of fibronectin matrix and fibrillar adhesions. *J Cell Sci*, *117*(2), 177-187.
- Jessen, K., & Mirsky, R. (2016). The repair Schwann cell and its function in regenerating nerves. *The Journal of physiology*.
- Jessen, K. R. (2004). Glial cells. *Int J Biochem Cell Biol*, *36*(10), 1861-1867.
- Jessen, K. R., & Mirsky, R. (2005). The origin and development of glial cells in peripheral nerves. *Nature Reviews Neuroscience*, *6*(9), 671-682.

- Jessen, K. R., & Mirsky, R. (2005). The origin and development of glial cells in peripheral nerves. *Nat Rev Neurosci*, *6*(9), 671-682. doi:10.1038/nrn1746
- Jessen, K. R., Mirsky, R., & Lloyd, A. C. (2015). Schwann cells: development and role in nerve repair. *Cold Spring Harb Perspect Biol*, a020487.
- Ji, Y., Shen, M., Wang, X., Zhang, S., Yu, S., Chen, G., Gu, X., & Ding, F. (2012). Comparative proteomic analysis of primary schwann cells and a spontaneously immortalized schwann cell line RSC 96: a comprehensive overview with a focus on cell adhesion and migration related proteins. *J Proteome Res*, *11*(6), 3186-3198. doi:10.1021/pr201221u
- Jones, B. A., Beamer, M., & Ahmed, S. (2010). Fractalkine/CX3CL1: a potential new target for inflammatory diseases. *Molecular interventions*, *10*(5), 263.
- Kaewkhaw, R., Scutt, A. M., & Haycock, J. W. (2012). Integrated culture and purification of rat Schwann cells from freshly isolated adult tissue. *Nat Protoc*, *7*(11), 1996-2004. doi:10.1038/nprot.2012.118
- Kaewkhaw, R., Scutt, A. M., & Haycock, J. W. (2012). Integrated culture and purification of rat Schwann cells from freshly isolated adult tissue. *Nat Protoc*, *7*(11), 1996-2004.
- Kishi, M., Mizuseki, K., Sasai, N., Yamazaki, H., Shiota, K., Nakanishi, S., & Sasai, Y. (2000). Requirement of Sox2-mediated signaling for differentiation of early Xenopus neuroectoderm. *Development*, *127*(4), 791-800.
- Klämbt, C. (2009). Modes and regulation of glial migration in vertebrates and invertebrates. *Nature Reviews Neuroscience*, *10*(11), 769-779.
- Klein, R. (2010). Cell sorting during regenerative tissue formation. *Cell*, *143*(1), 32-34. doi:10.1016/j.cell.2010.09.018
- Klein, S., Prantl, L., Vykoukal, J., Loibl, M., & Felthaus, O. (2016). Differential Effects of Coating Materials on Viability and Migration of Schwann Cells. *Materials*, *9*(3), 150.
- Koike, T., Wakabayashi, T., Mori, T., Takamori, Y., Hirahara, Y., & Yamada, H. (2014). Sox2 in the adult rat sensory nervous system. *Histochem Cell Biol*, *141*(3), 301-309. doi:10.1007/s00418-013-1158-x
- Lauro, C., Catalano, M., Trettel, F., Mainiero, F., Ciotti, M. T., Eusebi, F., & Limatola, C. (2006). The Chemokine CX3CL1 Reduces Migration and Increases Adhesion of Neurons with Mechanisms Dependent on the β 1 Integrin Subunit. *The Journal of Immunology*, *177*(11), 7599-7606. doi:10.4049/jimmunol.177.11.7599
- Le, N., Nagarajan, R., Wang, J. Y., Araki, T., Schmidt, R. E., & Milbrandt, J. (2005). Analysis of congenital hypomyelinating Egr2Lo/Lo nerves identifies Sox2 as an inhibitor of Schwann cell differentiation and myelination. *Proc Natl Acad Sci U S A*, *102*(7), 2596-2601. doi:10.1073/pnas.0407836102
- Ledent, V. (2002). Postembryonic development of the posterior lateral line in zebrafish. *Development*, *129*(3), 597-604.
- Lefcort, F., Venstrom, K., McDonald, J. A., & Reichardt, L. F. (1992). Regulation of expression of fibronectin and its receptor, alpha 5 beta 1, during development and regeneration of peripheral nerve. *Development*, *116*(3), 767-782.
- Lefort, C. T., Wojciechowski, K., & Hocking, D. C. (2011). N-cadherin cell-cell adhesion complexes are regulated by fibronectin matrix assembly. *Journal of Biological Chemistry*, *286*(4), 3149-3160.
- Letourneau, P. C., Roche, F. K., Shattuck, T. A., Lemmon, V., & Takeichi, M. (1991). Interactions of Schwann cells with neurites and with other Schwann cells involve the calcium-dependent adhesion molecule, N-cadherin. *J Neurobiol*, *22*(7), 707-720.
- Liao, Y. F., Gotwals, P. J., Koteliensky, V. E., Sheppard, D., & Van De Water, L. (2002). The EIIIA segment of fibronectin is a ligand for integrins alpha 9beta 1 and alpha 4beta 1 providing a novel mechanism for regulating cell adhesion by alternative splicing. *J Biol Chem*, *277*(17), 14467-14474. doi:10.1074/jbc.M201100200
- Limatola, C., & Ransohoff, R. M. (2014). Modulating neurotoxicity through CX3CL1/CX3CR1 signaling. *Frontiers in cellular neuroscience*, *8*, 229.

- Lou, X., Han, X., Jin, C., Tian, W., Yu, W., Ding, D., Cheng, L., Huang, B., Jiang, H., & Lin, B. (2013). SOX2 targets fibronectin 1 to promote cell migration and invasion in ovarian cancer: new molecular leads for therapeutic intervention. *OMICS*, *17*(10), 510-518. doi:10.1089/omi.2013.0058
- Lu, P., Takai, K., Weaver, V. M., & Werb, Z. (2011). Extracellular matrix degradation and remodeling in development and disease. *Cold Spring Harb Perspect Biol*, *3*(12). doi:10.1101/cshperspect.a005058
- Mao, Y., & Schwarzbauer, J. E. (2005). Fibronectin fibrillogenesis, a cell-mediated matrix assembly process. *Matrix Biol*, *24*(6), 389-399. doi:10.1016/j.matbio.2005.06.008
- Marchesi, F., Piemonti, L., Mantovani, A., & Allavena, P. (2010). Molecular mechanisms of perineural invasion, a forgotten pathway of dissemination and metastasis. *Cytokine Growth Factor Rev*, *21*(1), 77-82. doi:10.1016/j.cytogfr.2009.11.001
- Mathews, G. A., & Ffrench-Constant, C. (1995). Embryonic fibronectins are up-regulated following peripheral nerve injury in rats. *J Neurobiol*, *26*(2), 171-188.
- Milner, R., Wilby, M., Nishimura, S., Boylen, K., Edwards, G., Fawcett, J., Streuli, C., & Pytela, R. (1997). Division of labor of Schwann cell integrins during migration on peripheral nerve extracellular matrix ligands. *Dev Biol*, *185*(2), 215-228.
- Miller, S. J., Rangwala, F., Williams, J., Ackerman, P., Kong, S., Jegga, A. G., Kaiser, S., Aronow, B. J., Frahm, S., Kluwe, L., Mautner, V., Upadhyaya, M., Muir, D., Wallace, M., Hagen, J., Quelle, D. E., Watson, M. A., Perry, A., Gutmann, D. H., & Ratner, N. (2006). Large-scale molecular comparison of human schwann cells to malignant peripheral nerve sheath tumor cell lines and tissues. *Cancer Res*, *66*(5), 2584-2591. doi:10.1158/0008-5472.CAN-05-3330
- Miyamoto, Y., Torii, T., Yamamori, N., Eguchi, T., Nagao, M., Nakamura, K., Tanoue, A., & Yamauchi, J. (2012). Paxillin is the target of c-Jun N-terminal kinase in Schwann cells and regulates migration. *Cell Signal*, *24*(11), 2061-2069. doi:10.1016/j.cellsig.2012.06.013
- Morgenstern, D. A., Asher, R. A., Naidu, M., Carlstedt, T., Levine, J. M., & Fawcett, J. W. (2003). Expression and glycanation of the NG2 proteoglycan in developing, adult, and damaged peripheral nerve. *Molecular and Cellular Neuroscience*, *24*(3), 787-802.
- Moser, M., Legate, K. R., Zent, R., & Fässler, R. (2009). The tail of integrins, talin, and kindlins. *Science*, *324*(5929), 895-899.
- Mottaghitlab, F., Farokhi, M., Zaminy, A., Kokabi, M., Soleimani, M., Mirahmadi, F., Shokrgozar, M. A., & Sadeghizadeh, M. (2013). A biosynthetic nerve guide conduit based on silk/SWNT/fibronectin nanocomposite for peripheral nerve regeneration. *PLoS One*, *8*(9), e74417.
- Namgung, U. (2015). The Role of Schwann Cell-Axon Interaction in Peripheral Nerve Regeneration. *Cells Tissues Organs*. doi:10.1159/000370324
- Nikaido, M., Doi, K., Shimizu, T., Hibi, M., Kikuchi, Y., & Yamasu, K. (2007). Initial specification of the epibranchial placode in zebrafish embryos depends on the fibroblast growth factor signal. *Dev Dyn*, *236*(2), 564-571. doi:10.1002/dvdy.21050
- Okuda, Y., Ogura, E., Kondoh, H., & Kamachi, Y. (2010). B1 SOX coordinate cell specification with patterning and morphogenesis in the early zebrafish embryo. *PLoS Genet*, *6*(5), e1000936.
- Okuda, Y., Yoda, H., Uchikawa, M., Furutani-Seiki, M., Takeda, H., Kondoh, H., & Kamachi, Y. (2006). Comparative genomic and expression analysis of group B1 sox genes in zebrafish indicates their diversification during vertebrate evolution. *Dev Dyn*, *235*(3), 811-825. doi:10.1002/dvdy.20678
- Pankov, R., Cukierman, E., Katz, B.-Z., Matsumoto, K., Lin, D. C., Lin, S., Hahn, C., & Yamada, K. M. (2000). Integrin dynamics and matrix assembly. *J Cell Biol*, *148*(5), 1075-1090.

- Pankov, R., & Momchilova, A. (2009). Fluorescent labeling techniques for investigation of fibronectin fibrillogenesis (labeling fibronectin fibrillogenesis). *Extracellular Matrix Protocols: Second Edition*, 261-274.
- Parrinello, S., Napoli, I., Ribeiro, S., Wingfield Digby, P., Fedorova, M., Parkinson, D. B., Doddrell, R. D., Nakayama, M., Adams, R. H., & Lloyd, A. C. (2010). EphB signaling directs peripheral nerve regeneration through Sox2-dependent Schwann cell sorting. *Cell*, *143*(1), 145-155. doi:10.1016/j.cell.2010.08.039
- Peters, J. H., Chen, G., & Hynes, R. O. (1996). Fibronectin Isoform Distribution in the Mouse II. Differential Distribution of the Alternatively Spliced EIIIB, EIIIA, and V Segments in the Adult Mouse. *Cell Communication & Adhesion*, *4*(2), 127-148.
- Peters, J. H., & Hynes, R. O. (1996). Fibronectin isoform distribution in the mouse I. The alternatively spliced EIIIB, EIIIA, and V segments show widespread codistribution in the developing mouse embryo. *Cell Communication & Adhesion*, *4*(2), 103-125.
- Petrie, R. J., Doyle, A. D., & Yamada, K. M. (2009). Random versus directionally persistent cell migration. *Nature Reviews Molecular Cell Biology*, *10*(8), 538-549.
- Petrie, R. J., & Yamada, K. M. (2012). At the leading edge of three-dimensional cell migration. *J Cell Sci*, *125*(Pt 24), 5917-5926. doi:10.1242/jcs.093732
- Pinto-Teixeira, F., Viader-Llargués, O., Torres-Mejía, E., Turan, M., González-Gualda, E., Polamorell, L., & López-Schier, H. (2015). Inexhaustible hair-cell regeneration in young and aged zebrafish. *Biology Open*, *4*(7), 903-909. doi:10.1242/bio.012112
- Platt, C. I., Krekoski, C. A., Ward, R. V., Edwards, D. R., & Gavrilovic, J. (2003). Extracellular matrix and matrix metalloproteinases in sciatic nerve. *J Neurosci Res*, *74*(3), 417-429. doi:10.1002/jnr.10783
- Pope, A. J., Sands, G. B., Smaill, B. H., & LeGrice, I. J. (2008). Three-dimensional transmural organization of perimysial collagen in the heart. *American Journal of Physiology-Heart and Circulatory Physiology*, *295*(3), H1243-H1252.
- Previtali, S. C., Feltri, M. L., Archelos, J. J., Quattrini, A., Wrabetz, L., & Hartung, H.-P. (2001). Role of integrins in the peripheral nervous system. *Prog Neurobiol*, *64*(1), 35-49.
- Prewitz, M. C., Seib, F. P., von Bonin, M., Friedrichs, J., Stißel, A., Niehage, C., Müller, K., Anastassiadis, K., Waskow, C., & Hoflack, B. (2013). Tightly anchored tissue-mimetic matrices as instructive stem cell microenvironments. *Nature Methods*, *10*(8), 788-794.
- Pujol-Martí, J., & López-Schier, H. (2013). Developmental and architectural principles of the lateral-line neural map.
- Purves, D., Augustine, G. J., Fitzpatrick, D., Hall, W. C., LaMantia, A.-S., McNamara, J. O., & Williams, S. (2004). Neuroscience. Massachusetts. *Publishers Sunderland*.
- Qu, Q., Li, D., Louis, K. R., Li, X., Yang, H., Sun, Q., Crandall, S. R., Tsang, S., Zhou, J., Cox, C. L., Cheng, J., & Wang, F. (2014). High-efficiency motor neuron differentiation from human pluripotent stem cells and the function of Islet-1. *Nat Commun*, *5*, 3449. doi:10.1038/ncomms4449
- Ribeiro-Resende, V. T., Koenig, B., Nichterwitz, S., Oberhoffner, S., & Schlosshauer, B. (2009). Strategies for inducing the formation of bands of Büngner in peripheral nerve regeneration. *Biomaterials*, *30*(29), 5251-5259.
- Richard, L., Topilko, P., Magy, L., Decouvelaere, A.-V., Charnay, P., Funalot, B., & Vallat, J.-M. (2012). Endoneurial fibroblast-like cells. *Journal of Neuropathology & Experimental Neurology*, *71*(11), 938-947.
- Richard, L., Védrenne, N., Vallat, J.-M., & Funalot, B. (2014). Characterization of endoneurial fibroblast-like cells from human and rat peripheral nerves. *Journal of Histochemistry & Cytochemistry*, *62*(6), 424-435.
- Rieger, S., Senghaas, N., Walch, A., & Koster, R. W. (2009). Cadherin-2 controls directional chain migration of cerebellar granule neurons. *PLoS Biol*, *7*(11), e1000240. doi:10.1371/journal.pbio.1000240

- Rogers, S. L., Letourneau, P. C., Palm, S. L., McCarthy, J., & Furcht, L. T. (1983). Neurite extension by peripheral and central nervous system neurons in response to substratum-bound fibronectin and laminin. *Dev Biol*, *98*(1), 212-220.
- Rovasio, R. A., Delouee, A., Yamada, K. M., Timpl, R., & Thiery, J. P. (1983). Neural crest cell migration: requirements for exogenous fibronectin and high cell density. *J Cell Biol*, *96*(2), 462-473.
- Sakai, T., Larsen, M., & Yamada, K. M. (2003). Fibronectin requirement in branching morphogenesis. *Nature*, *423*(6942), 876-881.
- Sances, S., Bruijn, L. I., Chandran, S., Eggan, K., Ho, R., Klim, J. R., Livesey, M. R., Lowry, E., Macklis, J. D., & Rushton, D. (2016). Modeling ALS with motor neurons derived from human induced pluripotent stem cells. *Nat Neurosci*, *16*(4), 542-553.
- Schaller, M. D. (2001). Paxillin: a focal adhesion-associated adaptor protein. *Oncogene*, *20*(44), 6459.
- Scholz, J., & Woolf, C. J. (2007). The neuropathic pain triad: neurons, immune cells and glia. *Nat Neurosci*, *10*(11), 1361-1368.
- Sepp, K. J. (2003). RhoA and Rac1 GTPases mediate the dynamic rearrangement of actin in peripheral glia. *Development*, *130*(9), 1825-1835. doi:10.1242/dev.00413
- Shirai, T., Miyagi, S., Horiuchi, D., Okuda-Katayanagi, T., Nishimoto, M., Muramatsu, M., Sakamoto, Y., Nagata, M., Hagiwara, K., & Okuda, A. (2005). Identification of an Enhancer That Controls Up-regulation of Fibronectin during Differentiation of Embryonic Stem Cells into Extraembryonic Endoderm. *Journal of Biological Chemistry*, *280*(8), 7244-7252. doi:10.1074/jbc.M410731200
- Shivane, A., Parkinson, D. B., Ammoun, S., & Hanemann, C. O. (2013). Expression of c-Jun and Sox-2 in human schwannomas and traumatic neuromas. *Histopathology*, *62*(4), 651-656. doi:10.1111/his.12062
- Singh, P., Carraher, C., & Schwarzbauer, J. E. (2010). Assembly of fibronectin extracellular matrix. *Annu Rev Cell Dev Biol*, *26*, 397.
- Singh, P., Reimer, C. L., Peters, J. H., Stepp, M. A., Hynes, R. O., & Van De Water, L. (2004). The spatial and temporal expression patterns of integrin alpha9beta1 and one of its ligands, the EIIIA segment of fibronectin, in cutaneous wound healing. *J Invest Dermatol*, *123*(6), 1176-1181. doi:10.1111/j.0022-202X.2004.23485.x
- Tanaka, E. M., & Reddien, P. W. (2011). The cellular basis for animal regeneration. *Dev Cell*, *21*(1), 172-185. doi:10.1016/j.devcel.2011.06.016
- To, W. S., & Midwood, K. S. (2011). Plasma and cellular fibronectin: distinct and independent functions during tissue repair. *Fibrogenesis & tissue repair*, *4*(1), 1.
- Topilko, P., Levi, G., Merlo, G., Mantero, S., Desmarquet, C., Mancardi, G., & Charnay, P. (1997). Differential regulation of the zinc finger genes Krox-20 and Krox-24 (Egr-1) suggests antagonistic roles in Schwann cells. *J Neurosci Res*, *50*(5), 702-712.
- Triolo, D., Dina, G., Lorenzetti, I., Malaguti, M., Morana, P., Del Carro, U., Comi, G., Messing, A., Quattrini, A., & Previtali, S. C. (2006). Loss of glial fibrillary acidic protein (GFAP) impairs Schwann cell proliferation and delays nerve regeneration after damage. *J Cell Sci*, *119*(19), 3981-3993.
- Tzima, E., Del Pozo, M. A., Shattil, S. J., Chien, S., & Schwartz, M. A. (2001). Activation of integrins in endothelial cells by fluid shear stress mediates Rho-dependent cytoskeletal alignment. *The EMBO journal*, *20*(17), 4639-4647.
- Verge, G. M., Milligan, E. D., Maier, S. F., Watkins, L. R., Naeve, G. S., & Foster, A. C. (2004). Fractalkine (CX3CL1) and fractalkine receptor (CX3CR1) distribution in spinal cord and dorsal root ganglia under basal and neuropathic pain conditions. *European Journal of Neuroscience*, *20*(5), 1150-1160. doi:10.1111/j.1460-9568.2004.03593.x
- Vogelezang, M. G., Scherer, S. S., Fawcett, J. W., & Ffrench-Constant, C. (1999). Regulation of fibronectin alternative splicing during peripheral nerve repair. *J Neurosci Res*, *56*(4), 323-333.

- Vracko, R. (1974). Basal lamina scaffold-anatomy and significance for maintenance of orderly tissue structure: a review. *The American journal of pathology*, 77(2), 313.
- Wakamatsu, Y., Endo, Y., Osumi, N., & Weston, J. A. (2004). Multiple roles of Sox2, an HMG-box transcription factor in avian neural crest development. *Dev Dyn*, 229(1), 74-86. doi:10.1002/dvdy.10498
- Wakatsuki, S., Araki, T., & Sehara-Fujisawa, A. (2014). Neuregulin-1/glia1 growth factor stimulates Schwann cell migration by inducing alpha5 beta1 integrin-ErbB2-focal adhesion kinase complex formation. *Genes Cells*, 19(1), 66-77. doi:10.1111/gtc.12108
- Wang, G.-Y., Hirai, K.-I., Shimada, H., Taji, S., & Zhong, S.-Z. (1992). Behavior of axons, Schwann cells and perineurial cells in nerve regeneration within transplanted nerve grafts: effects of anti-laminin and anti-fibronectin antisera. *Brain Research*, 583(1), 216-226.
- Webber, C., & Zochodne, D. (2010). The nerve regenerative microenvironment: early behavior and partnership of axons and Schwann cells. *Experimental neurology*, 223(1), 51-59.
- Wegner, M., & Stolt, C. C. (2005). From stem cells to neurons and glia: a Soxist's view of neural development. *Trends Neurosci*, 28(11), 583-588.
- Weiss, T., Taschner-Mandl, S., Bileck, A., Slany, A., Kromp, F., Rifatbegovic, F., Frech, C., Windhager, R., Kitzinger, H., & Tzou, C. H. (2016). Proteomics and transcriptomics of peripheral nerve tissue and cells unravel new aspects of the human Schwann cell repair phenotype. *Glia*, 64(12), 2133-2153.
- White, E. S., Baralle, F. E., & Muro, A. F. (2008). New insights into form and function of fibronectin splice variants. *The Journal of pathology*, 216(1), 1-14.
- White, E. S., & Muro, A. F. (2011). Fibronectin splice variants: understanding their multiple roles in health and disease using engineered mouse models. *IUBMB life*, 63(7), 538-546.
- Whitworth, I., Brown, R., Dore, C., Green, C., & Terenghi, G. (1995). Orientated mats of fibronectin as a conduit material for use in peripheral nerve repair. *Journal of Hand Surgery (British and European Volume)*, 20(4), 429-436.
- Wierzbicka-Patynowski, I., & Schwarzbauer, J. E. (2003). The ins and outs of fibronectin matrix assembly. *J Cell Sci*, 116(16), 3269-3276.
- Wojciak-Stothard, B., Denyer, M., Mishra, M., & Brown, R. (1997). Adhesion, orientation, and movement of cells cultured on ultrathin fibronectin fibers. *In Vitro Cellular & Developmental Biology-Animal*, 33(2), 110-117.
- Xiao, Y., Faucherre, A., Pola-Morell, L., Heddleston, J. M., Liu, T.-L., Chew, T.-L., Sato, F., Sehara-Fujisawa, A., Kawakami, K., & López-Schier, H. (2015). High-resolution live imaging reveals axon-glia interactions during peripheral nerve injury and repair in zebrafish. *Disease Models & Mechanisms*, 8(6), 553-564. doi:10.1242/dmm.018184
- Zaidel-Bar, R., Milo, R., Kam, Z., & Geiger, B. (2007). A paxillin tyrosine phosphorylation switch regulates the assembly and form of cell-matrix adhesions. *J Cell Sci*, 120(1), 137-148.
- Zamir, E., Katz, M., Posen, Y., Erez, N., Yamada, K. M., Katz, B.-Z., Lin, S., Lin, D. C., Bershadsky, A., & Kam, Z. (2000). Dynamics and segregation of cell-matrix adhesions in cultured fibroblasts. *Nat Cell Biol*, 2(4), 191-196.

7. Appendix

7.1. Abbreviations

%	Percent
°C	Degree Celsius
μl	Microliter
μ	Micro
μg	Microgram
μm	Micrometer
μM	Micromolar
APS	Ammonium Persulfate
BDNF	Brain-derived neurotrophic factor
bp	base pair
BSA	Bovine serum albumin
cDNA	Complementary DNA
CHAT	Choline O-Acetyltransferase
ChIP	Chromatin Immunoprecipitation
cm	Centimeter
CNS	Central nervous system
CO ₂	Carbon dioxide
Cre	Causes recombination
DAB	3,3'-Diaminobenzidine
DAPI	4',6-diamidino-2-phenylindole
Db cAMP	N6,2'-O-Dibutyryl adenosine 3',5'-cyclic
DEPC	Diethyl pyrocarbonate
DMEM	Dulbecco's Modified Eagle Medium
DNA	Desoxyribonucleic acid
dNTP	Desoxynucleotide

DPBS	Dulbecco's phosphate-buffered saline
DRG	Dorsal root ganglion
DTT	Dithiothreitol
E	Embryonic day
ECM	Extra cellular matrix
EDTA	Ethylendiaminintetraacetic acid
eGFP	Enhanced GFP
FAK	Focal adhesion kinase
FB	Fibroblasts
FB ^{Fn1-/-}	Fibroblast Fibronectin Knock-out
FBS	Fetal bovine serum
FC	Fold change
FDR	False discovery rate
FN	Fibronectin
FndFBSDMEM	Fibronectin depleted serum
g	Gram
GDNF	Glial cell-derived neurotrophic factor
GFAP	Glial fibrillary acidic protein
GO	Gene ontology
h	hour
H ₂ O	Water
H3K4me	Histone H3 (methylation K4)
HCl	Hydrochloride
hFn1	Human Fibronectin gene
hiPSC	Human induced pluripotent cells
HMGU	Helmholtz-Zentrum München für Gesundheit und Umwelt
hMN	Human Motorneuron
hpf	Hours post fertilization
IGF	Insulin Growth Factor
ISH	<i>In situ</i> hybridization
ISL	Insulin gene enhancer protein
JNK	c-Jun-amino (N)-terminal kinase

kDa	Kilo Dalton
Kg	Kilo gram
KO	Knock-out
l	Liter
Lam	Laminin
LB	Luria broth
M	Molar (mol/l)
mA	Milliampere
mg	Milligram
MilliQ-H ₂ O	Ultrapure water, purified by a Milli-Q Water Purification System
ml	Milliliter
mM	Millimolar
MMPs	Matrix metalloproteases
MN	Motorneuron
mRNA	Messenger RNA
mut	Mutant
Mx	Matrix
n	Sample size
N	Number of independent experiments
N ^o	Number
NaCl	Sodium chloride
NFH	Neurofilament heavy
ng	Nanogram
NGF	Nerve growth factor
nM	Nanomolar
NRG	Neuregulin
n.s.	Non-significant

NT	Neurotrophin
NTMT	Alkaline phosphatase buffer
PAM	Protospacer adjacent motif
PBS	Phosphate buffered saline
PCR	Polymerase chain reaction
PFA	Paraformaldehyde
P-Fwd	Forward primer
pH	potential of hydrogen
PI	Propidium Iodide
pLL	Posterior lateral line
PNS	Peripheral nervous system
qPCR	Real time PCR
RGD	Arginylglycylaspartic-peptide
RIPA	Radioimmunoprecipitation assay buffer
RNA	Ribonucleic acid
rcf	Relative centrifugal force
RT-PCR	Reverse-transcription polymerase chain reaction
SC	Schwann cell line RSC96
SC ^{Sox2+}	Schwann cell line RSC96 overexpressing Sox2
SC ^{Sox2+/Fn1-/-}	Schwann cell line RSC96 overexpressing Sox2 and Fibronectin 1 knock-out
SCW	Schwannoma cell line RT4D6P2T
SDS	Sodium dodecyl sulfate
s.e.m.	Standard error of the mean

sgRNA	Single guide RNA
SHH	Sonic hedgehog
SSC	Saline-sodium citrate
TBS	Tris-buffered saline
TBS-T	Tris-buffered saline with 0.1% Tween 20
TE	Tris/EDTA buffer
TEMED	Tetramethylethylenediamine
Tris	Tris-Hydroxy-Methyl-Amino-Methane
tRNA	Total Ribonucleic acid
TSS	Transcription starting site
TUBB	Tubulin
TUBB3	Tubulin class III
Tyr	Tyrosine
U	Unit
wt/v	Weight/Volume
VEGF	Vesicular endothelial growth factor
vs.	Versus
v/v	Volume/Volume

7.2. Acknowledgements

I would like to thank all the people that have been part of my doctoral studies, with their support, collaboration, and suggestion I could finish my Ph.D. project. Especially, I would like to thank:

Prof. Wolfgang Wurst for giving me the opportunity to do my Ph.D. at the Institute of Developmental Genetics, and for his valuable advice during the development of my project.

My direct supervisor, Dr. Sabrina Desbordes, for giving me the opportunity to work in her lab, for all her guidance and mentorship during my Ph.D., for the independence that she gave me to develop my own ideas and for her trust in my scientific criteria. I am also very gratefully for all her help and advice to develop my scientific career.

Dr. Hernán López Schier, for giving me the opportunity to work in his lab and for his supervision during the development of my Ph.D. project.

The members of my HELENA and final thesis committee. Prof. Magdalena Götz for her valuable suggestions and recommendations during all my Ph.D. studies. Prof. Harald Luksch for taking the chair of my thesis evaluation.

Prof. Reinhard Fässler for his important advice during the development of my project.

To the HELENA graduate school for all their support and to the Gender Equality Office, at the TUM, for the Laura-Bassi award that helped me to finish my Ph.D. project.

Dr. Dietrich Trümbach for all his collaboration with the bioinformatic analysis. His work was an indispensable contribution to the project.

Dr.med. Charlotte Kleeberger and Dr.med Ulf Dornseifer for their collaboration with the rat sciatic nerve injury experiments and for having the time to teach me the procedure.

Dr. Kamyar Hadian and Kara Brenke for their collaboration with the high-content images analysis.

All the people working at the animal facilities at the Helmholtz Zentrum Muenchen and at the Klinikum Rech der Isar (TUM).

Dr. Hagen Scherb for his assistance with the statistic for the animal protocol.

Prof. Johan Graw and Erika Burke for providing me with animal tissue for my experiments.

The former and present lab members Anna, Stefan, Theresa, Tanja and all the students not only for very helpful scientific discussions and troubleshooting sessions but also for creating a nice, supportive and friendly environment. I learned a lot from all of you guys. Stefan and Theresa also thank a lot for all your help with German translations.

All the members of the SBO for their help and for a nice working atmosphere. Particularly Petra for helping me with all the administrative paperwork.

Laura and Oriol not only for help me troubleshooting technical problems during my Ph.D. thesis but also for being there during every important step. Marta Forn, for all her *stupndus* advice and support. Thanks guys for making my time in Munich an amazing experience full of good memories.

Arnaldo, I am very grateful for all his help, advice and support during all my postdoctoral studies and for being there unconditionally.

My grandmother for continuously encouraging and motivating me. And finally, my parents, for their support despite the distance, for helping me to develop all my goals, for encouraging me to pursue a scientific career and teaching me about science. This work is dedicated to you.